

*To my dad*





**UNIVERSITÀ DEGLI STUDI DI SALERNO**

**DIPARTIMENTO DI SCIENZE  
FARMACEUTICHE E BIOMEDICHE**



**Dottorato di Ricerca in  
Scienze Farmaceutiche**

**X ciclo NS (XXIV)**

**2008-2011**

**Design and Characterization of DPI  
(dry powder inhaler) for the pulmonary delivery  
of anti-inflammatory and antibiotic drugs  
in the treatment of cystic fibrosis disease**

**Tutor**

Prof. Rita Patrizia Aquino

**PhD Student**

Lucia Prota

**Coordinator**

Prof.ssa Nunziatina De Tommasi



## **TABLE OF CONTENTS**

### **LIST OF PUBLICATIONS**

### **AIM AND OUTLINE OF THE PhD PROJECT**

<b>1 INTRODUCTION</b>	<b>1-32</b>
1.1 Cystic fibrosis: general background	5
1.2 Inflammatory signalling in CF airway epithelium	6
1.2a Role of bacterial infection	6
1.2b Use of immortalized cell lines to study CF	7
1.2c Role of oxidative stress	9
1.3 CFTR: structure and function	10
1.4 Current CF therapies	14
1.4a Gene Therapy	14
1.4b Correction of CF functionality	15
1.4c Management of CF	16
1.5 Respiratory drug delivery	18
1.5a Anatomy and physiology of the respiratory system	19
1.5b Inhalanda	23
1.5c The inhalation process	24
1.5d Factors affecting aerosol deposition	26
1.5e Pulmonary delivery devices	27
1.5f The challenge of Excipients for DPI	30
<b>2 RESULTS AND DISCUSSION</b>	<b>33-66</b>
<b>Section A</b> Design and development of a DPI of naringin to	

treat intrinsic inflammation in CF patient	35-65
2A.1 Background, Rationale of the selection of Naringin, Aims	37
2A.2 Naringin dry-powders production and characterization	43
2A.3 Aerodynamic behaviour of naringin dry powders	50
2A.4 <i>In vitro</i> biological activities of N dry-powders in bronchial epithelial cell	55
2A.5 Conclusions	65
<b>Section B</b> Design and development of a DPI of stable gentamicin micronized powders based on supercritical assisted atomization or spray-drying techniques	67
<b>2B</b> Background, Rationale of the selection of Gentamicin, Aims	69
<b>2B Part 1</b> Production of micronized gentamicin powder by SAA (Supercritical Assisted Atomization)	73-94
2B 1.1 Background and Aim	76
2B 1.2 Preliminary SAA test on BSA and GS	78
2B 1.3 SAA test for BSA/GS microspheres production	83
2B 1.4 Solid state microsphere characterization	87
2B 1.5 Microsphere characterization: drug loading and release profiles	90
2B 1.6 Conclusions	93
<b>2B Part 2</b> Production of micronized inhalable gentamicin powder by Spray-drying	95-110
2B 2.1 Background and Aim	97
2B 2.2 Manufacturing and characterization of GS/leu co-spray-dried powders	98
2B 2.3 Aerodynamic behaviour of GS/leu powders	103
2B 2.4 Effect of GS/leu powders on viability of CF	

airways epithelium	107
2B 2.5 Conclusions	108
<b>3 EXPERIMENTAL PROCEDURES</b>	<b>111-142</b>
<b>Section A</b> Design and development of a DPI of naringin to treat intrinsic inflammation in CF patient	113-124
3A.1 Chemicals	115
3A.2 Powders preparation and yield	115
3A.3 Powders physico-chemical properties	116
3A.3a Particle size	116
3A.3b Particle morphology	117
3A.3c DSC analysis	117
3A.3d X-ray diffraction studies	118
3A.3e Bulk and tapped density	118
3A.4 Aerodynamic behavior evaluation	119
3A.5 Dissolution study	121
3A.6 Biological activity	122
3A.6a Cell lines and culture conditions	122
3A.6b Proliferation assay	122
3A.6c Western blot analysis	123
3A.6d Interleukin-8 (IL-8) and interleukin-6 (IL-6) release determination in CuFi1 cells	124
3A.7 Statistical analysis	124
<b>Section B</b> Design and development of a DPI of stable gentamicin micronized powders based on supercritical assisted atomization or spray-drying techniques	125-142
<b>3B Part 1</b> Production of micronized gentamicin powder by SAA (Supercritical Assisted Atomization)	127-132

## Table of Contents

---

3B 1.1 Material	129
3B 1.2 Supercritical apparatus	129
3B 1.3 Morphology and particle size distribution	129
3B 1.4 Solid state characterization	130
3B 1.5 Drug content and encapsulation efficiency	131
3B 1.6 Drug release studies	132
<b>3B Part 2</b> Production of micronized inhalable gentamicin powder by Spray-drying	133-142
3B 2.1 Materials	135
3B 2.2 Powders preparation	135
3B 2.3 Powders physico-chemical properties	136
3B 2.3a GS and leu quantification	136
3B 2.3b GS and leu solubility	137
3B 2.3c Particle size	137
3B 2.3d Scanning Electron Microscopy (SEM)	138
3B 2.3e Bulk and tapped density	138
3B 2.3f Moisture uptake	138
3B 2.4 Aerodynamic behavior evaluation	139
3B 2.5 Powder stability	141
3B 2.6 <i>In vitro</i> toxicity	141
3B 2.6a Cell lines and culture conditions	141
3B 2.6b Proliferation assay	141
3B 2.6c Viability assay	142
3B 2.7 Statistical analysis	142
<b>4 LIST OF ABBREVIATIONS</b>	143-144
<b>5 REFERENCES</b>	145-160

**List of publications, proceedings and communications at international and national congress related to the scientific activity performed during the three years PhD course in Pharmaceutical Sciences:**

**Papers:**

- ✓ G. Della Porta, R. Adami, P. Del Gaudio, **L. Prota**, R.P. Aquino, E. Reverchon. “Albumin/gentamicin microspheres produced by supercritical assisted atomization: Optimization of size, drug loading and release”, *J. Pharm. Sci.*, **2010**, 99(11), 4720-9.
  
- ✓ S. Pisanti , P. Picardi, **L. Prota**, M.C. Proto, C. Laezza, P.G. McGuire, L. Morbidelli, P. Gazzero, M. Ziche, A. Das, M. Bifulco. “Genetic and pharmacological inactivation of cannabinoid CB1 receptor inhibits angiogenesis”, *Blood*, **2011**, 117(20), 5541-50.
  
- ✓ **L. Prota**, A. Santoro, M. Bifulco, R.P. Aquino, T. Mencherini, P. Russo. “Leucine enhances aerosol performance of Naringin dry powder and its activity on cystic fibrosis airway epithelial cells”, *Int. J. Pharm.*, **2011**, 412(1-2), 8-19.
  
- ✓ P. Picerno, F. Sansone, T. Mencherini, **L. Prota**, R.P. Aquino, L. Rastrelli, M.R. Lauro. “Citrus bergamia Juice: Phytochemical and Technological Studies”, *Natural Product Comm.*, **2011**, 6 (7), 951-955.
  
- ✓ R.P. Aquino, **L. Prota**, G. Auriemma, A. Santoro, T. Mencherini, G. Colombo, P. Russo “Dry powder inhalers of gentamicin and leucine:

formulation parameters, aerosol performance and *in vitro* toxicity on CuFi1 cells”, *Int. J. Pharm.*, **2012**, *in press*

**List of proceedings with ISBN:**

- ✓ P. Russo, L. Prota, P. Del Gaudio, G. Dello Russo and R.P. Aquino. “Optimization of Aerosol Performance of Naringin Dry Powders using Amino Acids”, in: *Respiratory Drug Delivery*, 2010, Florida, April 25-29, Vol. 3, pag. 861-864, ISBN:1933722436.
- ✓ R. Adami, S. Liparoti, G. Della Porta, P. Del Gaudio, G. Auriemma, L. Prota, R. P. Aquino, E. Reverchon. “Gentamicin Loaded Albumin/Pectin Microspheres for Drug Release Obtained by SAA”, 9<sup>th</sup> Conference on Supercritical Fluids and Their Applications, September 5-8, 2010, Sorrento (Napoli), Italy. E. Reverchon Vol.1, pag.193-196 ISBN:8878970409
- ✓ A Santoro, L. Prota, M. Bifulco, R. P. Aquino, T. Mencherini, P. Russo. “Naringin Dry Powder Inhalers Reduce Cystic Fibrosis Intrinsic Inflammation *in vitro*”, XXX National Congress of Società Italiana di Patologia – Salerno, October 14-17, 2010. *Am J Pathol* 2010, 177(Suppl):S15 Abstract IM 04.
- ✓ S. Pisanti, P. Picardi, L. Prota, C. Laezza, P. G. McGuire, L. Morbidelli, P. Gazzo, M. Ziche, A. Das, M. Bifulco. “Cannabinoid CB1 Receptor is a Novel Target for Angiogenesis Inhibition: Genetic and Pharmacological Evidence”, XXX National Congress of Società Italiana di Patologia – Salerno, October 14-17, 2010. *Am J Pathol* 2010, 177(Suppl):S19 Abstract MTP 01.

**List of communications:**

- ✓ L. Prota, S. Pisanti, C. Borselli, A. Santoro, P. Gazzero, M. Bifulco. “Anti-angiogenic activity of cannabinoid CB1 receptor SR141716”, 3rd AItUN Annual Meeting on Pharmaceutical Technology Meets Tissue Engineering, March 6-7, 2009, Fisciano, Italy.
  
- ✓ F.Sansone, C. Fienga, P. Del Gaudio, L. Prota, R. P. Aquino and M. R. Lauro. “Hesperidin gastroresistant microparticles by spray-drying: preparation, characterization and dissolution profiles”, 3rd AItUN Annual Meeting on Pharmaceutical Technology Meets Tissue Engineering, March 6-7, 2009, Fisciano, Italy.
  
- ✓ F. Sansone, A. Rossi, L. Prota, T. Mencherini, P.Picerno, R.P. Aquino and M.R. Lauro. “Hesperidin gastroresistent microparticles by spray-drying: preparation, characterization and dissolution profiles”, Scuola dottorale nazionale in tecnologie farmaceutiche, Università degli Studi di Cagliari, 7-9 Settembre 2009.
  
- ✓ P. Russo, F. Sansone, L. Prota, G. Dello Russo, M. R. Lauro, R.P. Aquino. “Optimization of the aerodynamic properties of naringin spray-dried powders using aminoacids”, XXI Simposio A.D.R.I.T.E.L.F. Associazione Docenti e Ricercatori Italiani di Tecnologie e Legislazione Farmaceutiche “Veicolazione dei farmaci: aspetti tecnologici innovativi”, tenutosi a Cagliari, 10-13 Settembre 2009.
  
- ✓ G. Della Porta, R. Adami, P. Del Gaudio, L. Prota, R.P. Aquino, E. Reverchon. “Gentamicin loaded microspheres obtained by supercritical

assisted atomization”, XXI Simposio A.D.R.I.T.E.L.F. Associazione Docenti e Ricercatori Italiani di Tecnologie e Legislazione Farmaceutiche “Veicolazione dei farmaci: aspetti tecnologici innovativi”, tenutosi a Cagliari, 10-13 Settembre 2009.

- ✓ L. Prota, P. Russo, A. Santoro, G. Dello Russo, P. Del Gaudio, R.P. Aquino. “Naringin Dry Powder Inhalers: aerodynamic properties and *in vitro* biological activity on cystic fibrosis air way cell lines”, 4th AItUN Annual Meeting on Innovation in Pharmaceutics: “a glimpse” in the Biotech world, February 26-27, 2010, Napoli, Italy.
- ✓ S. Pisanti, P. Picardi, L. Prota, C. Laezza, P. G. McGuire, L. Morbidelli, P. Gazzo, M. Ziche, A. Das, M. Bifulco. “Genetic and pharmacological inhibition of cannabinoid CB1 receptor inhibits angiogenesis”, Workshop SIICA (Società Italiana di Immunologia Clinica e Allergologia), Certosa di Pontignano, Siena, 10-12 Maggio 2010.
- ✓ P. Russo, L. Prota, V. Ventre, R. P. Aquino. “Co-spray-dried gentamicin and leucine inhalable powders for treatment of bacterial infection in cystic fibrosis patients”, 15 th International Pharmaceutical Technology Symposium on Advanced Therapeutic Systems From Innovative Technology to Commercialization, September 13-15, 2010 – Antalya, Turkey.
- ✓ P. Russo, L. Prota, V. Ventre, R. P. Aquino. “Inhalable gentamicin powders for treatment of chronic bacterial infection in cystic fibrosis patients”, Meeting on Lactose as a Carrier for Inhalation Products, September 26-28, 2010 - Parma, Italy.

- ✓ L. Prota, L. M. de Angelis, V. Ventre, M. Stigliani, R. P. Aquino and Paola Russo. “Co-spray-dried gentamicin and leucine inhalable powders for treatment of cystic fibrosis patients”, 5th AItUN Annual Meeting on Vaccines: Prevention is better than cure. Current Status and Future Prospects, 11-12 Marzo 2011, Pavia, Italy.
  
- ✓ L. Prota, L. M. de Angelis, V. Ventre, M. Stigliani, R. P. Aquino and P. Russo. “Co-spray-dried gentamicin and leucine inhalable powders for treatment of cystic fibrosis patients”, 3rd Pharmaceutical Sciences Fair and Exhibition for the Future of Medicines, June 13 - 17, 2011, Prague, Czech Republic.
  
- ✓ A. Santoro, L. Prota, E. Esposito, E. Ciaglia, C. Laezza, A. D’Alessandro, R. P. Aquino, M. V. Ursini, M. Bifulco. “N<sup>6</sup>-Isopentenyladenosine (I<sup>6</sup>A) inhibits inflammatory response through STAT3 and NF-κB signaling pathways in different cell lines”, 3rd Meeting Cell stress and apoptosis - to Arturo, 23-25 Giugno 2011, Salerno.
  
- ✓ L. Prota, A. Santoro, E. Esposito, R. P. Aquino, M. V. Ursini, M. Bifulco. “Biological activity of phytocannabinoids on intrinsic and LPS-induced inflammation in Cystic Fibrosis bronchial epithelial cells”, 3rd Meeting Cell stress and apoptosis - to Arturo, 23-25 Giugno 2011, Salerno.
  
- ✓ A. Santoro, L. Prota, E. Ciaglia, E. Esposito, C. Laezza, P. Picardi, R. P. Aquino, M. V. Ursini, M. Bifulco. “Anti-inflammatory activity of N<sup>6</sup>-Isopentenyladenosine (I<sup>6</sup>A) in Cystic Fibrosis bronchial epithelial

cells”, Cell Biology and Pharmacology of Mendelian Disorders, 7-11  
October 2011 - Vico Equense, Italy.

## **Aim and outline of the PhD Project**

Pulmonary drug delivery systems have been mainly applied for the management of pulmonary diseases such as Asthma and COPD (chronic obstructive pulmonary disease). In the treatment of obstructive respiratory diseases, a \$10Bn market which continues to grow, a drug administered by the pulmonary route directly targets the airways. Consequently, systemic side effects are minimized, a rapid response is provided as well as the required dose reduced. A drug, when is delivered directly to the conducting zone of the lungs, may be absorbed through the deep lung into the bloodstream with relatively high bioavailability or, alternatively, may exert a local action. Due to the advancement in pharmaceutical technologies as well as strong interest in using the lung as a route to systemic drug delivery, nowadays the pulmonary delivery has been proposed to treat many pathologies, such as diabetes, angina pectoris, cancer, bone disorders, tuberculosis.

The origin of inhaled therapies seen in back 4000 years ago to India, where people smoked the leaves of *Atropa belladonna* to suppress cough. In the 19th and early 20th centuries, smoked anti-asthmatic cigarettes, that contained stramonium powder mixed with tobacco, were largely used to treat respiratory diseases.

Nowadays, pulmonary drug delivery remains the preferred route for the administration of various drugs and it is an important research area which impacts the treatment of illnesses including, over asthma and COPD, cystic fibrosis (CF).

CF, one of the so-called “orphan disease”, is caused by mutations in the gene encoding the CF transmembrane conductance regulator (CFTR). Severe lung damage is the main cause of morbidity and mortality in CF patients.

Clinically, mucus high viscoelasticity results in ineffective cough and poor airway clearance, leading to progressive airway obstruction, chronic infection and inflammation.

Therefore, current CF therapy is focused on attenuating disease progression and delaying the onset of irreversible lung damage by controlling airway infection and inflammation.

The development of an inhalation therapy that is effective and safe depends not only on pharmacologically active molecule, but also on the delivery system and its application. Generally, inhalation products are liquid, solid or pressurized preparations which must be aerosolized and inhaled to be deposited in the lung.

Good distribution throughout the lung requires particles with an aerodynamic diameter between 1 and 5  $\mu\text{m}$  and, thus, most inhaled products are formulated with a high proportion of drug in this size range, in order to target the alveolar region specifically. The traditional inhalers, namely nebulizers and MDIs, use either a propellant or the patients inspired effort to get drug into their lungs.

How much drug is delivered to the lungs depends on the patients' own inhalation efforts. Because of this phenomenon, children and older patients may not get the full dosage they require, because their inhalation may not be strong enough to carry the drug to the lungs. DPI (dry powder inhaler), solvent- and propellant-free, does the work for the patient and is independent of patient effort. DPI devices with its own energy source provides patients with uniform medication dosage every time. When a patient activates the inhaler, the active mechanism aerosolizes the powder that is tailored to the specific drug loaded in the device. This also means that DPI can deliver a broader range of drug formulations from a single technology platform.

Over the last past decade, the research group in Pharmaceutical Technology of the University of Salerno has been involved in developing new inhalation dry powders and, currently, has active projects in this area addressing topics such as aerosolized antibiotics and antioxidant therapy. In this context, the aim of the present PhD project was to design inhalable powder-based formulations for pharmaceutical products that may improve the treatment of pulmonary diseases, mainly cystic fibrosis, and may be easier for patients to use. Particularly, the present project aims to supply CF patients with flavonoids (Naringin) and aminoglycosides (Gentamicin sulfate) in a respirable form as a valid alternative over more conventional (oral or parenteral) anti-inflammatory and antibiotic therapy. As a matter of fact, in CF epithelial cells, antioxidant defense systems appear to be defective in their ability to control the amount of ROS produced and over abundance of ROS may cause tissue injury-events and modify intracellular signalling pathways leading to enhanced inflammatory processes, typical of CF airways. Overall, evidence suggests improved CFTR function *in vitro* when flavonoids, such as genistein, are used. For chronic *Pseudomonas aeruginosa* (*Pa*) infections in CF, gentamicin given by pulmonary route may play an important role.

In fact, it was observed that daily inhalation of some aminoglycosides from nebulized solution delays the acquisition of chronic *Pa* infections and decreases CF progression.

The project addresses a number of the key features that are outstanding in inhaled delivery, mainly - characteristic of the active drug; - properties of the drug formulation, particularly powder flow, particle size, shape, surface properties and drug/carrier interaction; - consistent dose delivery and high proportion of dose getting to the lung; - performance of the inhaler device, including aerosol generation and delivery. A balance among these

characteristics is necessary in the design of a drug formulation intended for pulmonary administration.

Utilizing proven (Spray-drying) or innovative (Supercritical Assisted Atomization) technology, stable and micronized powders usefull for dry powder inhaler (DPI) production have been developed. Moreover, the research has been based on *in vitro* product test methods to evaluate the health effects of produced powders and their aerodynamic behaviour through the pulmonary system. Optimized stability and bioavailability of the selected drugs, the achieving of therapeutically effective concentrations for the pulmonary care of cystic fibrosis have been other goals of the research. Technologies and products that the research is aimed to develop would be of interest to a number of pharmaceutical companies either in the respiratory area or trying to get a toehold in this market.

Specific objectives of this research have been:

- design and development of Dry Powder Inhalers (DPIs) containing flavonoids (Naringin) or aminoglycoside antibiotics (Gentamicin sulfate) micronized powder by spray drying production or by Supercritical Assisted Atomization (SAA);
- optimization of the aerodynamic characteristics of the powders, through the use of excipients (amino acids) not toxic for lung but able to improve the powder flow properties and dispersion which, in turn, may increase lung deposition of the drugs;
- *in vitro* evaluation of the biological activity of the engineered particles on a model of bronchial epithelial cell lines from patients with cystic fibrosis (CuFi1, F508del/F508del CFTR), in comparison to the activity of the same products on normal bronchial epithelial cell lines (NuLi1).



# **Introduction**



**RESPIRATORY DRUG DELIVERY  
AND CYSTIC FIBROSIS**



## 1.1 CYSTIC FIBROSIS: GENERAL BACKGROUND

Cystic Fibrosis (CF) is the most common lethal monogenic disorder in Caucasians, estimated to affect one per 2500-4000 newborns. The outlook for people affected by this pathology has improved substantially in the past 10-20 years (O'Sullivan et al., 2009).

CF is caused by mutations in the gene encoding the CF transmembrane conductance regulator (CFTR) (Cheng et al., 1990; Collins et al., 1990). The CFTR gene is located on the long arm of chromosome 7 (7q31) and contains 27 exons. The CFTR protein (Fig. 1), which is expressed in many epithelial and blood cells, is composed of 1480 amino acids and is a member of the ATP-binding cassette (ABC) transport protein super family.

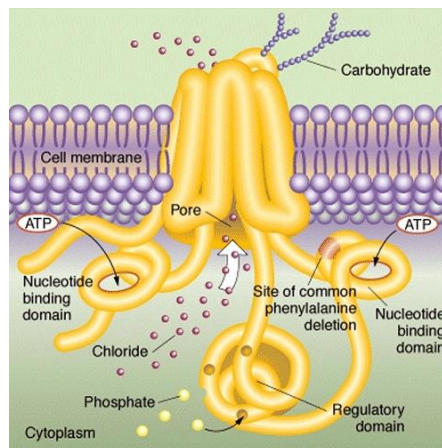


**Fig. 1.** CFTR protein.

Although CFTR acts mainly as a chloride channel, it has many other regulatory roles, including inhibition of sodium transport through the epithelial sodium channel, regulation of the outwardly rectifying chloride channel, regulation of ATP channels, regulation of intracellular vesicle transport, acidification of intracellular organelles and inhibition of endogenous calcium-

activated chloride channels (Reisin et al., 1994; Schwiebert et al., 1995; Stutts et al., 1995; Vankeerberghen et al., 2002; Mehta, 2005). CFTR is also involved in bicarbonate-chloride exchange (Quinton, 2008). Loss of functional CFTR promotes depletion and increases oxidation of the airway surface liquid, tissue injury, modification of intracellular signaling pathways, cell apoptosis and inflammatory processes.

Clinically, CF is dominated by chronic lung disease, which is the main cause of both morbidity and mortality in more than 90% of patients surviving the neonatal period. Airway obstruction by thick mucus and chronic infection by *Pseudomonas aeruginosa* (*Pa*) led to loss of pulmonary function (Rowe et al., 2005). Other CF symptoms include pancreatic dysfunction, elevated sweat electrolytes and male infertility.

## **1.2. INFLAMMATORY SIGNALLING IN CF AIRWAY EPITHELIUM**

### **1.2a. Role of bacterial infection**

Airway epithelial cell signalling in response to bacterial pathogens involves the activation of numerous receptors and signalling pathways and therefore leads to the release of a number of cytokines and chemokines that serve to recruit phagocytic cells to the airway epithelium (Gomez & Prince, 2008). Intact bacteria, removed from the lung by mucociliary clearance, are rarely in direct contact with airway epithelial cells well protected by mucins. In pathological conditions, components of the bacterial cell wall and flagella are major activators of epithelial proinflammatory signalling. Mutations in the CFTR gene in the airway epithelium cause decreased bacterial clearance, intrinsic hyperinflammation and decreased bacterial killing (Chmiel & Davis, 2003). Abnormal CFTR functional activity results in airway surface dehydration and modification of the properties of mucus clearance that participate in the susceptibility to chronic infection with pathogens such as

*Staphylococcus aureus* and *Pseudomonas aeruginosa*. In the lungs of CF patients, the inflammatory response to a defined bacterial load seems to be greater and more excessive than in normal lung (Chmiel & Davis, 2003; Davis et al., 1996). This lung inflammation is characterized by a sustained accumulation of neutrophils, high proteolytic activity and elevated levels of cytokines and chemokines (Balough et al., 1995; Sagel et al., 2007).

A growing body of evidence has emerged in support of the view that mutant CFTR may itself also contribute to defective regulation of the inflammatory response in lungs (Di Mango et al., 1995; Venkatakrisnan et al., 2000; Weber et al., 2001). Thus, Muhlebach et al. observed that bronchoalveolar lavage fluid (BALF) of CF non-infected and infected children had a higher pro-inflammatory state compared to non-CF disease controls (Muhlebach et al., 2004). It is not yet clear whether this hyperinflammatory process in the CF lung is the direct result of chronic bacterial infection or is due to the primary defect of mutated CFTR (Rubin, 2007).

### **1.2b. Use of immortalized cell lines to study CF**

The development of immortalized cell lines has been of significant benefit to the study of human disease, due to limitations in the availability of primary bronchial and lung epithelial cells, KO mice and human lung tissue (Gruenert et al., 2004). Immortalized CF lung epithelial cell lines have been critical to enhance our understanding of the pathophysiological and molecular mechanisms underlying the CF inflammatory process. Two major immortalized epithelial cell lines from CF patients are available: IB3-1 with a F508del/W1282X mutant genotype and CuFi1 cells derived from human CF bronchial epithelium which is homozygous for del508 (F508del/F508del CFTR mutant genotype). These cell culture systems exhibit enhanced proinflammatory signalling compared to non-CF cells (Muhlebach et al., 2004; Tabary et al., 2001; Wiszniewski et al., 2006). This intrinsic inflammation was

## Introduction

mainly characterized by an increased level of inflammatory mediators (e.g., IL-8 and IL-6) compared to non-CF bronchial epithelial cells, either in the absence (Hallows et al., 2006; Tabary et al., 1998) or in the presence of stimulation (DiMango et al., 1998; Kube et al., 2001). Interestingly, the origin of this proinflammatory state supports the concept that increased NF- $\kappa$ B signalling (NF $\kappa$ B activation, I $\kappa$ B degradation and IKK phosphorylation) leads to enhanced IL-8 production (Fig. 2) (Saadane et al., 2007; Verhaeghe et al., 2007; Weber et al., 2001).

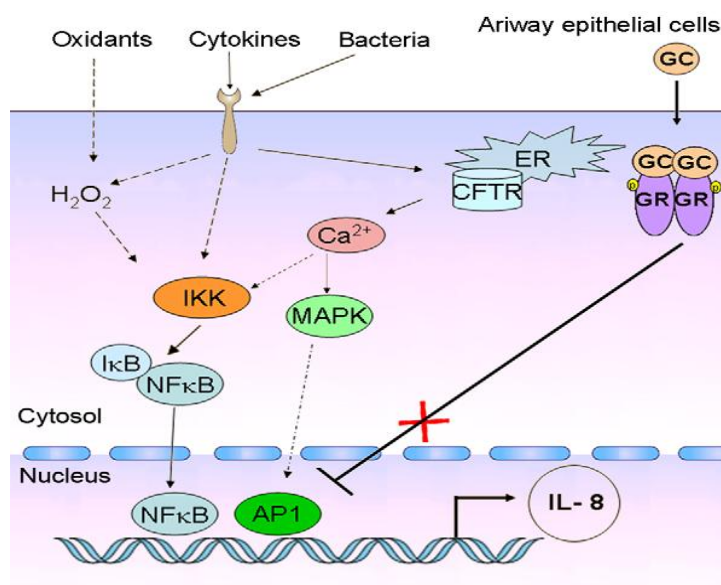


**Fig. 2.** CF airway epithelial cell responses to environmental agents. Signalling cascades are initiated through surface receptors and subsequent translocation of nuclear factors (NF- $\kappa$ B and AP-1) leads to transcriptional activation of pro-inflammatory cytokines, such as IL-8. In CF epithelial cells, glucocorticoids (GC) treatment fails to block IL-8 production. (Jacquot et al., 2008).

The proinflammatory molecular mechanisms in the CF lung epithelium remain partially understood and the NF- $\kappa$ B signalling pathway is not the only pathway implicated. While the release of IL-8 by CF lung epithelial cells was highly controlled by NF- $\kappa$ B, other pathways such as the mitogen-activated protein

kinase/extracellular signal-regulated kinase (MAPK/ERK) and activated protein (AP-1) pathways have been recently found to be involved in the lung inflammatory processes in the presence of different inducers (Boncoeur et al., 2008; Li et al., 2003; Verhaeghe et al., 2007). These findings provide a rationale for the potential use of MAPK and/or NF- $\kappa$ B inhibitors to control lung inflammation and, therefore, to limit deterioration of the lung function in CF patients.

### **1.2c. Role of oxidative stress**

Another important aspect of CF disease is the role of oxidative stress. Oxidative stress has been identified as an early complication in the airways of infants and young children with CF (Cantin et al., 2006; Kettle et al., 2004). Recent clinical data suggest that oxidative damage of pulmonary proteins during chronic infection may contribute to the decline of lung function in CF patients (Starosta & Griese, 2006). The massive infiltration of neutrophils in lungs of CF patients leads to the generation of oxygen-derived reactive oxygen species (ROS) and in particular  $H_2O_2$  that contributes to irreversible lung damage and ultimately to patient death. Activated neutrophils migrate to the airways and release large amounts of ROS. On the other hand, in CF epithelial cells antioxidant defense systems appear to be defective in their ability to control the amount of ROS produced (Boncoeur et al., 2008). Therefore, an over abundance of ROS and their products may cause tissue injury-events and modify intracellular signalling pathways leading to cell apoptosis and enhanced inflammatory processes in CF lung. In addition to its  $Cl^-$  channel function, CFTR has been proposed to conduct antioxidant-reduced glutathione. A recent study demonstrated that oxidative stress can suppress CFTR expression and function while increasing the cellular GSH content (Cantin et al., 2006).

### 1.3. CFTR: STRUCTURE AND FUNCTION

CFTR is made up of five domains: two transmembrane domains (TMD-1 and TMD-2) that form the chloride ion channel, two nucleotide-binding domains (NBD-1 and NBD-2) that are crucial to ATP binding and control the channel activity through an interaction with cytosolic nucleotides, and a regulatory (R) domain (Riordan, 2005).

While most ABC transporters consist of four domains (two membrane-spanning and two nucleotide-binding domains), CFTR is the only one known to possess a regulatory domain.

The R domain connects NBD-1 to TMD-2, and may be required to transmit signals between the two domains. Phosphorylation of the R domain, usually by cAMP-dependent protein kinase A and C, increases the apparent affinity of CFTR for ATP. The result is binding and hydrolysis of ATP by the nucleotide binding fold that causes the channel open (Fig. 3).

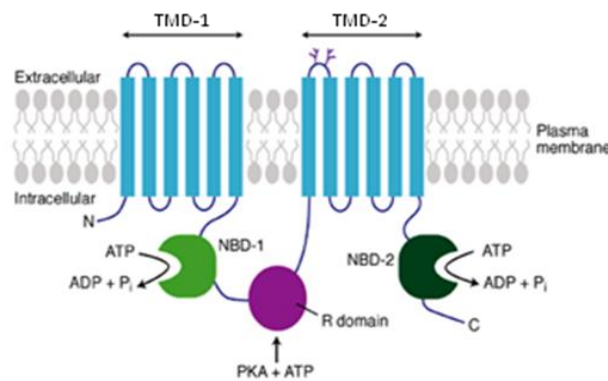


**Fig. 3.** Model of cystic fibrosis transmembrane regulator (CFTR).

CFTR forms a tightly regulated anion-selective channel that mediates anion flow across the apical membrane of epithelial cells (Sheppard et al., 1999) and

regulates the activity of other transport proteins in epithelial cells (Schwiebert et al., 1999). Dysfunction of CFTR in CF (Fig. 4) disrupts fluid and electrolyte transport across epithelial surface throughout the body and hence the function of a variety of organs, most notably the respiratory airways (Welsh et al., 2001; Rowe et al., 2005).

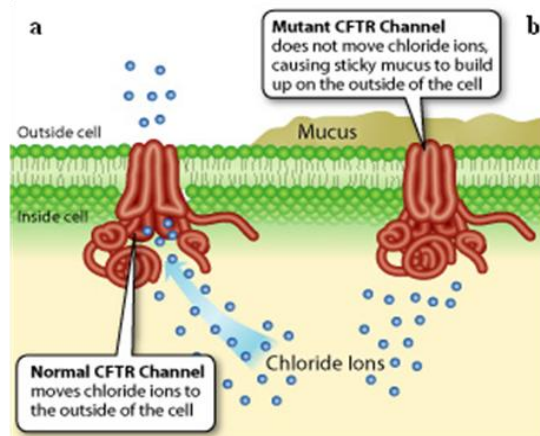


**Fig. 4.** Function (a) and dysfunction (b) of the CFTR channel.

### *CFTR Mutations*

To date, over 1500 mutations have been identified, but the functional importance of only a small number is known.

The most common mutation, a deletion of three nucleotides resulting in the deletion of phenylalanine at position 508 ( $\Delta F508$ ) (Fig. 5), is responsible for about 70% of all mutant CFTR alleles (Tsui, 1992), while 10–20 less common mutations represent a further 10–15% of all mutant alleles. The frequency depends on the ethnic background of the patient.

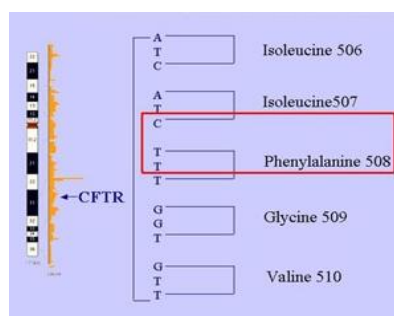


**Fig. 5.** Deletion of phenylalanine at position 508 ( $\Delta F508$ ).

The mutations can be classified into different groups according to the mechanism by which they disrupt CFTR function (Fig. 6).

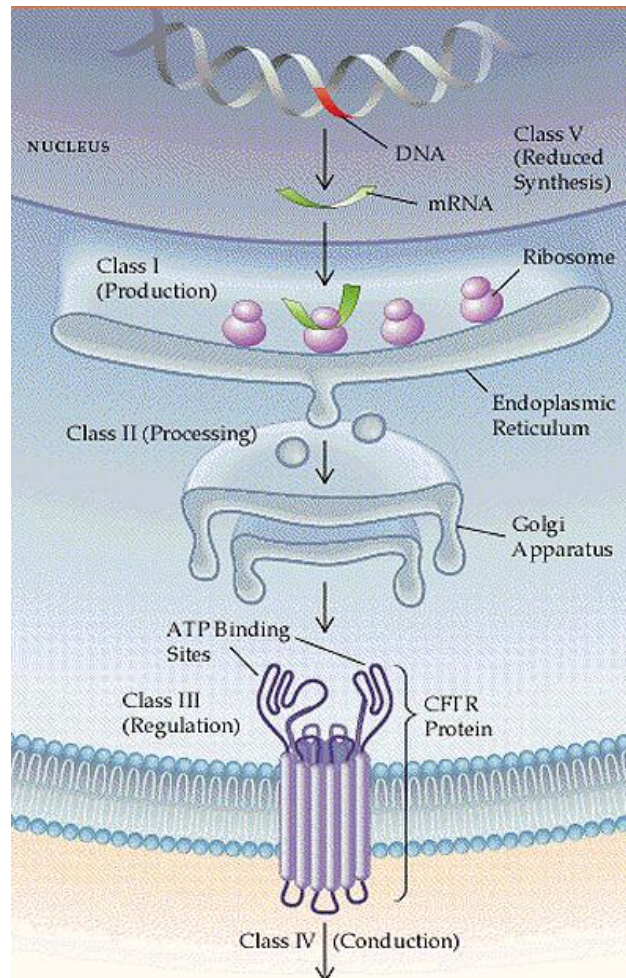


**Fig. 6.** CFTR class mutations.

**Class I Mutations affecting biosynthesis.** Class I mutations in the CFTR gene include the most severe CF phenotypes due to no protein being synthesised. These mutations, due either to nonsense mutations or premature stop codons, prevent the synthesis of a stable protein or result in the

production of a truncated protein due to the creation of a premature termination codon. The truncated proteins are usually unstable, are recognised by chaperone proteins in the endoplasmic reticulum (ER) and are rapidly degraded. G542X is the most common class I mutation.

**Class II Mutations affecting protein maturation and transport.** Class II mutations, including the most prevalent  $\Delta F508$ , result in the misprocessing of CFTR, producing a lack of functional protein at the cell membrane.  $\Delta F508$  CFTR is synthesised, but failed to mature or to proceed beyond the endoplasmic reticulum (ER) (Cheng et al., 1990).

**Class III Mutations affecting  $Cl^-$  channel regulation/gating.** Mutations of the *CFTR* gene in class III produce protein that is trafficked to the cell membrane but then does not respond to cAMP stimulation (Welsh et al., 1993). These mutations are located within the nucleotide-binding folds, and are likely to affect the binding of ATP or the coupling of ATP binding to activation of the channel, such as by preventing transmission of a conformational change. The missense mutation G551D is an example of a class III mutation.

These three classes usually lead to a classic CF phenotype with pancreatic insufficiency, although the severity of lung disease is highly variable.

**Class IV Mutations affecting  $Cl^-$  conductance.** Class IV mutations include cases where the *CFTR* gene encodes a protein that is correctly trafficked to the cell membrane and responds to stimuli but generates a reduced  $Cl^-$  current (for example R117H). Most of the class IV mutations analysed to date are located within the membrane-spanning domains.

**Class V Mutations affecting protein stability.** This class includes protein stability mutants (which result in inherent lability of the CFTR protein) lacking the last 70–98 residues of the CFTR C-terminus (Haardt *et al.*, 1999). Although the C-terminus is not required for the biogenesis and chloride

channel function of CFTR, it is indispensable for maintaining the stability of the complex-glycosylated CFTR.

The latter two classes are often associated with a milder phenotype and pancreatic sufficiency.

#### **1.4. CURRENT CF THERAPIES**

The understanding of the mechanisms by which mutations disrupt CFTR function provides the scientific basis for development of targeted drugs for CF treatment. Pharmaceutical research is currently proceeding on three different fronts:

- correcting CFTR defect (gene therapy);
- correcting protein function (pharmacological therapy);
- alleviating and improving the complex symptoms of CF patients.

##### **1.4a. Gene Therapy**

Since the discovery of the CFTR gene in 1989, CF has been considered a prime candidate for gene therapy, especially for treating the airways, since topologically they are easily accessible. Clinical trials using different gene transfer agent were conducted, but no clinical benefit has far been recorded. Gene therapy may yet provide the best solution, but the technical difficulties led to search for alternative approaches.

*In vivo* and *in vitro* studies on human CF nasal cells have indicated that boosting CFTR functional activity from less than 1% to as little as 5% of normal levels may greatly reduce disease severity or even eliminate the principal disease manifestations. Given the absence of other effective treatments, there has been an increasing interest in the possibility to restore the defective CFTR function by pharmacological means.

#### **1.4b. Correction of CF functionality**

An alternative strategy to gene therapy is, therefore, the approach termed “mutation-specific therapy”, which aims to correct the genetic defect according to the different classes of mutation.

A potential treatment for conditions caused by class I mutations includes agents that suppress the normal proofreading function of the ribosome. Recent studies showed that aminoglycoside antibiotics (gentamicin or G418), in addition to their antimicrobial activity, can suppress premature stop codons by enabling the incorporation of an amino acid, thus permitting translation to continue until the normal termination of the transcript (Clancy et al., 2001; Wilschanski et al., 2000; Wilschanski et al., 2003).

For class II mutations, therapy would require pharmacological methods to increase the levels of functional protein at the cell membrane, by increasing the efficiency of protein folding or suppressing the protein degradation processes. *Chemical, molecular or pharmacological chaperones*, generally called ‘correctors’ (Pedemonte et al., 2005), were reported to stabilize protein structure and promote folding, enabling cell-surface expression of processing mutants. Chemical chaperones such as glycerol have been shown to stabilise protein structure and to increase the stability and kinetics of oligomeric microtubule assembly (Sato et al., 1996; Zhang et al, 2003). Due to the high concentrations that would be required *in vivo* and their potential toxicity, glycerol and other chemical chaperones are unlikely to be useful. Another molecular chaperone is calnexin, a calcium-binding transmembrane protein chaperone in the ER that assists newly synthesized proteins to fold into a normal structure.

Sodium-4-phenylbutyrate (4-PBA) is an example of a possible corrector; it is a histone deacetylase inhibitor that promotes  $\Delta F508$  CFTR trafficking. It allows mutant CFTR to escape the ER, thereby permitting its glycosylation in the

## *Introduction*

---

Golgi apparatus, transportation to the plasma membrane and subsequent display of residual intrinsic channel activity.

Therapy for mutations in classes III and IV would require increased activation of the functional CFTR present at the cell membrane.

CFTR *activators* such as alkylxanthines and the flavonoid genistein overcome class III defects, acting as channel ‘potentiators’ (Andersson et al., 2000). Potentiators promote activity of mutant CFTR once delivered to the appropriate location in the cell. F508del-CFTR is also a class III mutant because membrane-localized channels also exhibit impaired gating (McCarty et al., 2002; Yang et al., 2003). Potentiators are also useful for class V mutants because they enhance the activity of normal channels already at the cell surface.

### **1.4c. Management of CF**

Gene or protein replacement, aimed to restore the CFTR activity in the involved tissues and organs, would be the ideal treatment of CF. Presently, the prospect of gene therapy remains a hope more than a reality. Although no specific treatment has been discovered for CF yet, many treatments have been developed to alleviate symptoms, slow the progress of the disease, prevent complications and, thereby, improve the quality of life for those who suffer from this severe disorder.

Currently, CF treatment comprises respiratory physiotherapy, antibiotic therapy, nebulisation with bronchodilators and mucolytic, making the pulmonary administration as one of the most effective therapies.

### ***Chronic pulmonary treatment***

The Cystic Fibrosis Foundation guidelines support the use of inhaled hypertonic saline, chronic azithromycin, ibuprofen, and inhaled  $\beta$  agonists in specific patient populations (Flume et al., 2007).

Despite the inflammatory nature of the disease, neither oral nor inhaled corticosteroids were recommended for routine use in patients with cystic fibrosis, because of an unacceptable adverse event profile of oral corticosteroids, and absence of proof of efficacy for the inhaled medication. (Flume et al., 2007; Balfour-Lynn et al., 2006). Intravenous colistin has been found to be beneficial in the acute setting when combined with another antipseudomonal antibiotic. (Conway et al., 1997). Inhaled colistin has been used widely in Europe as a chronic, suppressive treatment, but only two trials met the Cystic Fibrosis Foundation Pulmonary Guidelines Committee's eligibility criteria for inclusion in their report. Neither of these studies showed a benefit from inhaled colistin. (Jensen et al., 1987; Hodson et al., 2002). Frequent use of oral antibiotics to reduce symptoms such as cough and sputum production is warranted in the treatment of symptomatic cystic fibrosis patients.

### ***Pulmonary exacerbations***

Treating flares of cystic fibrosis lung disease aggressively, especially with intravenous antibiotics, improves pulmonary outcomes, and presumably extends life expectancy (Johnson et al., 2003; Szaff et al., 1983; Regelman et al., 1990). Unfortunately, what constitutes a pulmonary exacerbation of cystic fibrosis is not clearly defined.

Treatment for a pulmonary exacerbation of cystic fibrosis generally includes antibiotics (oral, inhaled, or intravenous), increased use of airway clearance techniques, and improved nutrition.

Since most patients with exacerbations will have *P aeruginosa* in their airways, the usual in-hospital treatment is a combination of a  $\beta$  lactam and an aminoglycoside (Doring et al., 2000). Home-based treatment with intravenous antibiotics is feasible (Wolter et al., 1997), but might not be as effective as hospital-based treatment (Thornton et al., 2004; Nazer et al., 2006). Use of

## *Introduction*

---

combined oral and inhaled antibiotics without hospital admission might be sufficient for milder exacerbation and allows the patient's daily life to continue unimpeded.

### *Airway clearance techniques*

There are many techniques used by patients with cystic fibrosis to augment clearance of tenacious airway secretions. These methods include percussion and postural drainage, active cycle of breathing techniques, airway-oscillating devices, high-frequency chest wall oscillation devices, and autogenic drainage (ie, chest physiotherapy in which the patient does a series of respiratory huffs and coughs designed to move mucus from distal to proximal airways so it can be coughed out) (O'Sullivan et al., 2009). The active cycle of breathing technique includes relaxation and breathing control, forced excretion technique, thoracic expansion exercises, and may also include postural drainage or chest clapping.

### *Lung transplantation*

Lung transplantation is the final therapeutic option for patients with endstage lung disease.

## **1.5. RESPIRATORY DRUG DELIVERY**

Inhalation drug therapy, in which drugs are delivered to the lungs in the form of micronized droplets or solid particles, is highly desirable especially in patients with specific pulmonary diseases such as cystic fibrosis, asthma, chronic pulmonary infections or lung cancer. The principal advantages include reduced systemic side effects and higher doses of the applicable medication at the site of drug action.

Although simple inhalation devices and aerosols containing various drugs have been used since the early 19th century for the treatment of respiratory disorders, a recent interest has arisen in systemic drug delivery via the pulmonary route.

The lungs are an efficient way for drugs to reach the bloodstream due to the large surface area available for absorption ( $\sim 100 \text{ m}^2$ ), the very thin absorption membrane (0.1–0.2  $\mu\text{m}$ ) and the elevated blood flow (5 l/min), which rapidly distributes molecules throughout the body. Moreover, the lungs exhibit relatively low local metabolic activity, and unlike the oral route of drug administration, pulmonary inhalation is not subject to first pass metabolism (Adjei and Gupta, 1997).

The product formulated for the inhalatory route has to be considered one of the more complex, because it is formed by an active, appropriately formulated medicine, and a special device. The effectiveness of an inhalation therapy, especially for a drug powder formulation, is dependent on factors that are related to the patient, the device and the characteristics of the formulation.

The anatomical organization of the respiratory tract (characterized by extensive bifurcation) and aerosol characteristics of drug molecules (especially aerodynamic particle size) generally determine the reproducibility of pulmonary drug administration.

### **1.5a. Anatomy and physiology of the respiratory system**

#### ***Structure and function of the lung***

The airways provide a pathway of normally low resistance to the flow of air into and out of the lung, where the alveoli perform the essential function of gas exchange. Based on this concept, the respiratory system comprises the conducting and respiratory regions (Weibel). The conducting zone consists of the first 16 generations of airways comprised of the trachea (generation 0),

## Introduction

---

which bifurcates into the two mainstem bronchi, which further subdivide into bronchi that enter two left and three right lung lobes. The intrapulmonary bronchi continue to subdivide into progressively smaller-diameter bronchi and bronchioles (Stevens). This zone ends with terminal bronchioles which are devoid of alveoli. Accordingly, the function of the conducting zone is to move air by bulk flow into and out of the lungs during each breath. The respiratory zone consists of all structures that participate in gas exchange and begins with respiratory bronchioles containing alveoli. These bronchioles subdivide into additional respiratory bronchioles, eventually giving rise to alveolar ducts and finally to alveolar sacs. The acinus is defined as the unit comprised of a primary respiratory bronchiole, alveolar ducts and sacs (Fig. 7).

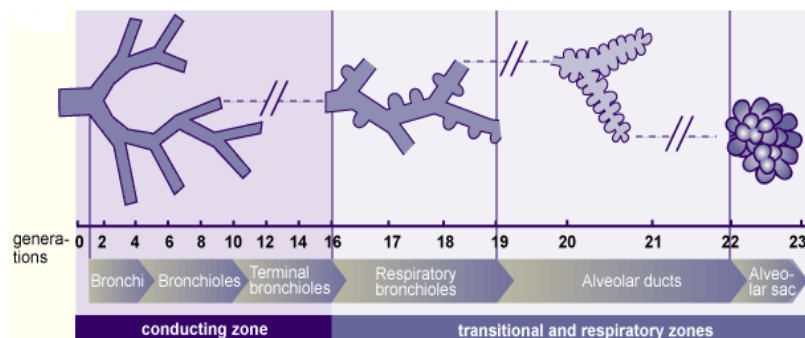


**Fig. 7.** Airways generations.

Two characteristic features of airway branching strongly influence lung function: decreasing airway caliber, and increasing airway surface area. The decrease in airway caliber (from 1.8 to 0.06 cm) along with a relatively small increase in total cross-sectional area from trachea to terminal bronchioles (from 2.5 to 180 cm<sup>2</sup>) ensures optimal conditions for bulk flow of air through the larger airways down to the terminal bronchioles. The total alveolar surface area approaches 140-160 m<sup>2</sup> in the adult human (Gehr et al., 1978). As a result of the enormous increase in surface area, bulk flow of air decreases rapidly

within the respiratory zone until movement of air within alveoli occurs entirely by diffusion.

### *Cell types lining the pulmonary airways*

The entire respiratory tract is lined with a continuous sheet of epithelial cells which vary in type and function throughout the tracheobronchial tree (Fig. 8) (Gail et al., 1983; Jeffrey, 1983).

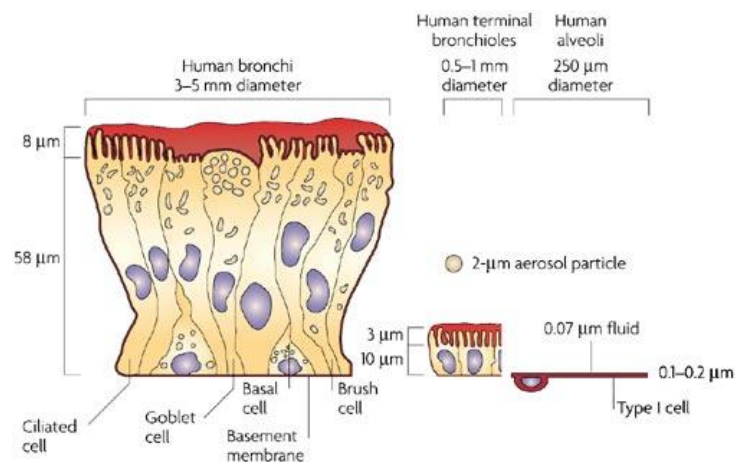


**Fig. 8.** Comparison of the lung epithelium at different sites within the lungs.

The respiratory epithelium lining the upper airways is classified as a ciliated pseudostratified columnar epithelium.

The most prominent epithelial cells are the **ciliated columnar cells**, that line the airways from the trachea through terminal respiratory bronchioles. From their apical surface protrude the cilia, that provide a sweeping motion of the mucus coat and play a crucial role in removing of small inhaled particles from the lungs.

**Goblet cells**, so named because they are shaped like a wine goblet, are columnar epithelial cells that contain membrane-bound mucous granules and secrete mucus, which helps maintain epithelial moisture and traps particulate material and pathogens moving through the airway. They are present

throughout the larger airways down to the small bronchi but are not found in bronchioles (Verdugo, 1990).

**Clara cells** are not ciliated cells that have a spheric-shaped apical surface founded among ciliated cells. They are secretory cells and prevent the luminal adhesion, particularly during expiration by secretion of a surface-active agent (a lipoprotein) (Evans et al., 1978).

The alveolar epithelium is composed of a thin, non-ciliated, non mucus-covered cell layer consisting mainly of **type I pneumocytes** and **type II pneumocytes** (Gail et al., 1983). The first ones cover about the 95% of the alveolar surface area and are squamous. It is through type I cells that gases diffuse to allow for oxygen and carbon dioxide exchange with pulmonary capillary blood. Type II cells have a more cuboidal shape and cover the remaining 5% of the alveolar surface. The main functions of type II cells are to produce pulmonary surfactant and to differentiate into type I cells after epithelial barrier injuries (Fehrenbach, 2001).

Drug uptake from the lung will be affected in rate and extent both by formulation characteristics (pH, ionic strength) and drug physicochemical properties (partition coefficient, solubility, molecular weight). In particular, macromolecules are absorbed to a degree that is inversely proportional to their molecular weight. At this level, the mucus (1-10  $\mu\text{m}$  thick) and the surfactant act as physical barriers to drug absorption, in particular in the case of peptides and protein. In addition, pulmonary enzymes deleterious for peptidic drug are present, even though at smaller concentrations than in the GI tract. Finally, the alveoli are populated by freely roaming macrophages acting as scavengers for inhaled particles, engulfing them and moving out of the respiratory tract with their payload.

### **1.5b. Inhalanda**

In general, inhalation products are liquid, solid or pressurized preparations to be aerosolized, inhaled and deposited in the lung or nose. Inhalation products are peculiar pharmaceutical dosage forms, since the product includes both the formulation and the device. Thus, the container closure system, which contains, protects and delivers the formulation, is also essential for the efficacy of the preparation together with the formulation (usually a solution, suspension or powder). These factors are the major difference with respect to other product (e.g. oral, parenteral administration), where the formulation alone constitutes the medicine able to deliver the drug dose at the desired time and site. With respect to the bioavailability of an inhaled drug, indeed the two components of the inhalation product have to be considered inseparable. Hence, any change in the formulation or in the device necessarily requires a bioequivalence assessment.

Given the physiological function of the respiratory apparatus, the safety of the inhalation of a drug product has to be considered at first. Any adverse reaction such as bronchoconstriction, irritation, cough and sneezing, that could derive from aerosol inhalation and interfere with respiration must be avoided. Moreover, the structural and functional integrity of the respiratory epithelium must be preserved from permanent damage of its protection mechanisms such as tight junctions and mucociliary clearance. Therefore, this limits the choice of excipients available for formulating an inhalation product and drives great attention to containers and packaging materials to avoid any risk of leakage, extraction and microbiological contamination.

Once safety is guaranteed, the effectiveness of the administration is expressed by the amount of drug absorbed and the rate at which absorption occurs. Bioavailability depends on several biopharmaceutical issues, some of which are common to oral and inhalation administration sites. Like oral dosage forms, solubility, dissolution rate, transit time and drug permeability across the

mucosal barrier can be limiting steps for adequate drug absorption. In contrast, formulation deposition at the proper absorption site is mostly relevant to inhalation product.

### **1.5c. The inhalation process**

The process of drug administration by inhalation can be divided in three steps, all relevant to the bioavailability of the drug (Brain et al., 1976):

- metering and delivery of the formulation,
- aerosol deposition at the absorption site,
- drug absorption (after dissolution and permeation).

For the drug to enter the respiratory tract, the proper amount of formulation has to be delivered outside the container in a form suitable for inhalation, i.e., an aerosol. An aerosol is a fine mist of spray released upon activation of an appropriate device and physically is a suspension of particles (solid or liquid) in a gas (usually air) that can be inhaled and impact into the airway walls. During aerosolization, device and formulation together play a role so that the dose is accurately metered and delivered to comply with the labeled drug dose. Metering and aerosolization do not exhaust the life of an inhalation product. Aerosol deposition at the appropriate site of the respiratory tract is required, since failure in depositing the formulation will result in poor drug absorption. Aerosol particles enter the airways with inspiration and fly following the air stream generated by the inspiration act, until they deposit onto the respiratory wall. Aerosol deposition occurs by various mechanism, depending on two major characteristics of inhaled aerosol, i.e. particle size (and shape) and velocity. Besides the differences in deposition due to patient variability, the most important mechanisms of particle deposition are: inertial impaction, sedimentation, diffusion, interception and electrostatic attraction (Fig. 9) (You & Diu, 1983).

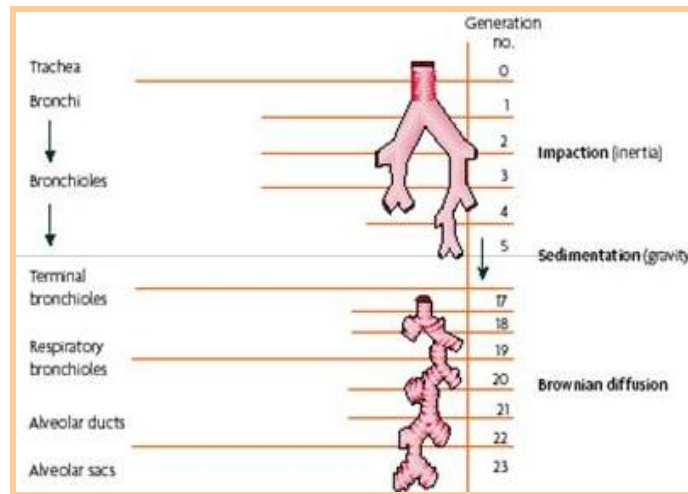


**Fig. 9.** Mechanisms of particle deposition at different sites within the lungs.

Inertial impaction is the dominant deposition mechanism for particles larger than  $1\ \mu\text{m}$  in the upper tracheobronchial regions. A particle with large momentum (large size or velocity or both) may be unable to change direction with the inspired air as it passes the bifurcations of the airways, and instead it will collide with the airway walls. Because impaction depends on the momentum of the particle, large or dense particles moving at a high velocity will show greater impaction (Heyder et al., 1986).

Gravitational sedimentation is an important mechanism for deposition of particles bigger than  $0.5\ \mu\text{m}$  and smaller than  $5\ \mu\text{m}$  in the small conducting airways (bronchioles and alveolar region) where the air velocity is very low. Deposition due to gravity increases with enlarging particle size and longer residence times but decreases as the breathing rate increases (Martonen and Yang, 1996).

Submicron-sized particles (especially those smaller than  $0.5\ \mu\text{m}$ ) acquire a random motion caused by the impact of surrounding air molecules. This Brownian motion may then result in particle deposition by diffusion, especially in small airways and alveoli, where bulk airflow is very low.

Therefore, to reach the lower respiratory tract and optimize pulmonary drug deposition, aerosols need to have aerodynamic diameters between 0.5 and 5  $\mu\text{m}$  (Zanen et al., 1996). In other words, particles larger than 5  $\mu\text{m}$  usually deposit in the oropharynx from which they are easily cleared. In contrast, particles smaller than 0.5  $\mu\text{m}$  may not deposit at all because they move by Brownian motion and settle very slowly.

Interception is likely to be the most effective deposition mechanism for aggregates and fibers. For such particles, deposition may occur when a particle contacts an airway wall, even though its centre of mass might remain on a fluid streamline (Darquenne, 2004; Yeh et al., 1976; Gerrity et al., 1983).

Electrostatic charges enhance deposition by increasing attractive forces to airway surfaces, in particular for fresh generated particles.

#### **1.5d. Factors affecting aerosol deposition**

Since geometry appears so relevant to the behavior of the inhaled particles, ultimately determining the respirability of an inhalation product, the concept of **aerodynamic diameter** has been introduced to measure the size of the inhaled particle. The aerodynamic diameter  $d_{ae}$  is defined as the diameter of a sphere of unitary density ( $\rho_0$ ) that has the same sedimentation velocity as the particle in consideration (De Boer et al., 2002):

$$d_{ae} = d \left( \frac{\rho}{\rho_0} \right)^{1/2} \quad \text{Eq. (1)}$$

where  $d$  is the actual diameter of the sphere,  $\rho_0$  and  $\rho$  are the unit and particle densities, respectively.

This is an ideal situation, since it considers only spherical particles. If the particle is not spherical, a correction factor called dynamic shape factor is applied to account for the effect of shape on particle motion. The dynamic shape factor  $\chi$  takes into account the non-sphericity of the particle: it is equal

to 1 for a sphere and greater than 1 for irregular particles. The dynamic shape factor is the ratio of the actual resistance force experienced by a non-spherical falling particle to the resistance force experienced by a sphere having the same volume (Hinds, 1999). Hence, when the inhaled particle is not spherical, equation 1 becomes:

$$d_{ae} = d_v \left( \frac{\rho}{\rho_0} \chi \right)^{1/2} \quad \text{Eq. (2)}$$

where  $d_v$  is the equivalent volume diameter.

Consequently, the aerodynamic behavior and respirability of a particle depend on its aerodynamic diameter, which is function of both particle geometry and density.

Good distribution throughout the lung requires particles with an aerodynamic diameter between 1 and 5  $\mu\text{m}$ , and thus most inhaled products are formulated with a high proportion of drug in this size range (Chrystyn, 1997). In order to target the alveolar region specifically, the aerosol droplets or solid particles diameter should not be higher than 3  $\mu\text{m}$ . Particles with diameters that are greater than 5  $\mu\text{m}$  are deposited in the oropharynx, whereas smaller particles (<1  $\mu\text{m}$ ) are exhaled during normal tidal breathing.

Only if the formulation deposited at the appropriate site of respiratory tract, the drug acts locally or can be absorbed and pass into the systemic circulation. In pulmonary drug delivery, the target site for an effective systemic administration is the deeper lung, namely the alveoli region, where the mucosa is thin and the vascularization highly developed. Solubility, dissolution rate and permeability are factors that can hinder drug absorption at this level.

### **1.5e. Pulmonary delivery devices**

Pulmonary drug delivery aims to bring the drug to the lung region, where the drug can be promptly absorbed. This is obtained by introducing (i.e., inhaling)

the drug formulation through the mouth into the respiratory tract using a suitable device. A good delivery device has to generate an aerosol of suitable size, ideally in the range of 0.5–5  $\mu\text{m}$ , and provide reproducible drug dosing. It must also protect the physical and chemical stability of the drug formulation. Moreover, the ideal inhalation system must be a simple, convenient, inexpensive and portable device.

Three types of devices are used to deliver an aerosolized drug to the lung: nebulizers, pressurized metered-dose inhalers (MDIs) and dry powder inhalers (DPIs), each class with its unique strengths and weaknesses. This classification is based on the physical states of dispersed-phase and continuous medium, and within each class further differentiation is based on metering, means of dispersion, or design.

**Nebulizers** have been the first devices developed for inhalation therapy market. They aerosolize aqueous solutions or suspensions containing the drug by means of a source of energy, which can be an air jet, a pump or ultrasounds. Then, the aerosol droplets enter the lungs over multiple breaths, thing that prolongs the duration of the treatment. Today nebulizers have become niche products, primarily for pediatric, geriatric and emergency department use (Grossman, 1994). Nebulizers have numerous disadvantages including delivery inefficiency, drug wastage, nonportability, poor reproducibility, great variability and high cost. Moreover, aerosol administration via nebulization is time consuming; approximately 30 min if set-up, drug administration and cleaning are taken into account. Thus, further improvement in aerosol delivery systems with greater efficiency and portability and shorter administration time could improve patient quality of life and compliance.

Therefore, **Pressurized Metered Dose Inhalers** (pMDIs) have been developed and since the 1950s they have been the mainstay of asthma inhalation therapy. In pMDIs the drug is dissolved or suspended with a

propellant in a pressurized dispenser and is aerosolized through an atomization nozzle using a metering valve and an actuator (Newman, 2005).

The most widely used propellants have always been the chlorofluorocarbons (CFCs), because of their non-toxicity, inertness and high vapor pressure. The medical application of CFC as propellants has been phased out, according to the 1987 Montreal Protocol on Substances that Deplete the Ozone Layer (UNEP, 1987). Gradually, the propellant CFC was substituted by hydrofluoroalkanes (HFA), given its safety profile (Emmen et al., 2000). However, this substitution was not straightforward since only a small fraction of the drug escaping the inhaler penetrates the patient's lungs due to a combination of high particle exit velocity and poor coordination between actuation and inhalation. The deposition of aerosolized drugs in the mouth and the oropharyngeal regions varies considerably according to the application technique, but losses using the pressurized devices are routinely greater than 70% and can exceed 90%. Particle losses that occur proximally to the lung are a long-documented problem that continues to compromise the effectiveness of current aerosol therapy protocols.

Given the problems encountered with nebulizers, alternative simple and small inhalers that do not use propellants have been more recently developed.

**Dry Powder Inhalers (DPIs)**, as the name suggests, deliver the drug to the pulmonary system as a dry powder aerosol. They contain a micronized drug substance with or without carrier. DPIs were designed to eliminate the coordination difficulties associated with pressurized MDIs. Patient coordination is not required for drug administration, because most DPIs are breath actuated (a respirable cloud is produced in response to patient inhalation). Nevertheless, one of the major advantages of DPIs products is that they are propellant-free and are thus environmentally friendly. Moreover, DPIs are preferred for their stability and processing since they are typically formulated as one phase, solid-particle blends. DPIs are a widely accepted

## Introduction

---

inhaled delivery dosage form, particularly in Europe where they are currently used by an estimated 40% of patients to treat asthma and chronic obstructive pulmonary disease (Atkins, 2005).

Today, there are essentially two types of DPIs:

- single dose or unit-dose devices, in which the drug is packaged in individual doses (capsules);
- multi-unit and multi-dose devices, that contain multiple doses in a foil-foil blister or a reservoir of drug from which the doses are metered (Fig. 10).



**Fig. 10.** Photographs of some currently available DPI devices.

A patient's DPI dose is dependent on four interrelated factors (Atkins, 2005): the physical properties of the drug formulation, particularly powder flow, particle size, shape and surface properties and drug carrier interaction; the performance of the inhaler device, including aerosol generation and delivery; correct inhalation technique for deposition in the lungs; and the inspiratory flow rate. Therefore, a balance among the design of an inhaler device, drug formulation and the inspiratory flow rate of the patient is required.

### 1.5f. The challenge of Excipients for DPI

The primary function of the lungs is respiration. To fulfill this purpose, the lungs have a large surface area and thin membranes. Many compounds that

could enhance drug delivery outcomes also have the potential to irritate or injure the lungs. (Telko and Hickey, 2005).

In general, excipients are used to enhance the physical or chemical stability of the drug, mechanical and/or bio-pharmaceutical properties such as dissolution and permeation. Excipients are inactive ingredients that are intentionally added to therapeutic products but not intended for exerting therapeutic effects at the established dosage, although they may act to improve product delivery or bioavailability. The Food and Drug Administration (FDA, 2009) favors the use of commercially established excipients as well as “generally recognized as safe” (GRAS) substances. It should be noted that the current excipients approved for respiratory drug delivery are very limited in number (Pilcer & Amighi, 2010). Table 1 presents a summary of excipients already approved for pulmonary delivery or presented as interesting additives for DPI formulations. The array of potential excipients is restricted to compounds that are biocompatible or endogenous to the lung and can easily be metabolized or cleared (Telko and Hickey, 2005). If particles deposit throughout the conducting airways, they are removed by mucociliary clearance. Particles will be eliminated in 24 - 48 h according to the number of cilia and their beat frequency. In the bronchioles and alveoli, particles will be cleared by direct absorption through the epithelial cells or uptake by the alveolar macrophages (Dalby et al., 1996).

## Introduction

**Table 1**

List of accepted or interesting additives for DPI formulations. (Pilcer et al., 2010).

Excipients	Description	Status
Sugars Lactose Glucose Mannitol Trehalose	Coarse/fine carrier	Approved and commonly used Approved (Bronchodual®) Approved (Exubera®) Promising alternative (Mao and Blair,2004)
Hydrophobic additives Mg stearate	Protection for drug moisture	Approved (SkyeProtect™)
Lipids DPPC, DSPC, DMPC, cholesterol	Used in liposomes, matrix, coating	Biocompatible and biodegradable, very interesting excipients (Myers et al., 1993; Sebti and Amighi, 2006; Chono et al.,2009)
Amino acids Leucine, trileucine	Improved aerosol efficiency	Endogenous substance but no data on lung toxicity (Rabbani and Seville, 2004; Lechuga-Ballesteros et al., 2008)
Surfactants Poloxamer	Production of light and porous particles	May not be pro-inflammatory at low dose (Steckel and Brandes, 2004; Vaughn et al., 2007)
Bile salts		Endogenous substances, May be accepted but at low dose (2–5%, w/w) (Yamamoto et al., 1997; Johannson et al., 2002; Pilcer et al., 2009b)
Absorption enhancers Hydroxypropylated-β-CD, natural γ-CD	Absorption for proteins & peptides	Promising results (Hussain et al., 2004; Salem et al., 2009)
Bile salts		Promising results but toxic in chronic use (Yamamoto et al., 1997; Johannson et al., 2002)
Chitosan, trimethylchitosan		Pro-inflammatory effect observed (Huang et al., 2005; Grenha et al., 2008)
Biodegradable polymers PLGA	Used in sustained release formulations	Immunogenicity effect observed (Zeng et al., 1995; Dailey et al., 2006)

# **RESULTS AND DISCUSSION**



**SECTION A**

***DESIGN AND DEVELOPMENT OF A DPI OF NARINGIN  
TO TREAT INTRINSIC INFLAMMATION IN CF PATIENTS***

**Based on the article:** L. Prota, A. Santoro, M. Bifulco, R.P. Aquino, T. Mencherini, P. Russo. “Leucine enhances aerosol performance of Naringin dry powder and its activity on cystic fibrosis airway epithelial cells”. *International Journal of Pharmaceutics*. **2011**, 412, 8 – 19.



## 2A.1 BACKGROUND, RATIONALE OF THE SELECTION OF NARINGIN, AIMS

In the airway epithelium of patients with cystic fibrosis, the combination of excessive absorption of sodium and defective regulation of the secretory chloride channel of the apical membrane leads to the dehydration of airway secretions. These ion-transport defects contribute to the abnormal rheologic feature and poor clearance of airway secretions, obstruction of airflow and chronic bacterial infection of the airways. Therefore, current CF therapy is directed to reduce the abnormal inflammation and abnormal mucus secretion, in order to delay the onset of CF lung tissue damage (Kieninger and Regamey, 2010; Ross et al., 2009). Only a few anti-inflammatory drugs are available for CF treatments, mainly oral corticosteroids and ibuprofen. In addition, high doses of N-acetylcysteine, a well known glutathione prodrug administered orally, have shown the ability to counter the redox imbalance in CF (Jacquot et al., 2008). However, the above drugs have limited beneficial effects in presence of considerable side effects. Among natural polyphenols such as flavonoids, Naringin (N) (Fig. 11) extracted from grapefruits has shown anti-inflammatory, antioxidant and anticarcinogenic effects (Limasset et al., 1993).

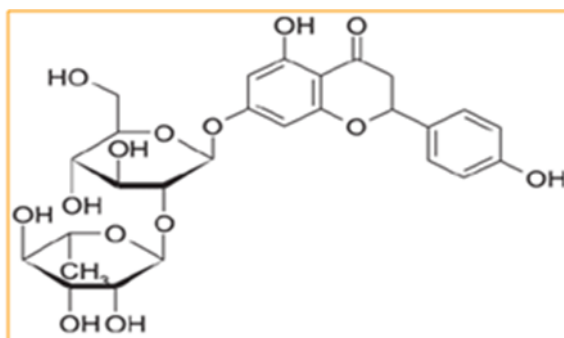


**Fig. 11.** Naringin 4,5,7-trihydroxyflavanone 7-rhamnoglucosyde.

In addition, recent studies have reported that flavonoids may act as CFTR direct activators, stimulating transepithelial chloride transport (Fig. 12) (Azbell et al., 2010; Pyle et al., 2009; Springsteel et al., 2003; Virgin et al., 2010; Wegrzyn et al., 2010).

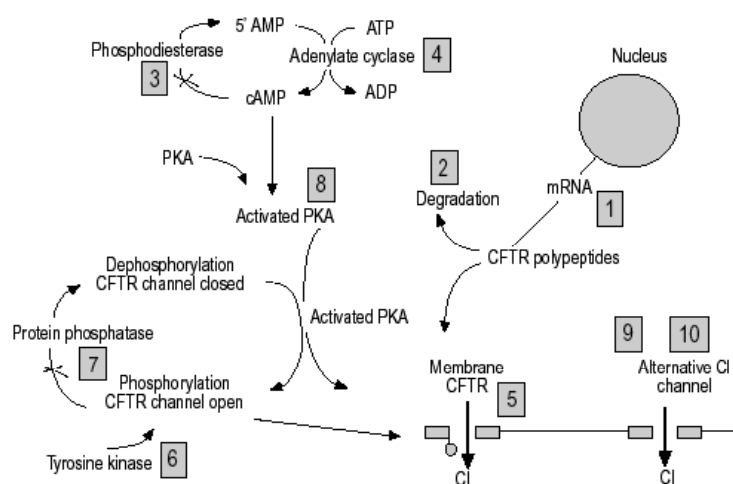


Fig. 12. CFTR activation by flavonoids.

Genistein, a soy-derived isoflavone, has been found to directly activate *in vitro* both wild-type and mutant CFTR and can overcome the affected ATP binding to G551D. Recent data indicated that the most likely explanation for the stimulatory effect of genistein was through direct binding to a nucleotide-binding domain (NBD) of phosphorylated CFTR. (Kerem, 2005; Kerem, 2006).

Genistein is also effective in human nasal epithelia – particularly on G551D-CFTR – but unfortunately, at higher concentrations, it inhibits ion transport (al Nakkash et al., 2001). Genistein may inhibit CFTR Cl<sup>-</sup> channels in two ways: first, it may interact with NBD1 to strongly inhibit channel opening; second, it may bind within the CFTR pore to weakly block Cl<sup>-</sup> permeation. (Becq et al., 2011). Moderate concentrations of genistein augmented CFTR maturation and

increased its localization to the cell surface (Schmidt et al., 2008). The encouraging results of pre-clinical studies with genistein provide a basis for clinical trials with CF patients. In fact, the Phase II clinical trial with a combined treatment (4- phenylbutyrate and genistein) of CF patients with the  $\Delta F508$  mutation has been started (Clunes et al., 2008). Further studies employing flavonoids such as apigenin, kaempferol and quercetin showed dose-dependent activation of cystic fibrosis trans membrane conductance regulator-mediated Cl currents in human airway epithelium. Flavonoid intake from a normal diet can result in a blood concentration of 1–2  $\mu\text{M}$  in humans and appear to be well tolerated thus far in human clinical trials (Lim et al., 2004).

In search of more effective activators of G551D-CFTR (Springsteel et al., 2003), some investigators have begun to examine the relationship between the chemical structure of flavonoids and their effects on CFTR Cl<sup>-</sup> channels. This study served to identify the pharmacophore portion of the skeletons and the molecular basis for interaction with the NBD (Fig. 13).

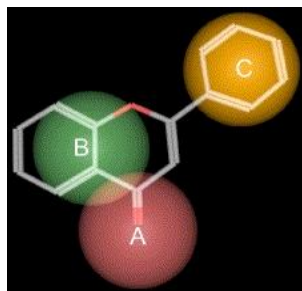


**Fig. 13.** Identified pharmacophore portions of flavonoids in CFTR activation (Springsteel et al., 2003).

Polyphenols with different structure such as pyrogallol has shown anti-inflammatory properties in CF bronchial epithelial cells exposed to *Pseudomonas aeruginosa* (Nicolis et al., 2008).

In the frame of the present PhD project, these findings suggest to design an inhalation Naringin form for delivering the drug directly to the site of action. Inhalation products (Chuchalin et al., 2009; Heijerman et al., 2009; Parlati et al., 2009) seem to be an alternative to oral and parenteral drug administration for long-term CF treatment. Among inhalation delivery systems, DPIs (dry powder inhalers) are versatile therapeutic systems, dispensing a metered quantity of powder in a stream of air, drawn through the device by the patient own inspiration in absence of propellants. In a previous study (Sansone et al., 2009) we reported that the N process *via* spray-drying, as commercial crystalline raw material, was able to produce amorphous material, showing improved aerodynamic properties with respect to the raw material. Such amorphous micronized form did not show completely satisfying pulmonary deposition profiles, probably due to the particles tendency to form aggregates. Several strategies (Pilcer and Amighi, 2010), including the use of coarse carrier or excipient systems, have been suggested to improve flowability and, consequently, aerosol efficiency of dry powders. However, current excipients approved for pulmonary drug delivery are limited to few sugars (lactose, mannitol and glucose) and an hydrophobic additive (magnesium stearate) (Pilcer and Amighi, 2010), due to potential toxicity for lung of other ingredients. As a matter of fact, safe and endogenous amino acids (AAs) co-spray-dried with few drugs showed the ability to modulate drug aerosolization behaviour (Chew et al., 2005a; Lucas et al., 1999; Najafabadi et al., 2004). To support AAs pulmonary safety, a formulation of Aztreonam and lysine (Cayston®, powder for instant solution and inhalation) has been recently approved by FDA for the management of CF patients.

From a pharmaceutical point of view, manufacture of powders for inhalation with aerodynamic diameter in the range of 0.5–5  $\mu\text{m}$  is a technical challenge because it requires production of particles reduced in size and respirable, while, as well known, small particles undergo strong cohesive forces, resulting in increased adhesion and poor flowability. A way to improve flow properties of micronized powders is through the addition of excipients, but those currently approved (mainly sugars) for pulmonary administration are very limited in number (Pilcer and Amighi, 2010). Thus, there is a special need for the development and test of other potentially promising excipients for DPI products able to increase drug deposition in the lung, acting on the powder flow, particle size, geometry and/or surface properties, and in the same time which are not toxic for airways.

Several features appeared to be critical in the design of inhalation form of Naringin. First, the manufacturing of dry powder with improved aerodynamic properties and satisfying pulmonary deposition profiles, as well as optimizing the system of powder micronization and aerosolizing, was required for effective delivery of the drug to the airway surfaces. Second, because few are materials accepted as pulmonary excipient, we proposed a series of AA (arginine, histidine, lysine, leucine, proline and threonine) on the basis of their endogenous source and safety profiles for use in human pharmaceuticals. In addition some AA, such as leucine and trileucine, may be able to improve powder dispersibility and flowability. Third, the outcome of this study on aerosolized polyphenol involved its efficacy in reducing CF intrinsic inflammation status on CF airways epithelial cell model.

With these aims, we selected spray-drying technology to transform a liquid feed containing N and AAs to produce N/AA powders. Morphology and surface, size distribution, density, dissolution rate of a number of N-AAs

powders were examined. Their aerodynamic properties were studied using Turbospin® as device with the objective to correlate the feed composition (ethanol/water and AA/drug ratios) and AA nature to aerodynamic behaviour. Finally, the potential anti-inflammatory activity of N and its formulations was investigated in CF and non-CF airways epithelial cells.

Spray drying has been used as atomizing technology because it is a one-step process widely used in the pharmaceutical industry that converts a liquid feed to a dried particulate form. The feed can be a solution, a coarse or fine suspension or a colloidal dispersion (e.g., emulsion, liposome, etc.). The fluid is first atomized to a spray form that is put immediately into thermal contact with a hot gas, resulting in the rapid evaporation of the droplets to form dried solid particles. The dried particles are then separated from the gas by means of a cyclone, electrostatic precipitator or bag filter. The three fundamental operations of the spray drying process are atomization, drying and separation. Atomization is the process whereby a liquid is broken up into a collection of droplets. Once the liquid is atomized, droplets dry to solid particles through intimate contact with heated gas in the drying chamber. After the spray-dried powder is formed, it must be separated from the circulating gas medium through a cyclone.

The main components of the spray dryer are (Fig. 14):

- heating system
- nozzle atomizer
- drying room
- aspirator
- cyclone

- container for collecting finished product.

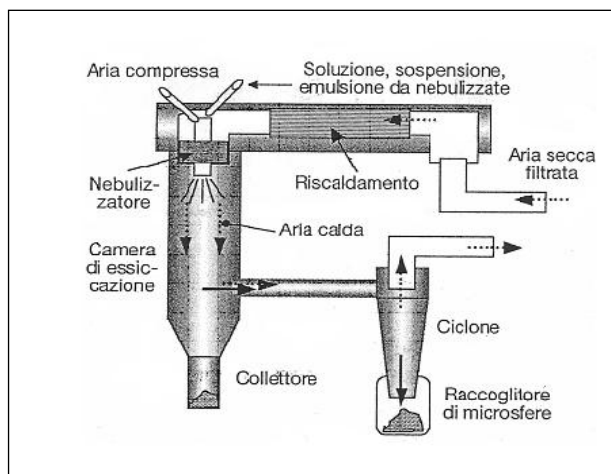


**Fig. 14.** Schematic representation of the spray dryer equipment.

The principal advantages of spray drying to obtain a powder suitable for pulmonary drug delivery are the ability to manipulate and control a variety of parameters such as solvent composition, solute concentration, solution and gas feed rate, temperature and relative humidity, droplet size, etc. This allows optimization of particle characteristics such as size, size distribution, shape, morphology and density, in addition to macroscopic powder properties such as bulk density, flowability and dispersibility (Sacchetti and Van Oort, 1996).

## 2A.2 NARINGIN DRY-POWDERS PRODUCTION AND CHARACTERIZATION

Co-spray-drying process of N with arginine, lysine (positively charged side chains) or threonine (polar neutral side chain), which display an isoelectric point (IP) far from the neutral pH of the feed solutions (Fig. 15), were performed in first place. The obtained powders were not respirable and

characterized by high particle size ( $d_{50} > 5 \mu\text{m}$ ) and high cohesiveness, resulting in low yield of the spray-drying process (<40%). Unsatisfying pulmonary distribution profiles upon activation of the device were also obtained (data not shown).

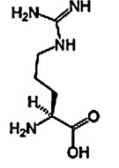
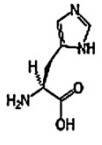
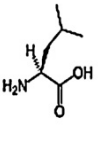
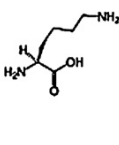
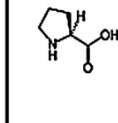
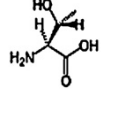
aa	Arginine	Histidine	Leucine	Lysine	Proline	Threonine
						
<b>IP</b>	10.76	7.60	6.01	9.60	6.30	5.60
<b>Water solubility (g/L)</b>	148.7	38.2	24	300	1500	200

Fig. 15. Isoelectric point (IP) and water solubility of AAs selected as pulmonary excipients.

Using leucine, histidine and proline (AAs with an IP next to 7), very interesting results were obtained in terms of flowability and aerodynamic performance determined by both SSGI and ACI. The powders were characterized in terms of particle size, morphology, bulk and tapped density, thermal properties and immediate solubility. Table 2 comprises all manufactured powders.

**Table 2.**

Formulation parameters and responses of N and N/AA dry powders.

Code #	% AA <sup>a</sup>	Feed solution <sup>b</sup>	Spray yield %	d <sub>50</sub> μm and () Span	Code #	% AA <sup>a</sup>	Feed solution <sup>b</sup>	Spray yield %	d <sub>50</sub> μm and () Span
N-1	-	3:7	59.4	5.20 (1.56)	N-pro 3	5	4:6	60.6	2.93 (2.05)
N-2	-	4:6	61.2	4.10 (1.68)	N-pro 4	10	4:6	67.8	2.99 (2.08)
N-3	-	1:1	55.9	6.99 (1.71)	N-pro 5	5	1:1	66.7	2.74 (1.77)
N-leu 1	5	3:7	60.7	3.31 (1.68)	N-pro 6	10	1:1	64.7	5.34 (1.93)
N-leu 2	10	3:7	54.4	2.88 (1.47)	N-his 1	5	3:7	51.3	2.99 (1.80)
N-leu 3	5	4:6	68.5	3.02 (1.70)	N-his 2	10	3:7	50.6	2.00 (1.85)
N-leu 4	10	4:6	60.6	2.82 (1.44)	N-his 3	5	4:6	62.6	4.21 (1.83)
N-leu 5	5	1:1	69.0	2.80 (1.74)	N-his 4	10	4:6	64.1	4.12 (1.92)
N-leu 6	10	1:1	63.2	2.75 (1.64)	N-his 5	5	1:1	72.0	4.44 (1.72)
N-pro 1	5	3:7	69.0	2.78 (1.73)	N-his 6	10	1:1	71.5	3.72 (1.77)
N-pro 2	10	3:7	60.0	3.42 (1.82)					

<sup>a</sup> Relative amount of AA by % in weight compared to the total amount of dry substance (2% w/v); <sup>b</sup> EtOH/water v/v content in the feed.

The presence of the AA in the feed formulation influenced the particle size distribution (Table 2) as well as the powder density and morphology, although the extent of these variations depends on the considered AA. The majority of the N-leu and N-pro powders showed a d<sub>50</sub> within a range of 2.75–3.42 μm, very lower than powders manufactured without AAs (d<sub>50</sub> 4.10–6.99 μm). Only formulation N-pro 6 has a diameter slightly above 5 μm. Increase in the ethanol ratio in the feed from 3:7 to 1:1 generally resulted in a higher process yield, ranging from about 50–60 up to 70%. Interestingly, for N-his the higher was the ethanol content, the larger were both the diameter and process yield (Table 2).

As showed by thermograms of N-leu 1 (Fig. 16c) reported as an example, DSC analyses indicated that N-AA powders produced by spray drying were amorphous materials. Spray-drying process causes the loss of crystalline habitus of both N-raw and Leu-raw as evidenced by the absence of the

endotherms corresponding to N crystal melting point at 247 °C (Fig. 16b) and Leu crystal melting point at 275 °C in DSC thermograms (Fig. 16a).

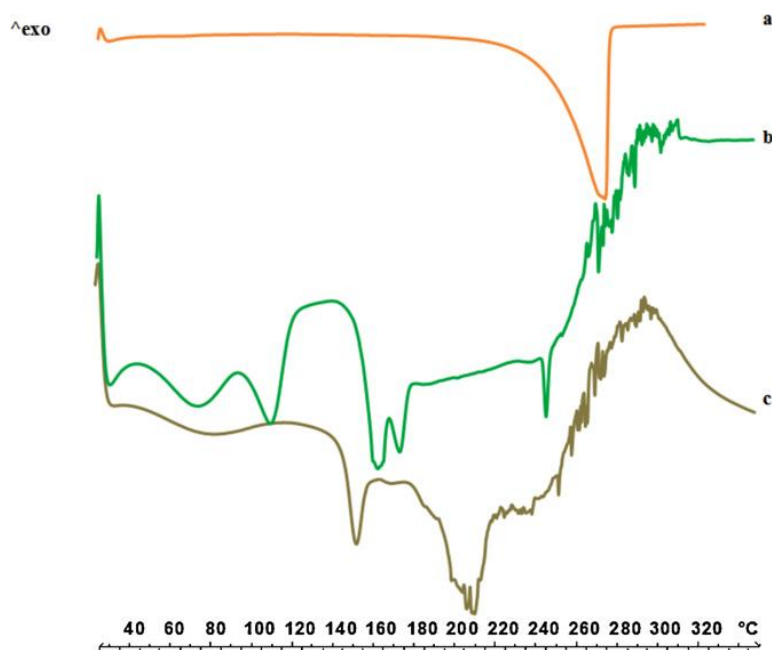


**Fig. 16.** Differential scanning calorimetry thermograms of leucine raw material (a), Naringin raw material (b) and N-leu 1 (c).

DSC results were confirmed by X-ray assessments, showing no crystalline diffractograms in N-AA powders. As an example, X-ray patterns of crystalline N (Fig. 17a) and Leu (Fig. 17b) as raw materials were reported in comparison with X-ray pattern of N-leu 1 (Fig. 17c).

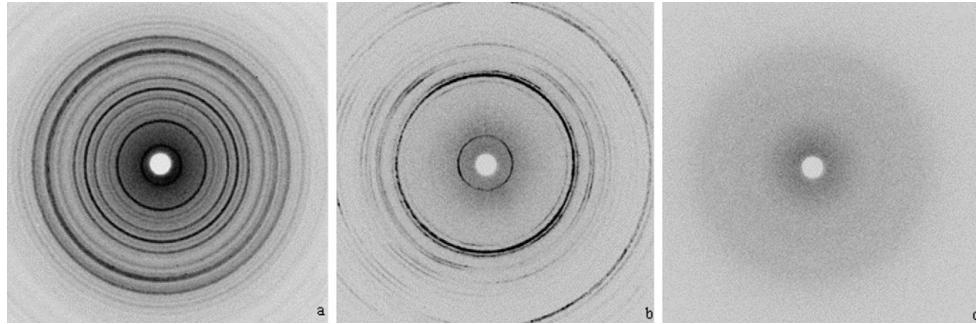


**Fig. 17.** X-ray patterns of Naringin raw material (a), leucine raw material (b) and N-leu 1 (c).

It is evident from Fig. 18 that powders containing AA possessed higher tapped density than those formulated without excipient. The density increased with the increase of both alcohol and AA content in the processed feeds. N-10% AA (Fig. 18b) powders showed the highest tapped density values and are expected to have the worst aerosolization properties.

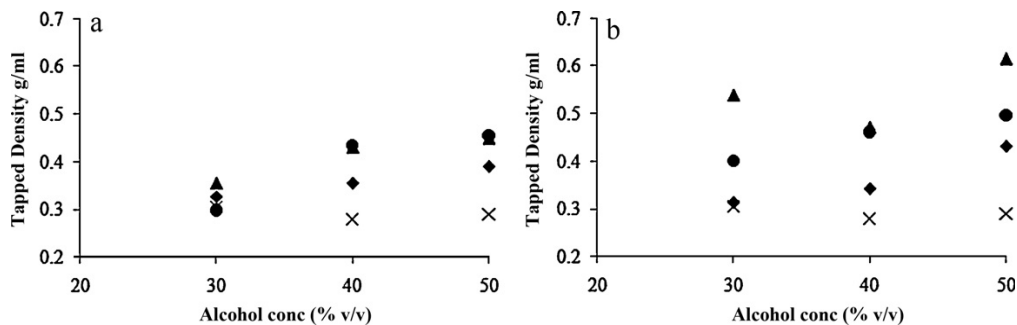


**Fig. 18.** Tapped density versus alcohol content in the liquid feed of RawN (X) and N-AA: (▲) leucine; (◆) proline, (●) histidine; a) 5% w/w AA; b) 10% w/w AA.

Microscopy observation revealed that the particles morphology was once again affected by the nature and percentage of AA as well as by ethanol content in the feed. Samples spray-dried from 3:7 ethanol/water feed and without AA, appeared as small particles, spherical in shape or very slightly corrugated, and their SEM micrographs showed widespread aggregation (Fig.

19a). By contrast, samples produced with 5% AA displayed well separated particles with corrugated, raisin-like surfaces (Fig. 19b), beneficial for particles intended for inhalation. In fact, previous reports suggested that improvement of the respirable fraction may be obtained not only by lowering the aerodynamic diameter, but also reducing interparticulate cohesion (Chew and Chan, 2001; Chew et al., 2005b). Corrugated particles might also be more appropriate for dissolution in the lung fluid due to a larger surface area. When the ethanol/water ratio increased (from 3:7 to 1:1), particles with smoother surface were observed (Fig. 19c and d). Considering that increasing the ethanol content in the feed results in higher solubility of N but lower solubility of the AA, we speculate that AA may precipitate from feeds on the particle surface, shaping smoother particles (Fig. 19d, N-his).

As it is well known, the spray drying process consists of spraying a liquid solution (in this case N/AA in ethanol/water) through a nozzle to obtain liquid droplets; then, these droplets are dried by solvent evaporation to form microparticles. As previously reported (Sansone et al., 2009), N has higher solubility in less polar solvents than in water (e.g. 0.11 g/100 g in water vs 1.1 g/100 g in ethanol). On the contrary, the solubility of AAs in water is higher than in alcohols (e.g. histidine 4.30 g/100 g in water vs 0.76 g/100 g in water/ethanol 1/1, v/v) (Nozaki and Tanford, 1971; Peijun et al., 2009).

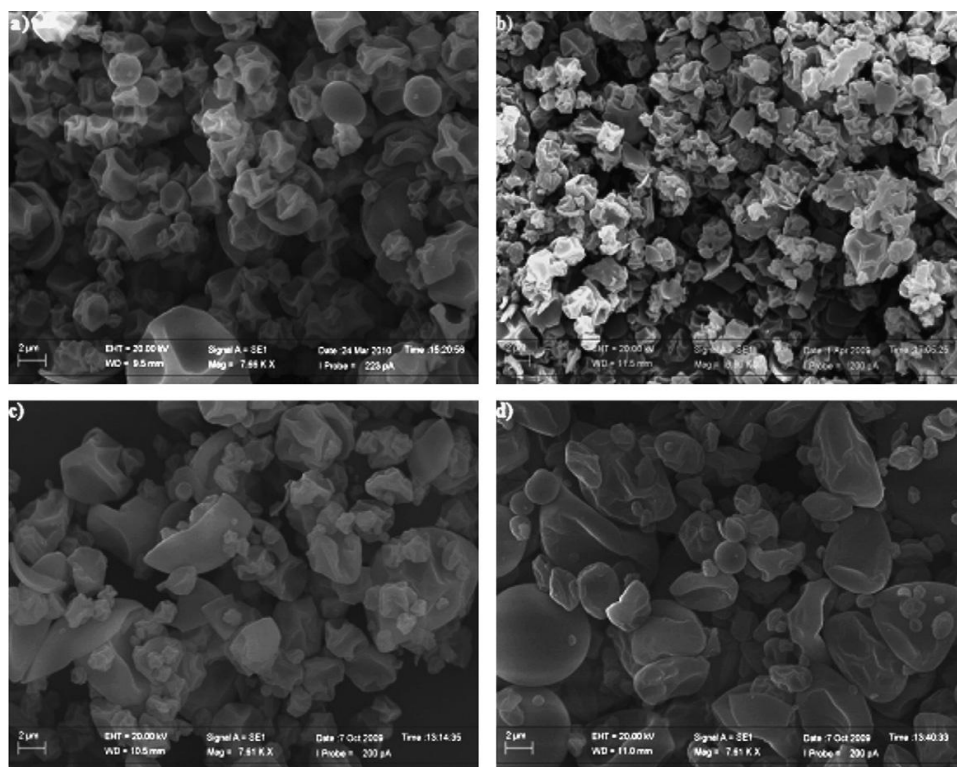


**Fig. 19.** SEM picture of (a) N-1 (ethanol/water ratio 3:7 N 2%, w/v) and N-5% histidine; (b) N-his 1 (ethanol/water ratio 3:7); (c) N-his 3 (ethanol/water ratio 4:6); (d) N-his 5 (ethanol/water ratio 1:1).

With this in mind, the immediate solubility of the batches was evaluated. Dissolution profiles of N-5% his powders, dried from 30, 40 or 50% (v/v) ethanol feeds, are reported as an example in Fig. 20.

An evident improvement of the immediate solubility was obtained for all N-AA powders with respect to crystalline rawN. In particular, we observed the maximum enhancement in powder immediate solubility for batches N-his 5 (Fig. 20) and N-leu 5 (data not shown). These microparticles were prepared from feeds with the highest ethanol content (1:1 (v/v) ethanol/water) and showed the highest AA accumulation on the particle shell.

In addition, as previously reported for rawN spray-dried powders (Sansone et al., 2009), also N-AA microparticles rapidly decrease their solubility in few minutes of exposure to solvent, reaching a nearly constant value after 30 min (Fig. 20).

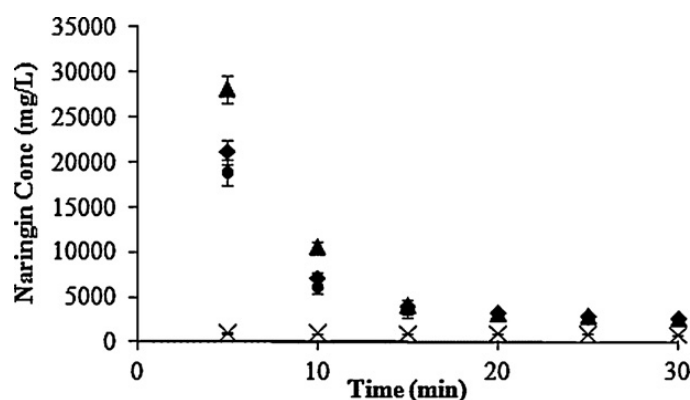


**Fig. 20.** Aqueous solubility at 37 °C of rawN (X) and N-5% histidine; (◆) N-his 1 (ethanol/water ratio 3:7; (●) N-his 3 (ethanol/water ratio 4:6); (▲) N-his 5 (ethanol/water ratio 1:1).

Similar profiles were observed for all the batches produced (data not shown). This behaviour may be justified by a rapid conversion of the amorphous spray-dried material to a crystalline status which is characterized by lower solubility (Hancock and Parks, 2000).

### 2A.3 AERODYNAMIC BEHAVIOUR OF NARINGIN DRY POWDERS

The *in vitro* aerosol deposition data are reported in Tables 3 and 4. The behaviour of N/AA powders was compared to that of rawN spray-dried powders (N-1, N-2, and N-3), used as controls. Results indicated that the AAs

generally improved the aerodynamic behaviour, in terms of fine particle fraction (FPF).

In SSGI experiments (Table 3), the mass of powder delivered from Turbospin® (emitted dose, ED) was from 81.6 to 92.5%, with the exception of N-leu 2 (73%). The last result indicates that more than 27% of powder was retained in the capsule and/or in the inhaler device. The reason for such lower emission (73%) may be found in the poor flow properties of the powder. Moreover, high cohesiveness of N-leu 2 was confirmed by low process yield (54.4%) and high tapped density.

**Table 3.**

Aerodynamic properties of N and N-AA dry powders after single stage glass impinger deposition experiments. All data are shown as mean  $\pm$ SD of three experiments.

Code #	ED %	FPF (%)	Code #	ED%	FPF (%)
N-1	92.7 $\pm$ 0.0	44.5 $\pm$ 1.5	N-pro 3	88.0 $\pm$ 9.7	43.3 $\pm$ 1.7
N-2	84.2 $\pm$ 6.5	40.9 $\pm$ 1.4	N-pro 4	86.6 $\pm$ 7.2	46.1 $\pm$ 1.3**
N-3	83.9 $\pm$ 2.4	38.5 $\pm$ 0.1	N-pro 5	85.7 $\pm$ 2.6	38.2 $\pm$ 3.9
N-leu 1	89.5 $\pm$ 4.8	51.3 $\pm$ 1.6**	N-pro 6	87.4 $\pm$ 3.5	34.1 $\pm$ 2.1*
N-leu 2	73.6 $\pm$ 7.5	40.2 $\pm$ 1.5*	N-his 1	91.8 $\pm$ 4.7	49.2 $\pm$ 1.1*
N-leu 3	89.0 $\pm$ 5.5	52.0 $\pm$ 1.1**	N-his 2	85.9 $\pm$ 8.3	47.1 $\pm$ 2.0
N-leu 4	83.3 $\pm$ 4.9	50.9 $\pm$ 3.9*	N-his 3	92.5 $\pm$ 3.0	41.5 $\pm$ 3.1
N-leu 5	81.6 $\pm$ 7.4	45.3 $\pm$ 1.1**	N-his 4	88.8 $\pm$ 1.2	34.4 $\pm$ 0.8**
N-leu 6	81.9 $\pm$ 7.4	44.0 $\pm$ 2.9*	N-his 5	86.5 $\pm$ 6.5	29.7 $\pm$ 1.6**
N-pro 1	92.1 $\pm$ 4.7	57.2 $\pm$ 1.4**	N-his 6	84.0 $\pm$ 5.0	37.3 $\pm$ 1.9
N-pro 2	92.0 $\pm$ 3.7	45.6 $\pm$ 2.9			

ED, emitted dose; FPF, fine particle fraction.

Despite the overall satisfying values of ED, a variation in FPF was observed depending on the AA used, its concentration and alcohol content in the feed. The highest FPFs (about 50%) were obtained for batches processed from 3:7

ethanol/water and 5% AA solutions. Generally, an increase in ethanol content (up to 40 or 50%, v/v) and AA (from 5 to 10%, w/w) concentration led to significantly lower FPFs (from 50% to 29.7%), indicating a worsening in the powders aerosolization properties.

MMAD, FPF and FPD values derived by ACI deposition studies confirmed the observed AA and alcohol concentration-dependent trends (Table 4). For inhalation into the lower airways and into the deep lung, a better dispersibility of particles with MMAD < 5 µm is definitely a prerequisite.

**Table 4.**

Aerodynamic properties of N and N-AA dry powders after Andersen cascade impactor deposition experiments. All data are shown as mean ± SD of three experiments.

Code #	MMAD	FPF %	FPD mg	Code #	MMAD	FPF %	FPD mg
N-1	3.72 ± 0.04	44.7 ± 1.5	7.54 ± 0.8	N-pro 3	2.81 ± 0.0**	60.7 ± 1.2**	8.53 ± 0.2*
N-2	3.85 ± 0.06	46.0 ± 0.9	6.87 ± 0.7	N-pro 4	3.42 ± 0.1**	44.8 ± 1.7	6.24 ± 0.1
N-3	3.89 ± 0.15	43.0 ± 0.5	6.56 ± 0.1	N-pro 5	3.92 ± 0.1	43.9 ± 0.6	6.52 ± 0.1
N-leu 1	2.77 ± 0.06**	63.4 ± 1.2**	8.47 ± 0.1	N-pro 6	3.90 ± 0.1	42.5 ± 0.9	5.30 ± 0.2**
N-leu 2	4.14 ± 0.21**	43.2 ± 2.1	5.93 ± 0.1	N-his 1	2.75 ± 0.0**	64.0 ± 0.2**	8.87 ± 0.6
N-leu 3	2.89 ± 0.16**	60.7 ± 1.9**	8.17 ± 0.0*	N-his 2	2.24 ± 0.1**	67.4 ± 1.2**	7.73 ± 0.3
N-leu 4	3.13 ± 0.15**	54.3 ± 3.2*	6.39 ± 0.1	N-his 3	3.94 ± 0.1	43.9 ± 0.9*	6.45 ± 0.5
N-leu 5	3.06 ± 0.31*	53.2 ± 1.9**	6.61 ± 0.1	N-his 4	4.13 ± 0.1**	35.9 ± 1.6**	4.57 ± 0.7
N-leu 6	3.91 ± 0.18	42.5 ± 0.7	5.30 ± 0.1**	N-his 5	n.d.	n.d.	n.d.
N-pro 1	2.68 ± 0.10**	63.4 ± 0.5**	9.55 ± 0.6*	N-his 6	n.d.	n.d.	n.d.
N-pro 2	3.61 ± 0.11	49.7 ± 0.9**	6.18 ± 0.3*				

MMAD, mass median aerodynamic diameter; FPF, fine particle fraction; FPD, fine particle dose.

As evident from Fig. 21, N-10% AA powders, spray-dried from 50% ethanol feeds had the lowest FPF, corresponding to an undesirable increase of the powders deposition into the throat. By contrast, N-his 1, N-leu 1 and N-pro 1

showed the best aerodynamic properties in terms of both FPF (about 64%) and FPD (8.47–9.55 mg) and gave satisfactory pulmonary deposition profiles (Fig. 21).

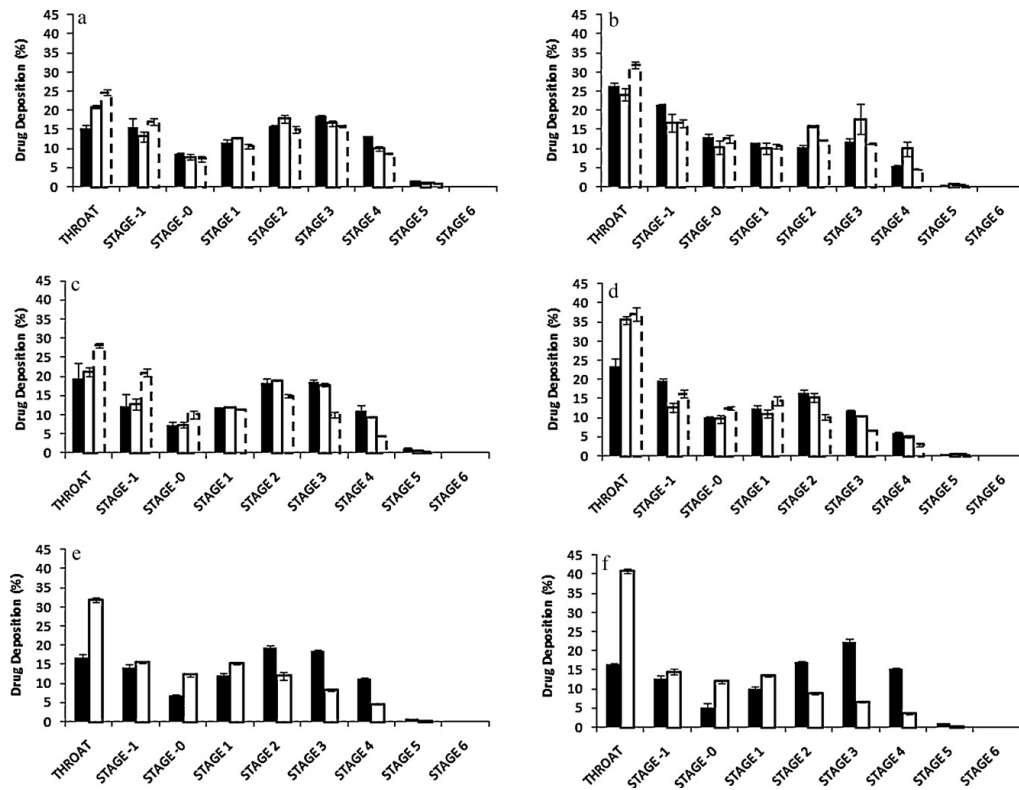


**Fig. 21.** Andersen cascade impactor deposition pattern of N dry powders from feeds containing: 30% (v/v) ethanol (black bars); 40% (v/v) ethanol (white bars); 50% (v/v) ethanol (dotted lines bars) and (a) 5% leucine, (b) 10% leucine, (c) 5% proline (w/w), (d) 10% proline, (e) 5% histidine, (f) 10% histidine.

Altogether our data indicate that, when compared to N spray-dried alone, powders processed with 5% AAs from 3:7 ethanol/water and, particularly, N-leu 1 show relatively high improvement of FPF. Higher FPF is due to two types of effects: a reduction in the capsule and device retention and/or an

increase in the powder dispersibility. The latter effect is likely related to the absence of aggregates and high degree of particle surface corrugation (Fig. 19). In agreement with previous reports, surface corrugation may decrease interparticulate cohesion by reducing Van der Waals forces between the particles and, consequently, increase the powder respirability (Chew and Chan, 2001; Chew et al., 2005b).

Another noteworthy finding of our research is the surprisingly high bulk density values observed for batches N-his 2 and N-leu 3, characterized by almost satisfying FPF (>60%) and FPD (>7.73 mg) (Table 5). From an industrial perspective, high bulk density values imply that the powders are easy to handle and can be introduced in increased amounts into the gelatine capsules; from a therapy point of view, an increased dosage imply a reduced dosage frequency. Therefore, the ACI deposition experiments were repeated on the capsules containing a double amount (40 mg vs 20 mg) of micronized powders. DPIs containing 40 mg of powders were able to emit almost doubled FPDs compared to DPIs charged with 20 mg (Table 5). This result allows to raise the FPD emitted after a single device actuation from about 6.9–8.2mg (N-1, N-2, N-his 2, and N-leu 3) to 16.2–18.6 mg (N-his 2 bis and N-leu 3 bis), keeping the FPF at about 60%. Higher dosages are more suitable for long-term treatment of CF patients and, moreover, we expected compliance to be major if dosage frequency is reduced.

**Table 5.**

Bulk density and aerodynamic properties after Andersen cascade impactor deposition experiments of selected N dry powders.

Code #	Bulk density g/cm <sup>3</sup>	FPF %	FPD mg
N-1	0.068	44.7 ± 1.5	7.54 ± 0.8
N-2	0.059	46.0 ± 0.9	6.87 ± 0.7
N-his 2 (20 mg)	0.094	67.4 ± 1.2	7.73 ± 0.3
N-leu 3 (20 mg)	0.095	60.7 ± 1.9	8.17 ± 0.0
N-his 2 bis (40 mg)	0.094	59.7 ± 1.2	16.2 ± 0.3
N-leu 3 bis (40 mg)	0.095	60.0 ± 2.6	18.6 ± 0.4

FPF, fine particle fraction; FPD, fine particle dose

#### **2A.4 IN VITRO BIOLOGICAL ACTIVITIES OF N DRY-POWDERS IN BRONCHIAL EPITHELIAL CELLS**

Aim of the research was also to investigate whether N and its formulations could affect intrinsic inflammation of airways epithelium in CF patients. For this scope, we tested rawN, N-1 and N-leu 1 in two immortalized cell lines as in vitro models: one, called CuFi1 (CF cells), was derived from human airway epithelial (HAE) cells of CFTR  $\Delta F508/\Delta F508$  mutant genotype, the other, called NuLi1 (normal lung), was derived from a non-CF subject and used as control. These cell lines exhibited transepithelial resistance, maintained the ion channel physiology expected for the genotypes and retained NF- $\kappa$ B responses to inflammatory stimuli (Dehecchi et al., 2008; Zabner et al., 2003).

***Effect of N and its formulations on cell viability***

Preliminary studies were performed to determine the cytotoxic drug concentration for these cell line models. After a 24 h treatment, rawN did not significantly affect cell viability, as determined by MTT assay in the concentration ranging from 15 to 150  $\mu$ M (data not shown), but it caused a dose-dependent reduction of cell growth of different extent in NuLi1 and CuFi1 cells, from 60 to 150  $\mu$ M (Fig. 22a). N-1 did not show a significant effect on proliferation in both cell lines (Fig. 22b), except a slight reduction of cell growth at the highest concentration (150  $\mu$ M,  $P < 0.05$ ). N-leu 1 induced a dose-dependent and significant cell growth inhibition only in normal bronchial NuLi1 cells (Fig. 22c), while it determined a 14% increase of cell proliferation in CuFi1 cells at the highest dose (150  $\mu$ M). In conclusion, neither rawN nor N-1 and N-leu 1 are cytotoxic or cytostatic in both CF and non-CF bronchial epithelial cells at concentrations lower than 60  $\mu$ M. To evaluate the contribution of the AA to the increased cell proliferation induced by N-leu 1 in CuFi1, Leu spray-dried alone was also tested. The AA did not show any significant effect in NuLi1 cells while it was able to increase CuFi1 cell proliferation at all the concentrations tested (Fig. 22d).

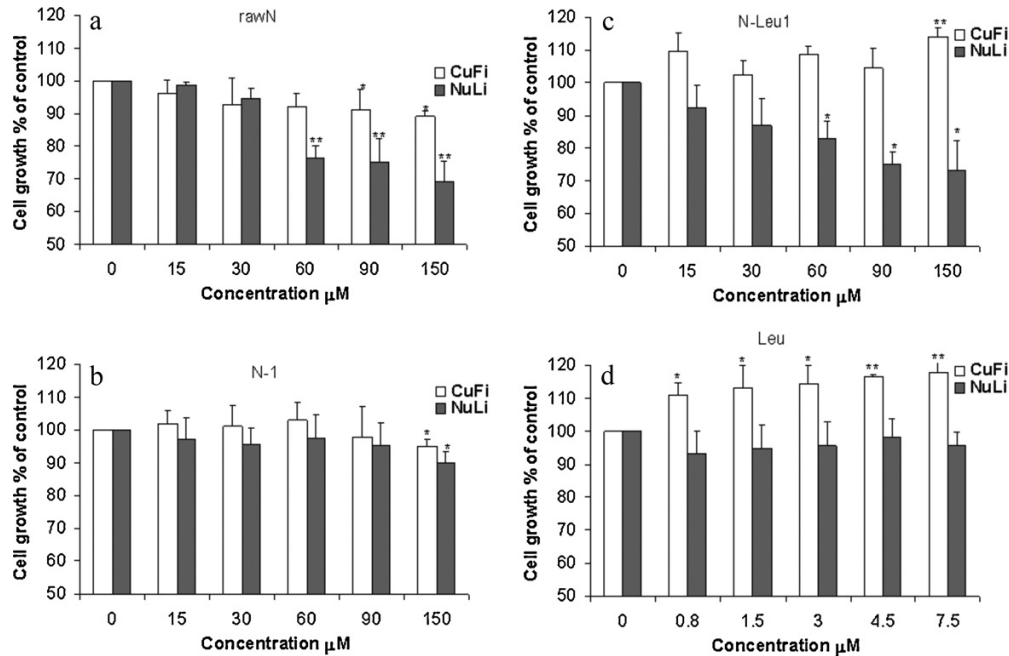


**Fig. 22.** Naringin and its DPI formulations do not inhibit CuFi1 and NuLi1 cell proliferation at concentrations lower than 60  $\mu\text{M}$ . Cells were treated for 24 h with: (a) raw Naringin (rawN), (b) spray-dried Naringin (N-1), (c) N co-sprayed with 5% leucine (N-leu 1) at concentrations from 15 to 150  $\mu\text{M}$ , and (d) spray-dried leucine (Leu) at concentrations corresponding to those contained in N-leu 1 (from 0.8 to 7.5  $\mu\text{M}$ ). Cell growth was determined using a colorimetric bromodeoxyuridine (BrdU) cell proliferation ELISA kit. The histograms report the percentage of growing cells in comparison with untreated cells (control, 100% proliferation). All data are shown as mean  $\pm$  SD of three independent experiments each done in duplicate (\* $P < 0.05$  and \*\* $P < 0.01$  vs control).

This finding suggests that the technological improvement of immediate drug solubility and powder flowability, as well as the presence of the AA in N-Leu 1, may increase the drug uptake and improve the CF cell altered metabolism, reducing the toxicity observed for unprocessed rawN (Fig. 22a). In accordance, increased and altered basal protein catabolism has been reported

in CF patients by many reports (Holt et al., 1985; Levy et al., 1985; Switzer et al., 2009).

***Effect of N and its formulations on NF- $\kappa$ B pathway***

To study the anti-inflammatory effects of N in CF cells, we investigated the main molecular targets of NF- $\kappa$ B and MAPK/ERK pathways in CuFi1 in comparison to normal bronchial NuLi1 cells. The NF- $\kappa$ B pathway is well known to play a crucial role in inflammatory process (Yamamoto and Gaynor, 2001). In resting cells, the transcription factor NF- $\kappa$ B exists as homo- or heterodimer, maintained inactive in the cytosol by a family of inhibitor proteins named I $\kappa$ Bs (I $\kappa$ B $\alpha$ ,  $\beta$ ,  $\epsilon$ ). In response to a wide range of stimuli such as cytokines and bacterial or viral products, I $\kappa$ B proteins are phosphorylated by I $\kappa$ B kinases (IKK $\alpha$  and  $\beta$ ), ubiquitinated and degraded by the 26S proteasome. As a consequence, NF- $\kappa$ B dimers can localize into the nucleus and positively regulate the transcription of proinflammatory genes (Hayden and Ghosh, 2004). This pathway is overactivated also in absence of any infection (Lyczak et al., 2002; Rottner et al., 2007; Verhaeghe et al., 2007) in CF cells, as previously reported.

In our experiments, CuFi1 cells exhibit higher expression levels of IKK $\beta$ , phosphoI $\kappa$ B $\alpha$  and phosphoERK 1/2 proteins compared to their normal counterpart NuLi1 cells (data from Western Blot analysis not shown). The effects of rawN, N-1 and N-Leu1 at sub-toxic concentrations (30  $\mu$ M) were evaluated at 2, 6 and 24 h on IKK $\beta$  and I $\kappa$ B $\alpha$  kinases, measuring both the expression levels and the phosphorylation status of the main molecular targets of the NF- $\kappa$ B pathway (i.e. IKK $\alpha$ , IKK $\beta$  and I $\kappa$ B $\alpha$ ). Results are reported in Fig. 23.

As regards to IKK $\alpha$ , N1 and N-leu1 caused a reduction of IKK $\alpha$  but rawN did not in CuFi1 cells, while all powders did not cause any significant effect in NuLi1 cells (Fig. 23b). As IKK $\beta$ , its expression was generally reduced in CuFi1 cells: the highest decrease was observed at 6 h in N-leu 1-treated cells (Fig. 23b). In normal bronchial epithelial cells, IKK $\beta$  expression was slightly reduced, particularly at 6 h (by N1) and 24 h (by N-leu1). Interestingly, the observed reduction of expression levels of both the enzymatic subunits of the IKK complex in CuFi led to a significant and prolonged decrease of I $\kappa$ B $\alpha$  phosphorylation. In fact, this effect started early (2 h) and was retained all over the treatment time (24 h) in CF bronchial epithelial cells (Fig. 23a). On the contrary, in normal bronchial epithelial cells only a delayed (24 h) decrease of I $\kappa$ B $\alpha$  phosphorylation was observed as a consequence of the reduction of IKK $\beta$  subunit only expression level. Leucine spray-dried alone did not give any significant result in all Western Blot analyses (data not shown).

Previous evidence indicates that IKK $\beta$  plays a more crucial role for NF- $\kappa$ B activation in response to pro-inflammatory cytokines and microbial products (Verhaeghe et al., 2007), even though both the catalytic subunits of the IKK complex are able to regulate NF- $\kappa$ B activation and have a complementary role in the control of inflammation (Descargues et al., 2008). These observations are in agreement with our results, showing that N formulations are effective in inhibiting both IKK subunits expression, and therefore caused a prolonged reduction of I $\kappa$ B $\alpha$  phosphorylation in CuFi1 cells, whereas the observed slight reduction of IKK $\beta$  subunit only may justify the delayed effect on I $\kappa$ B $\alpha$  observed in NuLi1 cells.

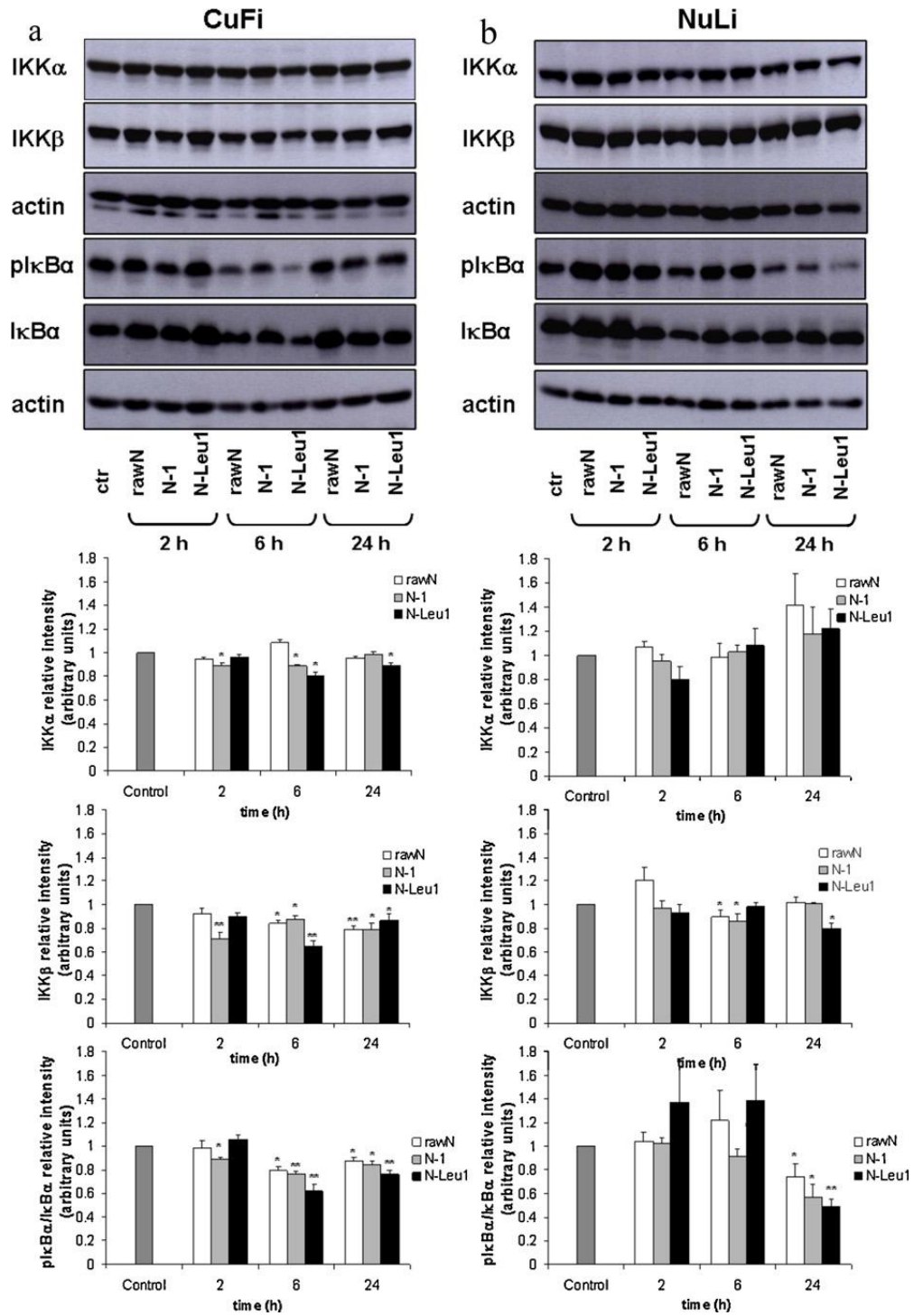


**Fig. 23.** Naringin and its DPI formulations inhibit the key enzymes of the NF- $\kappa$ B pathway in CF bronchial epithelial cells. CuFi1 (a) and NuLi1 (b) cells were treated with raw Naringin (rawN), spray-dried Naringin (N-1) and N co-sprayed with 5% leucine (N-leu 1) at 30  $\mu$ M concentration for the indicated time points. Cell lysates were analyzed by Western blot with antibodies against IKK $\alpha$ , IKK $\beta$  and pIKB $\alpha$ . Same filters were stripped and re-probed with total IKB $\alpha$  and anti-actin used as loading control. More representative results are shown (upper panels). Immunoreactive bands were quantified using Quantity One program. Densitometric analyses (mean  $\pm$  SD) of three independent experiments are reported as relative intensity of IKK $\alpha$ , IKK $\beta$  or pIKB $\alpha$ /IKB $\alpha$  on actin and expressed as arbitrary units vs control (lower panels). (\*P < 0.05 and \*\*P < 0.01 vs control).

#### ***Effect of N and its formulations on MAPK/ERK pathway***

As concerns the effect on the MAPK/ERK pathway, results (Fig. 24) showed that N and its formulations, in both NuLi1 and CuFi1 cells, modulate negatively the MAPK/ERK cell signaling pathway, which is known to activate the transcription factor AP-1 required for cytokine transcription and production (Karin, 1995).

However, the effect is very pronounced for N-Leu1 at 6 h and prolonged until 24 h in CF bronchial epithelial cells, with respect to non-CF NuLi1 cells. Also in this case, leucine alone did not induce any change in ERK 1/2 phosphorylation (data not shown).

Altogether our findings indicate that N-Leu 1 is able to inhibit both MAPK/ERK and NF- $\kappa$ B pathways, which are over activated in bronchial epithelial cells from CF patients also in absence of infections.

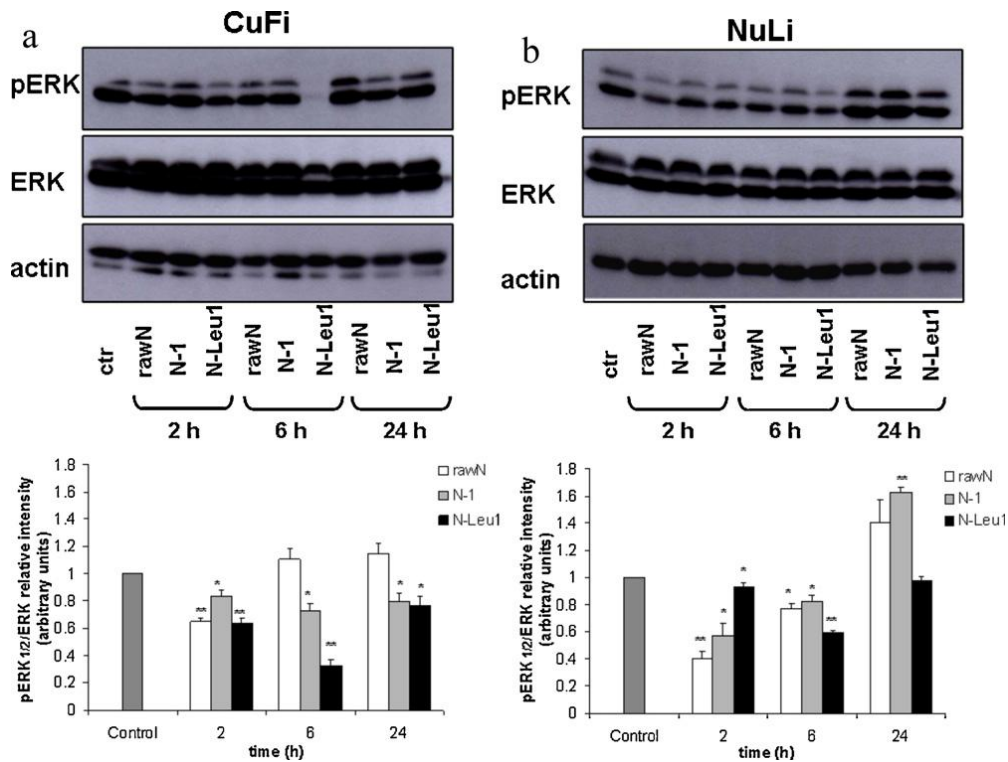


**Fig. 24.** Naringin and its DPI formulations reduce ERK1/2 phosphorylation in CF airway bronchial epithelial cells. CuFi1 (a) and NuLi1 (b) cells were treated with raw Naringin (rawN), spray dried Naringin (N-1) and N co-sprayed with 5% leucine (N-leu 1) at 30  $\mu$ M concentration for the indicated time points. Western blot analysis with anti-pERK1/2 (pERK) was performed on cell lysates. Membranes were stripped and re-probed with total ERK1/2 (ERK) and actin as loading control. More representative results are shown (upper panels). Immunoreactive bands were quantified using Quantity One program. Densitometric analyses (mean  $\pm$  SD) of three independent experiments are reported as relative intensity of pERK/ERK on actin and expressed as arbitrary units vs controls (lower panels). (\*P < 0.05 and \*\*P < 0.01 vs control).

***Effect of N and its formulation on Interleukin-8 (IL-8) and interleukin-6 (IL-6) release***

To further provide evidence about the anti-inflammatory activity of N-Leu1, we investigated the direct effect of N-Leu 1 on the main cytokines involved in inflammatory response, interleukin 8 (IL-8) and interleukin 6 (IL-6). To this aim, CuFi1 cells were treated with N-Leu1 at 30 and 60  $\mu$ M in the presence and absence of LPS-stimulation from *Pseudomonas aeruginosa*. Results (Fig. 25) showed that N-Leu1 inhibited both cytokine production in unstimulated as well as in LPS-stimulated CuFi1 cells. Particularly, N-Leu1 inhibited the production of IL-8 more than IL-6 and this effect was much evident in unstimulated cells.

These data indicate that the inhibition of NF $\kappa$ B and ERK pathways by N-Leu1 results directly in a reduction of the release of pro-inflammatory cytokines corroborating the efficacy of N-Leu 1 in controlling the pro-inflammatory status of CF cells in the presence as well as in the absence of bacterial stimulation. However, LPS-stimulated cytokine secretion is dependent on Toll-like receptor-4 (TLR-4) signaling. TLR-4 expression is reduced in the CF airway epithelial cells, possibly because of a diminished translocation of the receptor to the cell surface. This is associated with a reduced possibility of CF cells to counteract the LPS-induced inflammatory response from gram-negative bacteria maybe predisposing the CF lung to bacterial colonization and chronic infection (John et al., 2010).

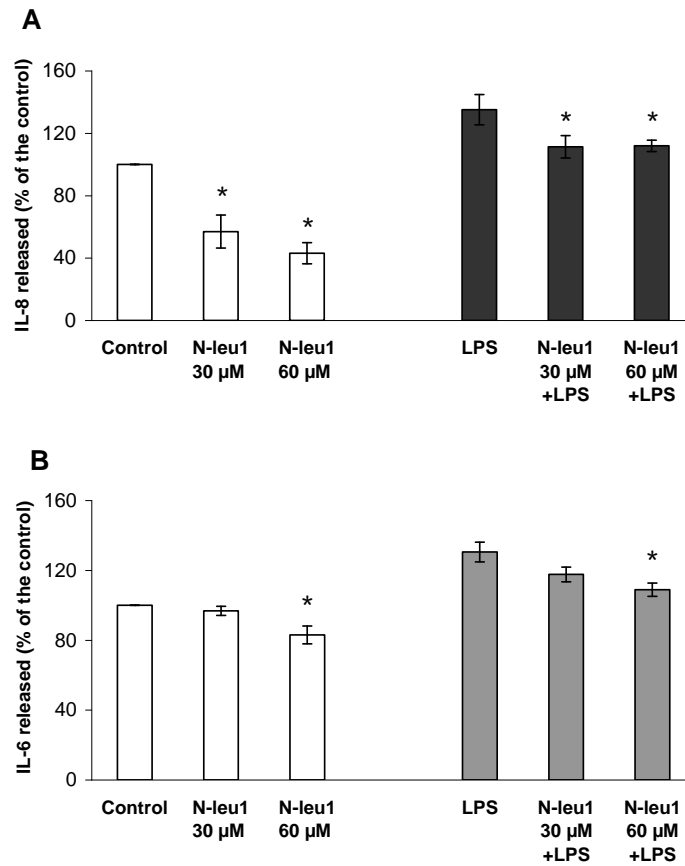


**Fig. 25.** Effect of Naringin co-sprayed with 5% leucine (N-leu 1) on basal and LPS-induced secretion of IL-8 (**A**) and IL-6 (**B**) in Cystic Fibrosis bronchial epithelial (CuFi1) cells. Data are presented as mean percentage of released cytokines in the control supernatants (untreated and unstimulated)  $\pm$  SD of two independent experiments each done in duplicate. (\* $P < 0.05$  vs control supernatants).

## 2A. 5 Conclusions

Naringin is a natural polyphenol with anti-inflammatory potential for cystic fibrosis treatment. N/AA dry powders, produced by co-spray drying N and AAs in the appropriate ratio, were found to have improved aerodynamic properties, showing high FPFs (> 60%), low impact loss, capsule and device retention. The use of leucine as excipient was useful to reduce adhesion between particles and improve powder dispersion when delivered from dry powder inhalers. Therefore, a careful formulation plays a key role in affecting the aerosol performance of N-dry powders. N-Leu1 was proposed as the formulation with optimized bulk and aerodynamic behavior.

N-Leu1, N1 and rawN were tested *in vitro* on CF and normal bronchial epithelial cells, to establish if the particle engineering has positive effect on biological activity. Since defective CFTR function induces the expression of pro-inflammatory mediators, CF cells show constitutive NF- $\kappa$ B hyperactivation and ERK upregulation, resulting in increased levels of pro-inflammatory mediators also in absence of any infection. Dry powder N-Leu1, at sub-toxic concentrations, is able to negatively modulate both NF- $\kappa$ B and MAPK/ERK pathways in absence of stimulation in bronchial epithelia, with higher effects in CF cells (CuFi1) than in normal (NuLi1) bronchial cells. In addition, N-Leu1 is able to reduce the overexpressed Il-8 and Il-6 production in CuFi1 cells both in basically and LPS-stimulated conditions, confirming the efficacy of this formulation in controlling CF chronic inflammation.

These findings, together with the already reported anti-inflammatory and antioxidant properties of Naringin, support a potential use of N/AA-DPI as MAPK and NF- $\kappa$ B inhibitors to treat lung intrinsic inflammation and prevent tissue damages in CF patients.



**SECTION B**

***DESIGN AND DEVELOPMENT OF STABLE GENTAMICIN  
MICRONIZED POWDERS BASED ON  
SUPERCRITICAL ASSISTED ATOMIZATION  
OR SPRAY-DRYING TECHNIQUES***



## 2B BACKGROUND, RATIONALE OF THE SELECTION OF GENTAMICIN, AIMS

Pulmonary infections are the major cause of morbidity and mortality in cystic fibrosis (CF), with *Pseudomonas aeruginosa* (*Pa*) acting as the principal pathogen. The viscous mucus lining the lung of CF patients impairs the mucociliary function, facilitating recurrent and chronic respiratory infections caused mainly by *Pa* but also by *Haemophilus influenzae*, *Burkholderia cepacia* (Mukhopadhyay et al., 1996; Ramsey et al., 1999). Treatment of lung disease by antibiotics is an accepted standard in CF cure aiming at reducing decline in lung function and number of hospitalizations (Prayle et al., 2010). Aminoglycosides, such as gentamicin sulfate (GS) (Fig. 26), are indicated in the management of acute exacerbations of CF as well as in the control of chronic infection and the eradication of *Pa* infections. Aminoglycosides are very commonly used for severe gram-negative infections.

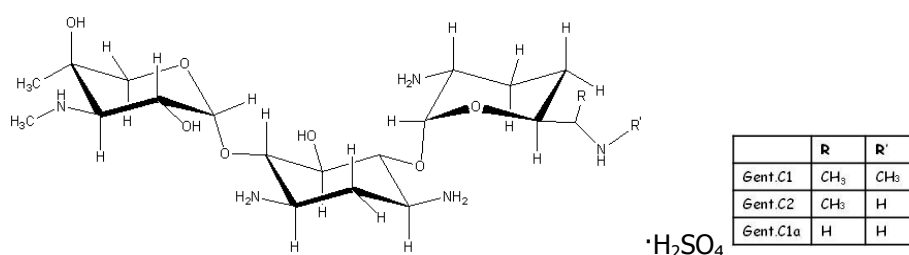


**Fig. 26.** Gentamicin sulfate structure.

The antibacterial activity results from binding to the bacterial 16S ribosome unit, causing misreading of messenger RNA codons. The drugs are routinely administered for its antibacterial effect both intravenously and topically. However, their use is limited by a lack of bioavailability owing to gastrointestinal absorption and by severe renal toxicity and ototoxicity at relatively low serum concentrations. Moreover, parenteral administration of aminoglycosides requires high doses due to their high polarity and, consequently, reduced penetration into the endobronchial space (Mendelman et al., 1985). Administration of aminoglycosides by inhalation has become a common and standard therapy in patients with cystic fibrosis and has minimal side effects. This route results in higher concentrations in the respiratory system than does the intravenous route, with very low serum concentrations. Aerosolized aminoglycosides may deliver the drug directly to the site of action and reduce systemic toxicity and side effects, including severe kidney damage and hearing loss (Geller, 2009; Parlati et al., 2009). Various clinical studies on gentamicin inhalation treatment in cystic fibrosis patients chronically infected with *Pseudomonas aeruginosa* have shown that antibiotic solutions for aerosol treatment produce both subjective and objective improvement. Interestingly, among aminoglycosides, GS has shown the ability to partially restore the expression of the functional protein CFTR (cystic fibrosis transmembrane conductance regulator) in CF mouse models bearing class I nonsense mutations (Clancy et al., 2001; Du et al., 2002; Wilschanski et al., 2000; Wilschanski et al., 2003). In particular, Du and coll. (Du et al., 2002) demonstrated that GS was able to induce the expression of a higher CFTR level compared to tobramycin. Aminoglycoside antibiotics can suppress premature termination codons by allowing an amino acid to be incorporated in

place of the stop codon, thus permitting translation to continue to the normal end of the transcript (Fig. 27).

Aminoglycoside antibiotics can reduce the fidelity of translation, predominantly by inhibiting ribosomal “proofreading”, a mechanism to exclude mismatched amino acyl-transfer RNA from becoming incorporated into the polypeptide chain. In this way aminoglycosides increase the frequency of erroneous insertions at the nonsense codon and permit translation to continue to the end of the gene, as has been shown in eukaryotic cells (Burke et al., 1985), including human fibroblasts (Buchanan et al., 1987). The susceptibility to suppression by aminoglycosides depends on the stop codon itself and on the sequences surrounding it.

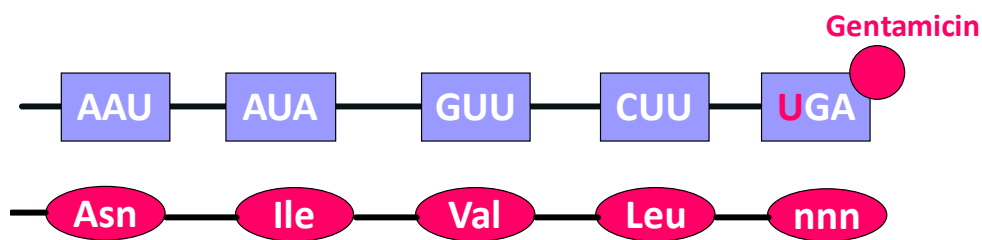


**Fig. 27.** Proposed mechanism for suppression of premature termination codon by gentamicin.

Howard et al. demonstrated that two CFTR-associated stop mutations could be suppressed by treating cells with low doses of an aminoglycoside antibiotic (Howard et al., 1996). Bedwell et al. demonstrated that after incubation of bronchial epithelial cell line IB3-1, which carries a W1282X mutation of CFTR, with aminoglycosides, cyclic AMP (cAMP)-activated chloride conductance and the expression of functional CFTR were restored to the apical membrane (Bedwell et al., 1997). Zsembery et al. isolated cholangiocytes from the liver of a patient carrying the G542X mutation of CFTR and

incubated them with gentamicin, resulting in the expression of cAMP-activated chloride transport (Zsembery et al., 2002). Thus, *in vitro*, gentamicin obviated the effect of stop-codon mutations on the transcription and translation of CFTR. This effect has subsequently been demonstrated in a number of models of other diseases caused by stop mutations, including muscular dystrophy (Barton-Davis et al., 1999), Hurler's syndrome (Keeling et al., 2001), cystinosis (Helip-Wooley et al., 2002), late infantile neuronal ceroid lipofuscinosis (Sleat et al., 2001), and disorders involving the p53 gene (Keeling et al., 2002).

Although aerosolized antibiotics were first introduced in therapy in the '50s, recently approved products for life-threatening lung infections in CF are limited to solutions for nebulization (TOBI<sup>®</sup>, Bramitob<sup>®</sup> and Cayston<sup>®</sup>). Generally, aqueous solutions for inhalation are time consuming, difficult in the dose handling and require routine maintenance in order to avoid bacterial contamination. Moreover, liquid formulations may deliver low and variable drug amount when nebulized and cause drug chemical instability, as well. Dry powder inhalers (DPI) decrease the burden of treatment and offer more freedom to patients as they are breath-actuated, propellant-free and easy to be transported (Khassawneh et al., 2008). In addition DPI containing drugs as micronized powder are able to aerosolize and deliver a metered and high amount of the active principle to the respiratory tract. They seem to be more suitable than liquid nebulizer products especially for antibiotic pulmonary therapy, which requires larger drug doses compared to bronchodilator or steroidal therapy.

As for other drugs, the exposure to organic solvents, interfaces, and stringent physical conditions of temperature and cavitation or shear forces can lead to structural changes which can have an effect on gentamicin integrity, although gentamicin sulphate is stable in aqueous buffers over a wide pH and

temperature range (Prior et al., 2000). Among physico-chemical properties of gentamicin sulfate (highly water soluble polar cation, highly hydrophilic, H-donor) influencing its stability, some authors pointed out the high hygroscopicity (Della Porta et al., 2010). For an inhalation product, hygroscopicity can interfere with the production of respirable particle during aerosol generation. In addition, as particles enter the airways, they may be subject to hygroscopic growth due to the highly humid environment, which reduces lung deposition.

Therefore, the first aim of the research was to develop micronized gentamicin powders, easy to handle and stable for long time; the second goal was to obtain a dry powder suitable for pulmonary administration. Final purpose of the project was also to compare spray-drying versus a new atomization technology, supercritical fluids assisted atomization (SAA), in the processing of gentamicin sulphate.



**PART 1: PRODUCTION OF MICRONIZED GENTAMICIN  
POWDER BY SAA (Supercritical Assisted Atomization)**

**Based on the article:** G. Della Porta, R. Adami, P. Del Gaudio, **L. Prota**, R.P. Aquino, E. Reverchon. “Albumin/Gentamicin Microspheres Produced by Supercritical Assisted Atomization: Optimization of Size, Drug Loading and Release”. *Journal Pharmaceutical Sciences*. **2010**, 99: 4720 – 9.

## **2B 1.1 BACKGROUND AND AIM**

The first part of the project was devoted to verify the feasibility of Supercritical Assisted Atomization (SAA) process in the production of gentamicin sulphate (GS) powders with decreased hygroscopicity and particle size.

Preliminary experiments showed that neat GS powders processed by SAA technology retained its high hygroscopicity; therefore, the next step of the research was aimed to load GS on a biodegradable and biocompatible carrier, able to prevent physical and chemical degradation. Polymers such as cellulose, alginates, chitosans, pectins, chemically inert, non-toxic, biocompatible and easily sterilized, have been used for this scope. Recent studies have demonstrated that proteins could be a viable alternative to polysaccharides (Das et al., 2005; Kim et al., 2004; Haswani et al., 2006). A pharmaceutical-grade albumin, the most abundant of the whey protein, has recently been proposed as drug carriers. Such microsystems, for albumin non-antigenic properties, biodegradable, biocompatibility (Willmott et al., 1985), are able to control the release of drugs, particularly antibacteric drugs. Therefore, in the frame of the present PhD project, BSA was selected as proteic carrier of GS and SAA as processing technology to obtain stable microsystems.

The SAA process (Fig. 28) consists of dissolving the SC-CO<sub>2</sub> in a liquid solution and, then, spraying this mixture using a 80 µm injector device to obtain droplets; then, these droplets are evaporated by warm nitrogen to form microparticles, as performed in conventional spray-drying.

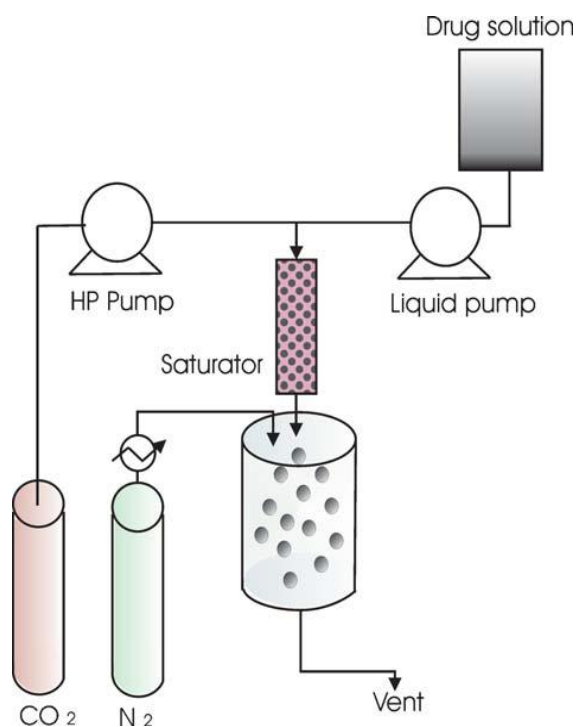


**Fig. 28.** Schematic representation of SAA apparatus.

The enhanced atomization obtained by SAA is due not only to the *pneumatic* atomization obtained by means of injector, but, also to the so-called *decompressive* atomization that is due to the fast release of solubilized CO<sub>2</sub> from the primary droplets, forming smaller secondary droplets (Della Porta G et al., 2007). Moreover, the presence of dissolved CO<sub>2</sub> reduces the surface tension of the liquid, inducing a more efficient pneumatic atomization: as a result, more uniform and smaller droplets (i.e., particles) can be obtained by SAA process. The solubilization of SC-CO<sub>2</sub> in the liquid solution inside the saturator is one of the key steps controlling the efficiency of the SAA process. The solubility of SC-CO<sub>2</sub> in liquids depends on the solvent chemical nature and on temperature and pressure in the saturator. Moreover, it can also be influenced by the presence of solute dissolved in the liquid. In the SAA

process, gas and liquid flow rates are selected to obtain residence times of some minutes (from 5 to 8 min) in the saturator to assure efficient gas dissolution in the liquid solution. The selected mass flow ratio between CO<sub>2</sub> and liquid solution is related to the equilibrium of the system CO<sub>2</sub>/solvent/solutes in the saturator. Indeed, when pressure and temperature are set, the mass flow ratio between CO<sub>2</sub> and the liquid solution fixes the position of the process operating point in the pressure-composition plane. The most efficient decompressive atomization (that enhances the efficiency of SAA process) is obtained when the operating conditions of pressure and temperature are chosen into the one phase region, since all CO<sub>2</sub> will dissolve into the liquid solution and a supercritical solution is obtained. However, when water is selected as liquid solvent (as in our case), at pressures and temperatures between 10–10.5 MPa and 80–90°C, the solubility of CO<sub>2</sub> in the aqueous solutions is low; that is, the operating point always falls into a two phase gas–liquid region. Therefore, when aqueous solutions are used, the effect of the mass flow ratio on the composition of the phases formed in the saturator is reduced and the decompressive atomization is weakly influenced by this process parameter.

## **2B 1.2 PRELIMINARY SAA TEST ON BSA AND GS**

The first step of the research was to verify the SAA processability of GS and BSA as pure, single compounds.

Following the consideration reported above, GS was micronized by SAA using a concentration of 10 mg/mL of drug in water, a mass flow ratio (R) between CO<sub>2</sub> and water of 1.8, temperature in the saturator of 80°C and a pressure of 10.5 MPa; the temperature in the precipitator was set at 100°C. A

SEM image of the produced powder is reported in Figure 29 and shows that the particles obtained are spherical, with a mean size of 1.3  $\mu\text{m}$  ( $\text{SD} \pm 0.5 \mu\text{m}$ ). The precipitated powder was light yellow; whereas the untreated GS is a white powder, suggesting that the drug was partly degraded during the process. This hypothesis was confirmed by HPLC–UV analysis performed on the micronized GS that revealed the presence of 3.3% of decomposed drug after SAA processing. As stated before, the residence time in the pre-mixing chamber is of 5–8 min at 80°C; therefore, GS should not degrade during this part of the process, whereas, it is reasonable to assess that the drug degradation occurred when it was warmed up to 100°C in the precipitator chamber where, the residence time of the micronized drug is much higher (25 min, for example, for a SAA run in which are processes 500 mL of solution).

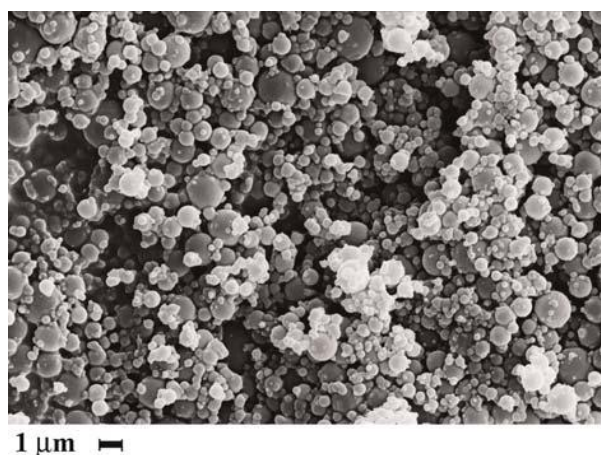


**Figure 29.** SEM image of GS precipitated from water. Saturator conditions: 80°C and 10.5 MPa; Precipitator temperature: 100°C; concentration injected: 10 mg/mL.

BSA micronization was performed using the same mass flow ratio between  $\text{CO}_2$  and water ( $R = 1.8$ ); the saturator pressure and temperature conditions

were of 85°C and 10.5 MPa with a temperature in the precipitator of 100°C. In these conditions, spherical and well separated particles have been obtained and a characteristic SEM image of the produced particles is reported in Figure 30.

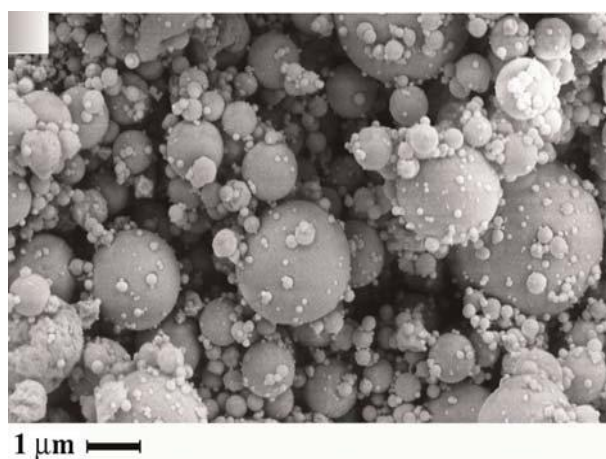


**Figure 30.** SEM image of BSA precipitated from water. Saturator conditions: 85°C and 10.5 MPa; Precipitator temperature: 100°C; concentration injected: 20 mg/mL.

BSA denaturation is fundamental for the use of this protein as a controlled release device, indeed it is the heat treatment that increases the hydrolytic resistance of the protein generating the unfolding of the  $\alpha$ -helices and the following formation of the disulfide bridges. In this sense, the SAA technology may combine the micronization and the thermal denaturation of the protein with the microencapsulation of GS in the protein. To select the better operation temperature for BSA denaturation, FTIR analyses were performed on the protein increasing the temperature from 30 to 150°C; the obtained signals showed that at temperatures higher than 90°C some modifications occurred in the range between 3200 and 3700  $\text{cm}^{-1}$ , confirming the protein unfolding process. Following the FTIR spectra indications, some tests of BSA micronization were also performed using precipitation

temperatures of 110 and 130°C and the corresponding SEM images of the particles obtained are reported in Figure 31a and b, respectively. In all cases microparticles were obtained and the water solubility of the processed BSA was significantly decreased; that is, the microparticles were formed by stable hydrophobic aggregates due to the irreversible unfolding of the protein. However, especially when operating at 130°C more collapsed particles were produced (see SEM images in Fig. 31b).

Particularly, collapsed BSA particles were collected always when operating at temperatures up to 100°C in the precipitation chamber; this phenomenon can be due to faster water evaporation from the droplets which can modify their shape. Indeed, as suggested by Iskandara et al. (Iskandara et al., 2003), when increasing the air temperature into a conventional spray-drier, local temperature gradients are created on the droplet surface. This causes two types of effects: the thermophoretic displacement of the solute toward the surface of the droplet and specific microcirculations inside a droplet. The solute particles move towards the peripheric regions of the droplet, and, as a result, a stronger droplet deformation occurs. Collapsed microparticles are undesirable due to an expected less uniform drug release with respect to the spherical shaped particles; therefore, a precipitating chamber temperature of 100°C was selected in the following part of the study.

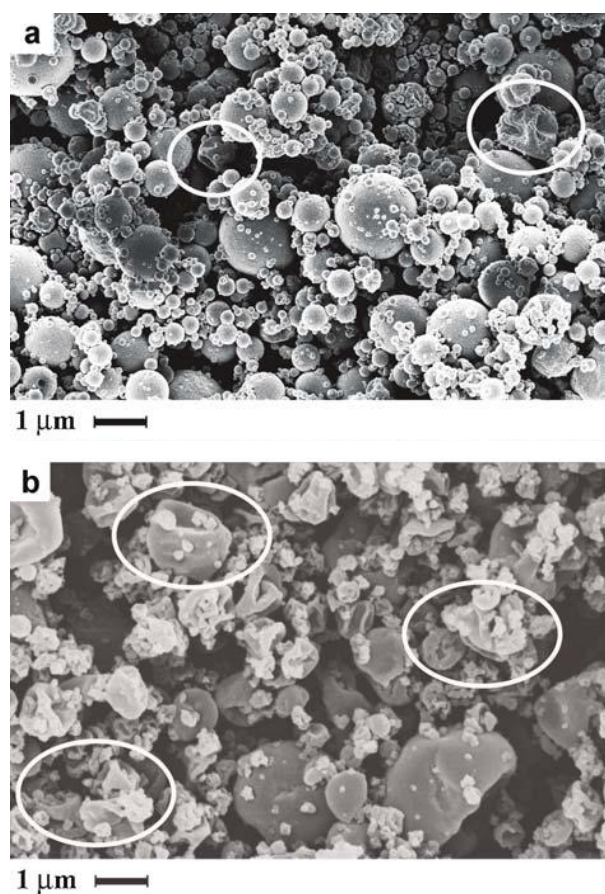


**Fig. 31.** SEM images of BSA microspheres obtained by SAA from water solutions at different precipitator temperatures: (a) 110°C, (b) 130°C. Saturator conditions: 85°C and 10.5 MPa; concentration injected: 20 mg/mL. Some collapsed particles are produced in both cases, however, they are more evident when a temperature of 130°C was used in the precipitator.

### **2B 1.3 SAA TEST FOR BSA/GS MICROSPHERES PRODUCTION**

After verifying the SAA processability of the two pure compounds, systematic coprecipitation tests

were performed to prepare BSA/GS loaded microparticles from the ternary system formed by BSA and GS dissolved in water. This ternary system can have very complex behavior at high pressure in presence of SC-CO<sub>2</sub> and could show significative different behaviors from the binary ones: BSA/water and GS/water. Indeed, in the SAA saturator a quaternary mixture is formed and the interactions between these components may influence the process results in terms of process stability and particle morphology. The operating SAA conditions (pressure, temperatures, and flow ratios) at which both BSA and GS individually showed good results, in terms of particles morphology were used and protein/drug ratios ( $r_{\text{BSA/GS}}$ ) of 1:1, 2:1, 4:1, 8:1 were chosen. Well-defined spherical microparticles with uniform morphology were produced at all ratios tested. Moreover, in all the experiments a white powder was always obtained, suggesting that BSA also acts as a protecting agent covering GS and avoids its thermal degradation during the process. SEM images of the microspheres obtained at the different  $r_{\text{BSA/GS}}$  are reported in Figure 32a–d.

From the proposed images it is possible to observe that at lower  $r_{\text{BSA/GS}}$  value (see SEM image reported in Figure 32d for the particles obtained with  $r_{\text{BSA/GS}}$  of 1:1) the micronized particles start again to collapse; this effect may be also due to the decrease of the amount of BSA in the coprecipitate which gives a less rigid spherical shell to the produced microspheres.

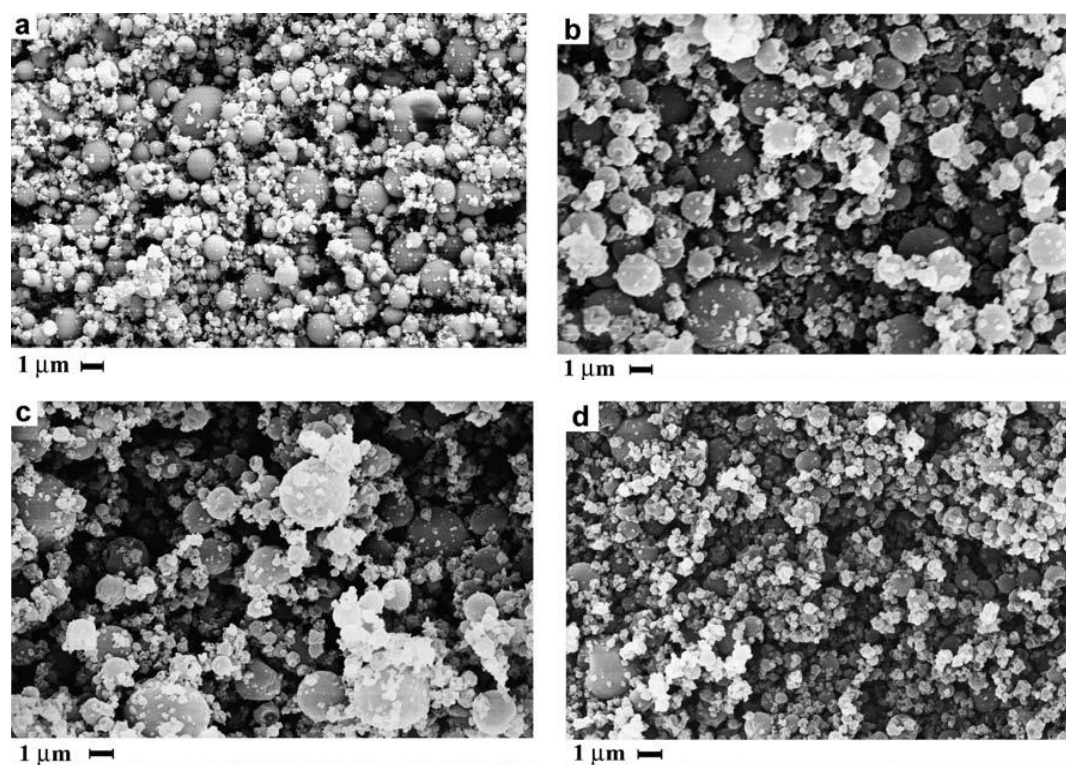


**Figure 32.** SEM images of BSA/GS microspheres obtained by SAA from water solutions at different  $r_{\text{BSA/GS}}$  values of (a) 8:1, (b) 4:1, (c) 2:1, (d) 1:1. Concentration injected: 20 mg/mL. Saturator conditions: 85°C and 10.5 MPa; precipitator condition: 100°C.

The Particle size distributions (PSDs) data of the produced microspheres are reported in Table 6; they were measured by SEM image analysis and by laser scattering. For all BSA/GS ratios studied the particles mean sizes (MSs) ranged between 1.5 and 2.5 μm ( $SD \pm 0.8 \mu\text{m}$ ) and a very moderate increase of the mean diameter was observed increasing the amount of GS loaded.

**Table 6.** Particle size distributions data of BSA/GS microspheres manufactured by SAA at different protein/drug ratio measured by Scanning Electron Microscopy-Image Analysis (SEM) and Laser Scattering (LS).

BSA/GS Ratio	Mean ( $\mu\text{m}$ )		SD ( $\pm$ ) ( $\mu\text{m}$ )		D <sub>10</sub> ( $\mu\text{m}$ )		D <sub>50</sub> ( $\mu\text{m}$ )		D <sub>90</sub> ( $\mu\text{m}$ )	
	SEM	LS	SEM	LS	SEM	LS	SEM	LS	SEM	LS
<b>8/1</b>	1.8	2.1	0.83	1.03	0.87	0.58	1.70	1.19	2.55	2.45
<b>4/1</b>	1.7	2.0	0.94	1.10	0.89	0.56	1.89	1.14	2.83	2.34
<b>2/1</b>	1.5	2.3	0.88	1.02	0.73	0.69	1.52	1.23	2.62	2.56
<b>1/1</b>	1.6	2.5	0.98	1.05	1.18	0.78	2.24	1.54	3.22	2.98

The PSDs of the microspheres produced with an  $r_{\text{BSA/GS}}$  of 1:4 and 1:8 are also illustrated in Figure 33a and b using a cumulative curve representation, respectively and a comparison between the distributions obtained using the two different evaluation methods is also proposed. Both measurement techniques confirmed that microspheres diameters are almost included in the range of 0.8 and 3  $\mu\text{m}$ ; however, SEM images analysis tends to overestimate the particles smaller than 1  $\mu\text{m}$  and to underestimate the particles larger than 3  $\mu\text{m}$  showing a D<sub>50</sub> of around 1.8  $\mu\text{m}$ , in both sample proposed. On the contrary, LS distribution curves indicate that particles with diameters included in the range of 0.7–1  $\mu\text{m}$  are almost the 50% of the distribution and show a relatively long tail included in the range of 4–6  $\mu\text{m}$ .

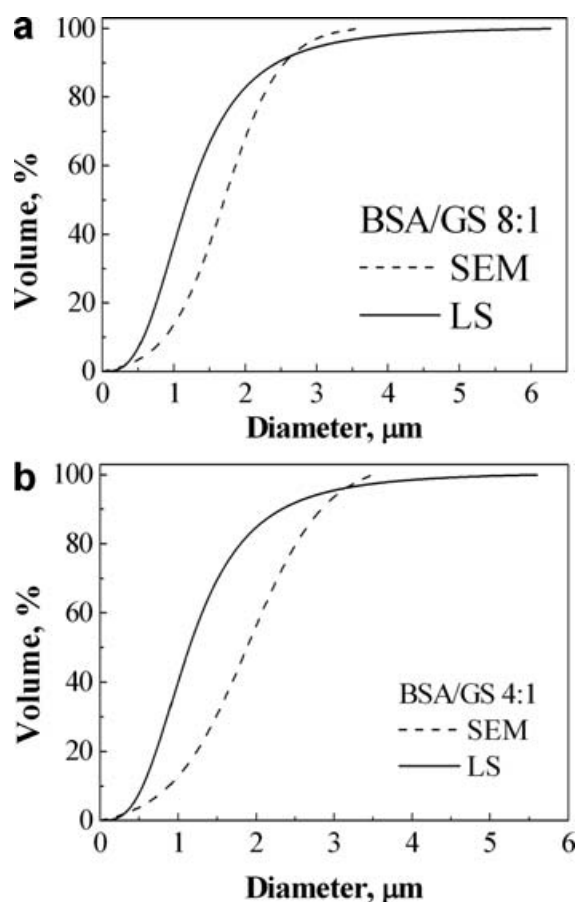


**Fig. 33.** Comparison between PSDs obtained by SEM images analysis (dashed line) and by LS (continuous line) for SAA microspheres produced at different BSA/GS ratios (a)  $r_{\text{BSA/GS}} = 8:1$  and (b)  $r_{\text{BSA/GS}} = 4:1$ .

It is well known that different techniques provide different particle size distributions and no one representation of the particle size can be claimed to be more accurate than another; in the case of drug production, for example, it is more important to understand how the mass or volume of material is distributed between particles of different sizes. So that, by image analysis it is calculated the volume occupied by the equivalent spheres and by the laser diffraction technology, it is possible to have a detailed idea of the bulk

properties of the suspension, with a more sensitive indication of the presence of oversized material. In conclusion, all the microspheres produced at different BSA/GS ratio are almost included in the size range of 1–3  $\mu\text{m}$ .

## 2B 1.4 SOLID STATE MICROSPHERE CHARACTERIZATION

X-ray analyses were performed to have information about the solid state of the produced materials. In the case of microspheres formed by an intimate solid solution on the two components, an amorphous state is expected. The diffraction pattern of coprecipitated microparticles produced at different  $r_{\text{BSA/GS}}$  values are reported in Figure 34. The XRDs of the SAA processed GS and BSA alone are also reported, for comparison. XRD analyses show that all the coprecipitated particles obtained by SAA are amorphous, at all the ratios explored.

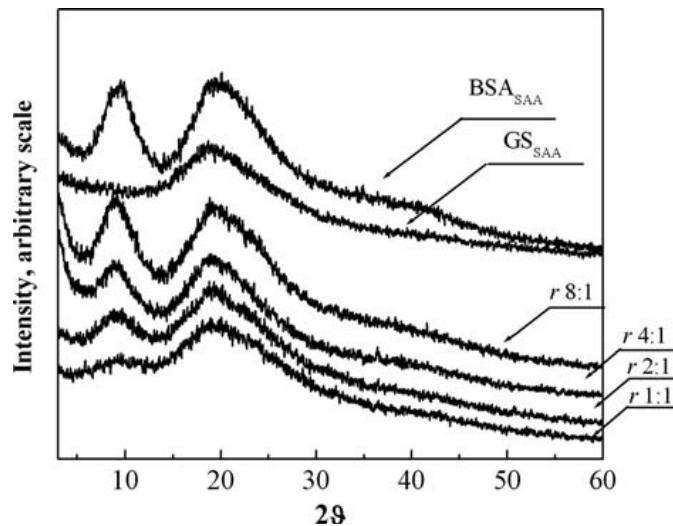


**Figure 34.** XRD of single BSA and GS micronized by SAA and microspheres obtained at different BSA/GS ratios ( $r$ ).

The observed patterns can be justified in the hypothesis that, during the particle formation, the drug and the polymer have no time to separate. The formation of this solid solution is due to the rapid evaporation of the solvent from the droplets that causes the entrapment of drug molecules into the polymeric matrix. The organization of GS molecules into a crystalline structure is hindered by the presence of the BSA chains and the powder is amorphous.

DSC traces of the BSA/GS coprecipitates are reported in Figure 35; the trace of the single BSA and GS micronized by SAA are also reported in the same Figure, for comparison. DSC analyses were also performed on the unprocessed BSA and GS and the resulted DSC traces showed that no substantially differences emerging between untreated and the SAA micronized powders.

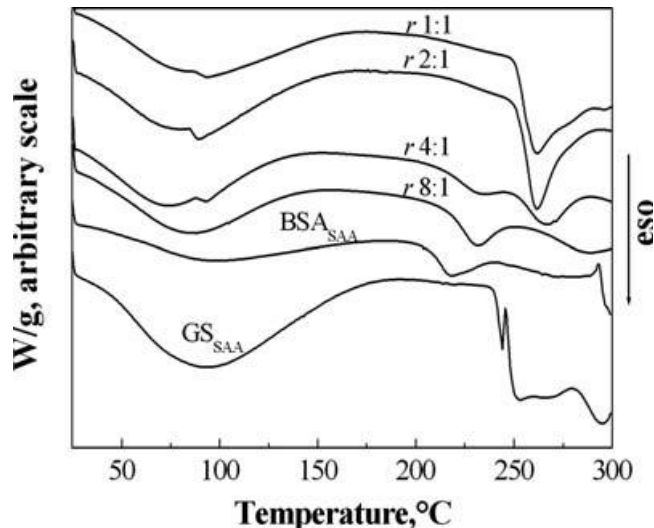


**Fig. 35.** DSC of single BSA and GS micronized by SAA and microspheres obtained at different BSA/GS ratios ( $r$ ).

Looking at the thermal profiles of all the microspheres produced by SAA, it can be confirmed the XRD data; indeed, a thermal behavior that is similar to the single traces of the drug and the carrier is observed. Particularly, the peak of GS decomposition (at 240°C) is more evident decreasing the BSA/GS ratio confirming the decrease of the amount of carrier in the microspheres.

The FT-IR analyses, reported in Figure 36, show the presence of GS inside the BSA microspheres because in all traces it is possible to observe the peaks at 619 and 960–1234  $\text{cm}^{-1}$ , characteristic of GS. It is also clear that no chemical link between the drug and the carrier occurred because no changes in the wavelength of the characteristic peaks are detected: that is, no modifications of the bonds took place.

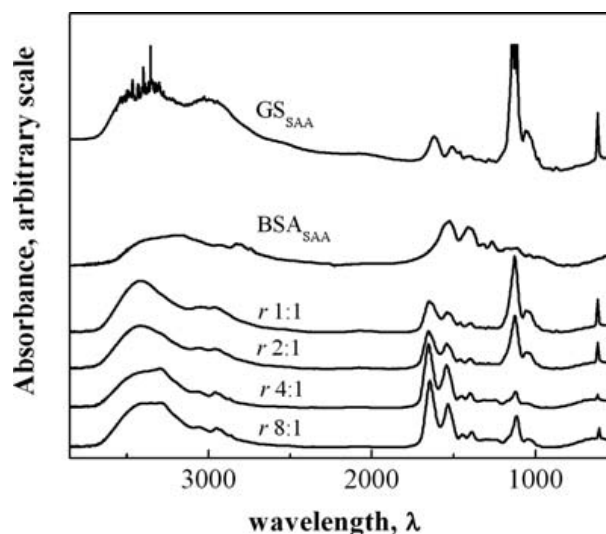


**Fig. 36.** FTIR of single BSA and GS micronized by SAA and microspheres obtained at different BSA/GS ratios ( $r$ ).

## 2B 1.5 MICROSPHERE CHARACTERIZATION: DRUG LOADING AND RELEASE PROFILES

Drug content, encapsulation efficiency and moisture content of BSA/GS microspheres were reported in Table 7.

As expected, the GS content increases by increasing the drug/protein ratio used to formulate the coprecipitates. Encapsulation efficiency is very high for all the microsphere batches tested and it reaches values over 100% when solutions with BSA/ GS ratio higher than 2:1 were processed. This phenomenon might be due to a slight loss of BSA into the saturator leading to a lower BSA/GS ratio before the microparticles formation into the precipitation chamber. Indeed, during the SAA experiments SC-CO<sub>2</sub> and liquid solution are injected in the premixing chamber, fixing the carbon dioxide molar fraction at value of 0.42. The addition of carbon dioxide can induce the precipitation of small quantities of BSA from the solution, generating the so called anti-solvent effect (Reverchon et al., 2006) by SAA.

**Table 7.** Drug Content, Encapsulation Efficiency, and Moisture Content of BSA/GS microspheres manufactured by SAA at different protein/drug ratio.

<b>BSA/GS Ratio</b>	<b>Drug Content (%)</b>	<b>Encapsulation Efficiency (%)</b>	<b>Moisture Content (%)</b>	<b>Moisture Content after 60 days (%)</b>
<b>1:1</b>	47.8 ± 0.3	95.6 ± 0.2	12.38 ± 0.42	16.57 ± 0.75
<b>2:1</b>	32.6 ± 0.1	97.8 ± 0.2	11.31 ± 0.68	15.43 ± 0.76
<b>4:1</b>	20.5 ± 0.2	> 100	10.19 ± 0.53	13.85 ± 0.62
<b>8:1</b>	12.2 ± 0.4	> 100	9.32 ± 0.39	12.31 ± 0.38

The drug content and encapsulation efficiency were calculated correcting the sample weight after the moisture content evaluation. Each point represents the mean ± SD (n = 3).

However, the phenomenon is more evident when the solutions processed have a higher BSA/GS ratio: that is, when a fixed the amount of carbon dioxide is added, the more is the BSA solubilized in the solution injected, the higher is the BSA oversaturation value reached.

Water content of GS processed by SAA, as well as, of other BSA/GS microspheres was obtained by titration. In the case of BSA, it was found to be 6.85% (w/w) ( $\pm 0.58$ ); whereas, the SAA micronized GS exhibited 15% (w/w) ( $\pm 1.38$ ) of water residue and the unprocessed GS had water content of 10% (w/w) ( $\pm 1.98$ ). The difference in water content can be due to the higroscopicity of both raw material and SAA processed GS. Indeed, when GS is exposed to air at ambient conditions is able to uptake a larger amount of water reaching a water content more than 20% (w/ w). On the contrary, BSA/GS microspheres produced by SAA showed lower water content and less water uptake in time than pure GS (see also data reported in Tab. 7). Moreover, the higher was the content of BSA into the formulated coprecipitates the lower were both the primary content and the uptake of water; that is, the less hygroscopic component was able to reduce the interaction between GS and air moisture after its encapsulation.

GS release studies were performed to evaluate the ability of BSA microspheres to control the release of the loaded drug. Franz cells methods was selected to simulate the drug release profile when inserted in a wound dressing structure, while covering and protecting the wound. Initially, the permeation of GS across membrane was studied using pure GS processed by SAA. The profile of GS transport is reported in Figure 37 and it is almost linear with the square root of time, without any time-lag, as expected for a free diffusion of the drug through the membrane.

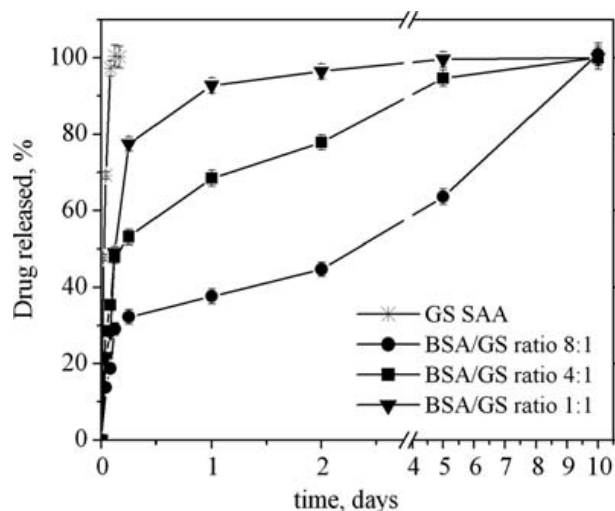


**Fig. 37.** Release profiles of BSA microspheres ( $MS = 2\mu m$ ;  $SD = \pm 1\mu m$ ) manufactured by SAA with different drug loading (mean  $\pm$  SD;  $n = 6$ ).

The results of *in vitro* release of BSA/GS formulations at three different  $r_{BSA/GS}$  values of 1:8, 1:4, and 1:1 are also reported in Figure 37, where the GS concentration in the releasing medium during 10 days of study, is presented. As expected, a higher amount of BSA in the microspheres produces a slower release of the drug, since BSA acts as a barrier to the fast diffusion of GS. Indeed, the diffusion rate is inversely proportional to drug concentration into the microdevices.

All formulations show an intensive release of gentamicin in the first 6 h of the permeation experiment. To be more precise the release is between 30% and 75% for BSA/GS microparticles obtained with  $r_{BSA/GS}$  values of 8:1 and 1:1, respectively. This behavior might be explained by the presence of GS close to the particles surface that is easily delivered to the medium before the swelling of BSA. High release rate of the antibiotic at the beginning of a therapy are very important because the efficiency of the antibiotics is strictly correlated to a high concentration of the drug at the site of infection at the beginning of the therapy (Huang et al., 2001). Moreover, both formulations with  $r_{BSA/GS}$  values

of 4:1 and 8:1, after the preliminary burst effect, are able to release the GS continuously over 10 days, whereas, formulation with a  $r_{\text{BSA/GS}}$  value of 1:1 microspheres releases more than 90% of the drug in less than 2 days.

## **2B 1.6 Conclusions**

SAA was proposed for the production of microparticulate carriers to be employed as drug controlled release system. This is the first time that this technology has been tested for the thermal coagulation of proteic microstructured devices with a mean diameter of around 2  $\mu\text{m}$ . Indeed, all the microspheres produced by SAA exhibited large drug content and very high encapsulation efficiency.

Water content was significantly reduced in BSA/GS microspheres because of the encapsulation of gentamicin in the matrix of BSA denaturated by the SAA process. In fact, pure GS and also SAA micronized GS alone are able to uptake high quantity of moisture by air; whereas, this adverse effect is strongly reduced in the BSA/GS microspheres produced leading to an increase in stability of the drug in these formulations.

The release of GS from the microspheres was found to be diffusion controlled and correlated with BSA concentration. In fact, the higher was the concentration of BSA used to manufacture the microparticles the more prolonged was the release rate of the drug.

BSA/GS are not microsystems usefull to inhalation products; however, formulations with a BSA/GS ratio of 1:4 and 1:8 would be proposed for topical application, as an example, in the treatment of wound infections. In fact, the microsystems may maintain the antibiotic concentration over the

*Results and Discussion*

---

minimal inhibition concentration able to control the growth of various pathogens for more than a week of treatment.

**PART 2: PRODUCTION OF MICRONIZED INHALABLE  
GENTAMICIN POWDER BY SPRAY-DRYING**

**Based on the article:** R.P. Aquino, **L. Prota**, G. Auriemma, A. Santoro, T. Mencherini, G. Colombo, P. Russo. “Dry powder inhalers of gentamicin and leucine: formulation parameters, aerosol performance and *in vitro* toxicity on CuFi1 cells”. *International Journal of Pharmaceutics*. **2012**, *In press*



## **2B 2.1 BACKGROUND AND AIM**

As previously mentioned, the major obstacle to the formulation of a stable and respirable dry powder of gentamicin is the drug hygroscopicity and instability that make unable aerosolization and respirability. In order to produce microparticulate GS powders suitable for inhalation, we investigated the feasibility of the use of spray-drying technology, in particular, the co-spray-drying of GS and an excipient suitable for pulmonary delivery (L-leucine).

As a matter of fact, aminoacids (AAs) are considered to be safe as pulmonary excipients and were recently used to improve aerosolization behavior of several drugs (Ibrahim et al., 2010; Pilcer et al., 2010; Thai et al., 2010; Wang et al., 2009). Among AAs, L-leucine (leu) shows a hydrophobic side chain which potentially may help to reduce G water absorption. Moreover, in a previous part of this PhD thesis, we demonstrated that leu may increase the dispersibility and, consequently, respirability of dry polyphenol powders processed by spray-drying (Prota et al., 2011).

The aim of the present part of the research was to develop, by particle engineering via spray drying, stable GS powders with improved aerodynamic properties and good stability profile which may be used for the treatment of *Pa* infections in CF. Microparticles were designed while studying the effect of leu, feed composition and process parameters on particle formation, physico-chemical properties and aerosol performance. In addition, the effect of the produced powders on cell viability and cell proliferation of bronchial epithelial cells bearing a CFTR F508/ F508 mutant genotype (CuFi1) was investigated.

## 2B 2.2 MANUFACTURING AND CHARACTERIZATION OF GS/LEU CO-SPRAY-DRIED POWDERS

Due to its high polarity, GS powder as raw material was deliquescent, becoming liquid after 1 hour of exposure to room conditions. In order to reduce hygroscopicity and to increase powder dispersibility, GS was spray dried alone or with leu as flowability enhancer using water or water-co-solvent systems with different dielectric constant (water, water/ethanol or water/IPA mixtures): mixtures): batches processed from hydro-alcoholic solutions containing ethanol are indicated as Get and those containing IPA as Giso.

Preliminarily, the solubilities of the drug and excipient in the feed systems were determined; GS freely soluble in water exhibited the lowest solubility in water/IPA 7/3 (v/v) system, the poor solubility of leu is even lower in water-co-solvent systems (Table 8).

**Table 8.** Gentamicin and L-leucine solubility in liquid feeds used for spray drying at pH 7.0±0.1.

Liquid feed composition	G mg/ml	Leu mg/ml
Water	Freely soluble	24.2±1.0
Water/ethanol 8/2 (v/v)	519.4±97.0	14.6±0.3
Water/ethanol 7/2 (v/v)	242.0±25.1	10.1±0.5
Water/IPA 8/2 (v/v)	351.8±25.1	11.2±0.5
Water/IPA 7/3 (v/v)	135.9±24.6	9.5±0.2

As reported in Table 9, addition of the organic co-solvents into the water feed was extremely helpful in terms of spray drying process yield. In particular, less polar IPA led to higher process yield than ethanol. Batch dried from a 7/3

v/v water-IPA solution showed a 30% increase in yield, compared with powder dried from water, suggesting a reduction in powder cohesiveness and, therefore, a potential enhancement of the aerosolisation properties (Li et al., 2005). Differently, leu addition did not have a linear effect on spray drying yield, especially in hydro-alcoholic solutions (Table 9).

**Table 9.** Physical characteristics of spray dried particles: liquid fees composition, process yield, particle size and bulk density.

	Code #	Leu content % w/w	Process yield (%)	d <sub>50</sub> (µm) and ( ) span	Bulk density (mg/ml)		Code #	Leu content % w/w	Process yield (%)	d <sub>50</sub> (µm) and ( ) span	Bulk density (mg/ml)
20% v/v ethanol	Get2	0	61.2 ±5.4	4.42 (1.98)	0.13 ±0.02	20% v/v IPA	Giso2	0	78.0 ±3.8	4.74 (2.10)	0.11 ±0.02
	Get2-Leu5	5	77.6 ±2.2	4.03 (1.55)	0.22 ±0.01		Giso2-Leu5	5	73.9 ±0.5	6.19 (1.88)	0.16 ±0.02
	Get2-Leu10	10	58.0 ±3.2	4.58 (2.04)	0.36 ±0.01		Giso2-Leu10	10	65.0 ±5.5	4.07 (1.81)	0.29 ±0.01
	Get2-Leu15	15	69.3 ±0.3	4.65 (1.94)	0.35 ±0.02		Giso2-Leu15	15	84.6 ±3.3	3.72 (1.58)	0.34 ±0.00
	Get2-Leu20	20	72.6 ±1.1	4.46 (1.88)	0.32 ±0.01		Giso2-Leu20	20	77.5 ±0.6	4.82 (1.73)	0.33 ±0.01
	30% v/v ethanol	Get3	0	74.8 ±2.5	4.01 (1.82)		0.15 ±0.01	30% v/v IPA	Giso3	0	85.5 ±0.7
Get3-Leu5		5	69.4 ±2.2	4.34 (1.81)	0.24 ±0.02	Giso3-Leu5	5		86.6 ±1.2	3.77 (1.36)	0.17 ±0.01
Get3-Leu10		10	82.5 ±3.1	3.59 (1.57)	0.29 ±0.00	Giso3-Leu10	10		85.9 ±0.9	3.69 (1.51)	0.26 ±0.02
Get3-Leu15		15	68.2 ±4.1	4.16 (1.71)	0.34 ±0.00	Giso3-Leu15	15		82.0 ±2.1	3.90 (1.62)	0.34 ±0.01
Get3-Leu20		20	68.9 ±2.1	4.65 (1.88)	0.31 ±0.01	Giso3-Leu20	20		80.8 ±1.3	4.11 (1.90)	0.30 ±0.00

HPLC analysis evidenced that the amount of GS and leu detected in all produced batches was almost 100% of nominal load, therefore indicating that the spray drying process on the selected conditions neither determined loss nor modified G/leu ratio in the final product. Particle size analysis showed that spray-drying allowed to obtain micronized powders with d<sub>50</sub> (ranging from 3.6 µm to 4.8 µm) similar for all batches produced (Table 9), with no evident effect of co-solvent and leu content on the particles diameter.

Organic co-solvent had a massive effect on hygroscopicity too (Fig. 38). In particular, by adding 30% v/v of IPA into the aqueous feed, humidity uptake by G powders was reduced from 10.5% (water) to 4.8% (water/IPA) after exposure at room conditions. In the presence of 10% w/w leu, GS lost its water avidity (0.9% weight gained after 80 min). These effects may be explained by the addition of the lower-soluble component (leu) into the liquid feeds, able to reach the critical concentration for shell formation as the droplet evaporation progresses during spray-drying process (Vehring, 2008). Such enrichment in leu at the particle surface may slow down water uptake of GS in agreement with previous observations (Shur et al., 2008) and, potentially, increase powder flowability.

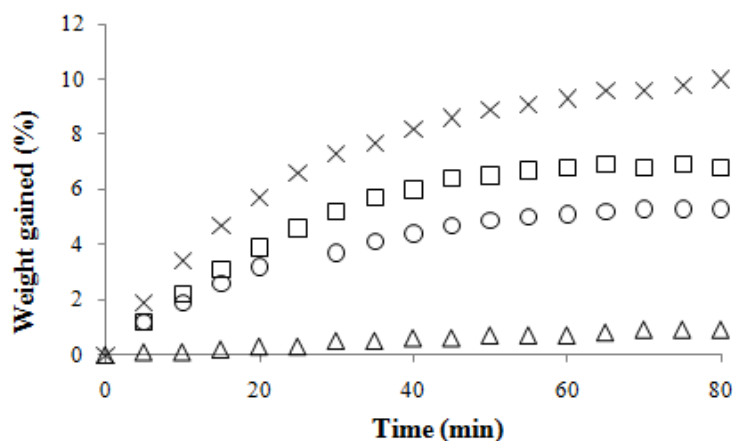


**Fig. 38.** Weight gained after 80 min of exposure at room conditions by G raw material (cross), G spray-dried from 7:3 water-ethanol (squares) or water-IPA (circles) v/v systems, and G/10%leu spray-dried from water-IPA 7:3 v/v mixture (triangles).

Leu effect on spray-dried powders appears clearly, after microscopy studies, as an evident increase in particle corrugation. Morphology studies showed an increase in particle corrugation as an effect of leu presence in spray-dried

powders. As an example, SEM pictures of particles dried from 8:2 water/ethanol ratio solutions were reported in Fig. 39.

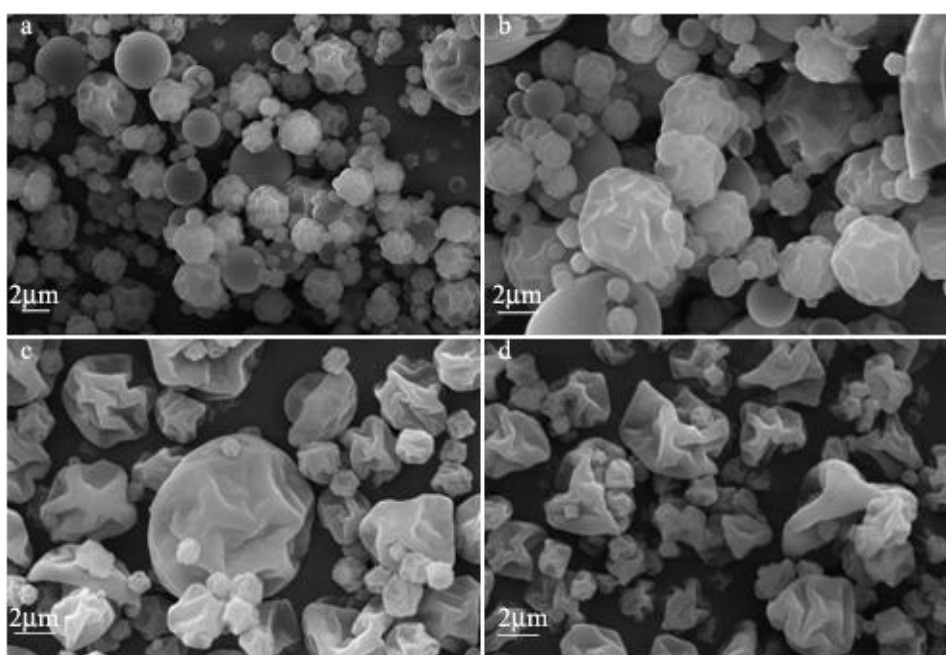


**Fig. 39.** SEM pictures of powders dried from water/ethanol 8:2 v/v systems containing: a) GS; b) GS/5% leu; c) GS/10% leu; d) GS/20% leu.

As well known, the morphology of spray-dried particles is strongly influenced by the solubility of the components and their initial saturation in the liquid feeds. GS, freely soluble in water, led to the formation of spherical particles when spray dried alone (Fig. 39a, GS). According to previous observations (Lechuga-Ballesteros et al., 2008), during the co-spray drying process, the saturation of the lower-soluble component (leu) may increase faster than that of hydrophilic one (GS), due to the preferential evaporation of alcohol and the associated change in the solvent/co-solvent ratio. This led to the formation of a primary solid shell which collapsed, hence corrugated microparticles were

formed. As the relative amount of the less soluble component increased, particle corrugation was more and more evident; particles from almost spherical became raisins like (Fig. 39b, GS/5%leu) or irregularly wrinkled (Fig. 39d, GS/20%leu). Such surface modification has been shown to be beneficial for particles intended for inhalation (Chew et al., 2001): a corrugated surface improves powder dispersibility by minimizing contact areas and reducing interparticulate cohesion and, therefore, corrugated particles disperse better than spherical ones.

By modifying particle shape and corrugation degree, leu influenced powder bulk density too (Table 9). In fact, powders processed from hydro-alcoholic systems showed lower bulk density values than those spray-dried from water (Table 9), whereas leu inclusion up to 15% w/w led to higher density powders. Further increase in leu content up to 20% w/w produced powders with similar or slightly lower bulk density.

As well known, differences in bulk density influence the amount of powder chargeable into the capsules for the inhalation, which shifted from 60 mg for neat GS to 120 mg for GS/10-20%leu. As a consequence, an important effect on the patient compliance can be achieved in the case of antibiotics such as GS requiring the administration of high doses. Previously, a pilot study on effectiveness and toxicity of GS administered as dry powder inhaler, (Crowther Labiris et al., 1999) reported that 32 actuations of the device were necessary to emit 160 mg of GS nominal dose. In the case of GS/10-20%leu DPI, the possibility to charge higher amount of drug into the device allows the administration of 108 mg (GS/10%leu) or 96 mg (GS/20%leu) of GS each time, with a dramatic reduction in the number of actuations required.

## 2B 2.3 AERODYNAMIC BEHAVIOR OF GS/LEU POWDERS

The preliminary screening of the powder aerosol performance was carried out by Single Stage Glass Impinger using Turbospin<sup>®</sup> as inhaler device. Capsules were filled with different amount of dry powder (60-120 mg), depending on its bulk density.

Batches dried from water were hygroscopic, cohesive powders, difficult to insert into and come out from the capsule and with unsatisfying aerodynamic properties (data not shown). In particular, neat GS dried from water was a cohesive and sticky material, unable to be aerosolized.

Results from *in vitro* SSGI deposition experiments for batches different in co-solvent and aminoacid content are reported in Table 10.

**Table 10.** Aerodynamic properties of spray-dried powders after single stage glass impinger deposition experiments. All data are shown as mean  $\pm$  SD of three experiments.

Code #	Leu content % w/w	Charged Dose (mg)	Emitted Dose (%)	FPF (%)	FPD (mg)	Code #	Leu content % w/w	Charged Dose (mg)	Emitted Dose (%)	FPF (%)	FPD (mg)		
20% v/v ethanol	Get2	0	60	95.6 $\pm 1.4$	17.3 $\pm 3.8$	10.4 $\pm 2.3$	20% v/v IPA	Giso2	0	60	95.8 $\pm 1.9$	14.5 $\pm 7.8$	8.7 $\pm 4.7$
	Get2-Leu5	5	90	98.0 $\pm 0.3$	23.7 $\pm 9.2$	20.2 $\pm 7.9$		Giso2-Leu5	5	80	98.0 $\pm 0.2$	21.9 $\pm 5.1$	16.6 $\pm 3.9$
	Get2-Leu10	10	120	99.2 $\pm 0.1$	28.9 $\pm 5.2$	31.3 $\pm 5.6$		Giso2-Leu10	10	120	99.4 $\pm 0.1$	32.6 $\pm 5.6$	35.2 $\pm 6.0$
	Get2-Leu15	15	120	99.3 $\pm 0.3$	31.0 $\pm 1.5$	31.6 $\pm 1.5$		Giso2-Leu15	15	120	99.6 $\pm 0.2$	46.8 $\pm 0.5$	47.7 $\pm 0.5$
	Get2-Leu20	20	120	99.2 $\pm 0.1$	40.8 $\pm 1.5$	39.2 $\pm 1.5$		Giso2-Leu20	20	120	99.3 $\pm 0.3$	50.9 $\pm 1.0$	48.8 $\pm 0.9$
	30% v/v ethanol	Get3	0	60	95.7 $\pm 2.2$	18.9 $\pm 4.8$		13.4 $\pm 2.9$	30% v/v IPA	Giso3	0	60	90.9 $\pm 7.9$
Get3-Leu5		5	80	98.0 $\pm 0.5$	14.9 $\pm 1.5$	11.4 $\pm 1.1$	Giso3-Leu5	5		70	97.2 $\pm 0.5$	22.3 $\pm 3.0$	14.8 $\pm 2.0$
Get3-Leu10		10	100	98.5 $\pm 0.6$	38.6 $\pm 5.7$	34.7 $\pm 5.1$	Giso3-Leu10	10		110	99.4 $\pm 1.1$	28.8 $\pm 5.0$	28.4 $\pm 5.0$
Get3-Leu15		15	120	98.9 $\pm 0.2$	43.6 $\pm 2.7$	44.5 $\pm 2.8$	Giso3-Leu15	15		120	99.1 $\pm 0.3$	49.4 $\pm 0.8$	50.4 $\pm 0.8$
Get3-Leu20		20	120	99.0 $\pm 0.1$	46.5 $\pm 1.5$	44.7 $\pm 1.4$	Giso3-Leu20	20		120	99.2 $\pm 0.0$	50.2 $\pm 1.0$	48.2 $\pm 0.9$

FPF, fine particle fraction; FPD, fine particle dose

GS spray drying from water/organic co-solvent (e.g. water/ethanol-based Get2 and Get3, water/IPA-based Giso2 and Giso3) reduced powder cohesivity and enabled the aerosolization process; however, the resulting aerodynamic properties were still not satisfying (FPF less than 15%). The inclusion of leu substantially increased emitted doses (ED up to 99.6% for #Giso2-Leu15) and fine particle fractions (FPF up to 49.4% for #Giso3-Leu15). Taking into account the relative reduction in drug content, further increase in the excipient/drug ratio up to 20/80 w/w did not improve DPI performance. As to the effect of organic co-solvents, the use of IPA led to the best FPF and FPD values. As example, Giso3-Leu15 formulations, containing 15% w/w of leu and obtained from 30% v/v of IPA/water feed, emitted 50.4 mg of fine GS after one actuation of the Turbospin device, compared to a FPD of 44.5 mg of Get3-Leu15, containing the same amount of leu and co-solvent, but processed from ethanol. These results are in agreement with previous studies (Chew et al., 2001; Chew et al., 2005; Weiler et al., 2010) evidencing the enhancement of powder aerosol performance as particle surface corrugation goes up to a certain degree; further corrugation enhancement did not improve aerodynamic properties. Plotting FPF values of powder dried from 20% IPA feed versus growing leu amounts (Fig. 40) and in relation to SEM micrographs, a dramatic increase in both particle corrugation and FPF was shown as the leu content enhanced.

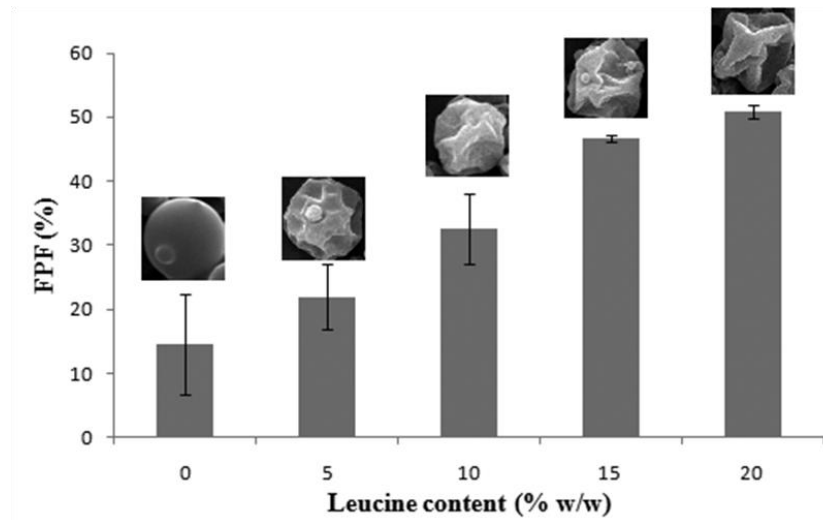


**Fig. 40.** FPF and SEM images of G powders spray-dried from liquid feeds containing 20% IPA and increasing amount of leu.

On the basis of these interesting preliminary results, powders containing 15 or 20% w/w of leu were analyzed by means of Andersen cascade impactor too, in order to study details of their aerodynamic properties. Results are reported in Table 11.

**Table 11.** Aerodynamic properties of G spray-dried powders containing 15 or 20% w/w leu after Andersen cascade impactor deposition experiments.

Batch	Feed Solution composition		MMAD ( $\mu\text{m}$ )	FPF (%)	FPD (mg)
	% Leu (w/w)	solvent (v/v)			
Get2-Leu15	15	Water/ethanol 8/2	$4.20 \pm 0.28$	$39.2 \pm 1.2$	$38.9 \pm 1.5$
Get2-Leu20	20	Water/ethanol 8/2	$4.06 \pm 0.10$	$42.8 \pm 0.7$	$40.9 \pm 2.5$
Get3-Leu15	15	Water/ethanol 7/3	$4.31 \pm 0.25$	$40.6 \pm 4.6$	$47.5 \pm 3.9$
Get3-Leu20	20	Water/ethanol 7/3	$3.93 \pm 0.20$	$45.3 \pm 2.0$	$41.9 \pm 2.1$
Giso2-Leu15	15	Water/IPA 8/2	$4.02 \pm 0.13$	$46.0 \pm 2.7$	$49.3 \pm 1.7$
Giso2-Leu20	20	Water/IPA 8/2	$4.17 \pm 0.12$	$42.5 \pm 0.2$	$39.3 \pm 0.3$
Giso3-Leu15	15	Water/IPA 7/3	$3.45 \pm 0.16$	$58.1 \pm 3.6$	$56.4 \pm 1.1$
Giso3-Leu20	20	Water/IPA 7/3	$3.31 \pm 0.11$	$58.0 \pm 0.5$	$54.7 \pm 2.2$

MMAD, mass median aerodynamic diameter; FPF, fine particle fraction; FPD, fine particle dose.

MMAD, FPF and FPD values obtained by ACI deposition studies confirmed the previously observed trend. Capsules charged with 120 mg of powder emitted almost the whole dose from the device after the pump actuation, as indicated by  $ED \geq 99\%$ . Increase of leu content from 15 to 20% w/w did not enhance the powder aerosol efficiency, whereas a reduction in particles MMAD values as well as a general improvement in powder aerosol performance was observed for batches processed from higher amount of co-solvent, especially IPA (Giso). Among all batches produced, Giso3-Leu15 (GS/15%leu from 30% v/v of IPA/water feed) showed very satisfying aerodynamic properties as proved by MMAD of 3.45  $\mu\text{m}$ , FPF 58.1% and FPD of 56.4 mg (Table 11).

For a preliminary screening of stability, powders were stored in a climatic chamber for 6 months at  $25\text{ }^{\circ}\text{C} \pm 2\text{ }^{\circ}\text{C}/60\% \text{ RH} \pm 5\% \text{ RH}$ . During this time, no variation in powder weight was observed, GS content remained unaltered and no GS degradation product was recorded by HPLC analyses of aged powders. Moreover, in order to evidence possible changes in inhalation performance, ACI studies were repeated on 15% leu powders. Results (Table 12, black rows) showed that ED, FPF and FPD values of aged powders were not significantly different with respect to the fresh ones except for #Get2leu15 showing slightly lower FPD (from 38.8 mg to 33.7 mg). These findings confirmed that GS/Leu systems designed are not hygroscopic and are able to preserve a high dispersibility even after 6 month storage.

**Table 12.** Aerodynamic properties of G spray-dried powders containing 15 or 20% w/w leu after Andersen cascade impactor deposition experiments (t=0). Experiments were repeated on powders containing 15% leu w/w after 6 month storage: results are reported in black rows.

	Code #	ED (%)	MMAD (μm)	FPD (mg)	FPF (%)		Code #	ED (%)	MMAD (μm)	FPD (mg)	FPF (%)
ethanol	Get2-Leu15 (t=0)	99.2 ±0.3	4.2 ±0.3	38.8 ±1.5	39.2 ±1.2	IPA	Giso2-Leu15 (t=0)	99.7 ±0.3	4.0 ±0.1	49.3 ±1.7	46.0 ±2.7
	Get2-Leu15 (t=6 months)	99.4 ±0.3	4.4 ±0.2	33.7 ±2.3	35.4 ±1.5		Giso2-Leu15 (t=6 months)	99.3 ±0.2	3.5 ±0.1	50.6 ±2.0	49.0 ±1.8
	Get3-Leu15 (t=0)	99.5 ±0.3	4.3 ±0.2	47.5 ±3.9	40.6 ±4.6		Giso3-Leu15 (t=0)	99.2 ±0.3	3.4 ±0.2	56.4 ±1.1	58.1 ±3.6
	Get3-Leu15 (t=6 months)	99.4 ±0.3	3.8 ±0.3	46.7 ±3.2	44.4 ±1.8		Giso3-Leu15 (t=6 months)	99.2 ±0.4	3.3 ±0.2	56.1 ±0.6	52.5 ±0.0

ED, emitted dose; MMAD, mass median aerodynamic diameter; FPF, fine particle fraction; FPD, fine particle dose.

## 2B 2.4 EFFECT OF GS/LEU POWDERS ON VIABILITY OF CF AIRWAYS EPITHELIUM

In order to establish whether the particle engineering has any cytotoxic or cytostatic effect on bronchial epithelial cells bearing a CFTR F508/ F508 mutant genotype (CuFi1) (Dehecchi et al., 2008; Zabner et al., 2003), CuFi1 cells were treated for 24 h with increasing concentrations (from 0.0002 to 2 μM expressed as GS content) of Get3 or Get3-Leu15 powders in comparison to rawGS. Results indicated that neither rawGS nor its formulations generally inhibited cells viability as determined by MTT assay (Fig. 41B). At concentrations higher than 0.02 μM, a slight but significant decrease in cell survival was detected only for rawGS. An interesting observation is that an increase in leu content up to 15%, as in Get3-Leu15, faintly but not significantly decreased CuFi1 viability at concentration ranging from 0.02 to 0.2 μM (P<0.05) (Fig. 41B) whereas at 2.0 μM did not. As previously reported (Holt et al., 1985; Prota et al., 2011; Switzer et al., 2009), this effect seems to

be related to leu ability to improve cell proliferation and metabolism of bronchial epithelial CF cells.

Furthermore ELISA BrdU immunoassay evidenced that rawGS slightly reduced CF cell growth only at the highest concentration (2  $\mu\text{M}$ ,  $P<0.01$ ) (Fig. 41 A).

Therefore, particle engineering producing GS/leu systems had no cytotoxic or cytostatic effect on CF epithelial lung cells (CuFi1 model), compared to neat rawGS, at concentrations up to 2  $\mu\text{M}$ .

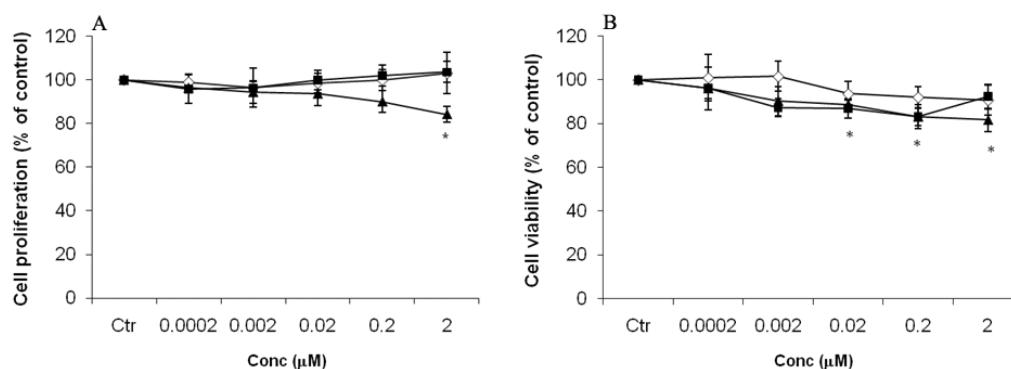


**Fig. 41.** Effect of Gentamicin and its DPI formulations on CuFi1 cell proliferation and viability. Cells were treated for 24 h with: raw Gentamicin (rawG, ▲), spray-dried Gentamicin (Get3 ◇) and G co-sprayed with 15%w/w leucine (Get3-Leu15 ■) at concentrations from 0.0002  $\mu\text{M}$  to 2  $\mu\text{M}$ . Cell growth (A) was determined using a colorimetric bromodeoxyuridine (BrdU) cell proliferation ELISA kit. Cell viability (B) was determined by MTT assay. All data are shown as mean  $\pm$  SD of three independent experiments, each done in duplicate (\* $P<0.05$  and \*\* $P<0.01$  vs control).

## 2B 2.5 Conclusions

The engineering process by spray drying and the use of water-co-solvent systems as liquid feed reduced GS hygroscopicity and stickiness, allowing its aerosolization. Moreover, the addition of small amount of safe excipient, as

leu, led to powder with an excellent emitted dose and good aerodynamic properties after actuation of the Turbospin device. In particular, dry powder inhalers containing 15% of leu (Giso 3-Leu 15) was able to deliver almost 100 mg of GS with a 58% of FPF after a single actuation. Preliminary stability studies evidenced that dry powders preserved good inhalation performance after a 6 month storage at room conditions. Finally, the engineered particles showed no cytotoxic or cytostatic effect on bronchial epithelial cells bearing a CFTR F508/ F508 mutant genotype.

These findings together with the well known GS antibiotic activity and ability to partially restore CFTR expression in class I nonsense mutation, support the use of GS/leu DPI as a valid alternative to antibiotics already used in the management of *Pa* infections.

Oncoming advance of the present project is to test whether the processing alters the drug bioactivity, investigating the antibacteric activity of GS/Leu formulations as related to effect of spray-drying process, leucine presence and storage conditions of the engineered particles.



# **EXPERIMENTAL PROCEDURES**



**SECTION A**

***DESIGN AND DEVELOPMENT OF A DPI OF NARINGIN  
TO TREAT INTRINSIC INFLAMMATION IN CF PATIENTS***

**Based on the article:** L. Prota, A. Santoro, M. Bifulco, R.P. Aquino, T. Mencherini, P. Russo. “Leucine enhances aerosol performance of Naringin dry powder and its activity on cystic fibrosis airway epithelial cells”. *International Journal of Pharmaceutics*. **2011**, 412, 8 – 19.



### **3A.1 Chemicals**

Naringin, l-aa (arginine, histidine, leucine, lysine, proline, threonine), dimethyl sulphoxide (DMSO) and sodium hydroxide anhydrous pellets were supplied by Sigma–Aldrich (Milan, Italy). Ethanol 96% and dichloromethane (for analysis, USP grade) were purchased from Carlo Erba Reagents (Milan, Italy). Size 2 gelatine capsules were kindly offered by Qualicaps Europe S.A. (Madrid, Spain). The device used for aerodynamic tests was Turbospin<sup>®</sup> kindly donated by PH&T SpA (Milan, Italy). All the cell culture reagents were purchased from Lonza.

### **3A.2 Powders preparation and yield**

Micronized particles were prepared by co-spray drying N and the aa (total powder concentration 2%, w/v) from different hydro-alcoholic feeds. Formulation parameters were (i) kind of AA, (ii) N to excipient ratio (100:0, 95:5 and 90:10 (w/w), respectively) and (iii) ethanol/water ratio, ranging between 3:7 (v/v) to 1:1 (v/v). N was solubilized into ethanol and the selected AA into water. The solutions were neutralized with 1 N sodium hydroxide (about 200  $\mu$ L) and spray-dried using a Buchi B-191 mini spray dryer (Fig. 42) (Buchi Laboratoriums-Tecnik, Switzerland).

Applied process parameters, selected on the basis of pilot experiments, were: inlet temperature 110° C, approximate outlet temperature 68–72 °C, drying air flow 500 L/min, aspirator capacity 100%, air pressure 6 atmospheres, feed rate 5 ml/min, nozzle 0.5 mm. As a reference, powders of neat AA (0.2%, w/v) from 3:7 (v/v) ethanol/water feed were produced under the same operative conditions.



**Fig. 42.** Buchi B-191 mini spray dryer.

Each preparation was carried out in triplicate. All the spray-dried powders were collected and stored under vacuum for 48 h at room temperature. Production yields were expressed as weight percentage of the final product over the total amount of sprayed material.

### **3A.3 Powders physico-chemical properties**

#### **3A.3a Particle size**

Particle size of both raw materials and microparticles were determined using a light-scattering laser granulometer equipped with a micro-liquid module (LS 13 320 Beckman Coulter Inc., FL, USA). The LS 13 320 uses a 5 mW laser diode with a wavelength of 750 nm and reverse Fourier optics incorporated in a fibre optic spatial filter and binocular lens systems. In preliminary studies, dichloromethane was chosen as suspending medium of choice (Sansone et al., 2009). Samples were suspended in dichloromethane and sonicated for 2 min: few drops of each sample were poured into the small-volume cell to obtain an

obscuration between 8 and 12%. Particle size distributions were calculated by instrument software, using the Fraunhofer model. Results were expressed as  $d_{50}$  and span, defined as  $[d(90) - d(10)]/d(50)$ , where  $d(10)$ ,  $d(50)$  and  $d(90)$  indicate diameters at the 10th, 50th and 90th percentiles of the particle size distribution, respectively.

### **3A.3b Particle morphology**

Morphology of raw materials and microparticles was examined using a scanning electron microscope (SEM) Zeiss EVO MA10 (Carl Zeiss SMT AG, München-Hallbergmoos, Germany) operating at 14 kV.

### **3A.3c DSC analysis**

Differential scanning calorimetry (DSC) was performed with an Indium-calibrated Mettler Toledo DSC 822e (Fig. 43) (Mettler Toledo, OH, USA).



**Fig. 43.** DSC 822<sup>e</sup>.

Accurately weighed samples (3–5 mg) (MTS Mettler Toledo microbalance, OH, USA) were placed in a 40  $\mu$ L aluminium pan, which was sealed, pierced and exposed to two thermal cycles, as reported elsewhere (Sansone et al., 2009). In the dehydration cycle measurements, the sample was heated up to 130 °C at a heating rate of 20 °C/min and kept at 130 °C for 15 min to remove

the residual solvent. Afterwards, the samples were cooled down to 25 °C and heated up to 350 °C at a heating rate of 10 °C/min.

### **3A.3d X-ray diffraction studies**

Dried samples were studied by means of X-ray diffraction measurement (XRD) with a Rigaku D/MAX-2000 diffractometer (Rigaku Corporation, Tokyo, J) using a Ni-filtered Cu-K $\alpha$  radiation (40 kV, 20 A).  $2\theta$  range was set from 5 to 50, step size 0.03/ $2\theta$  and 5 s counting time per step. A Rigaku imaging plate, mod. R-AXIX DSBC, was used for digitizing the diffraction patterns.

### **3A.3e Bulk and tapped density**

The bulk and tapped density of the spray-dried powders were measured as described elsewhere (Sansone et al., 2009). Briefly, powders were loaded into a bottom-sealed 1 mL plastic syringe (Terumo Europe, Leuven, Belgium) capped with laboratory film (Parafilm<sup>®</sup> “M”, Pechiney Plastic Packaging, Chicago, IL, USA) and tapped on a hard bench until no change in the volume of the powder was observed. The bulk density was calculated from the difference between the weight of the plastic syringe before and after loading divided by the volume of powder in the syringe. The tapped density was calculated from the difference between the weight of the plastic syringe before and after loading divided by the volume of the powder in the syringe after tapping. Experiments were performed in triplicate.

### 3A.4 Aerodynamic behaviour evaluation

The *in vitro* deposition of the micronized powders was evaluated using a single-stage glass impinger (SSGI, apparatus A European Pharmacopoeia 6.0, Copley Scientific Ltd., Nottingham, UK) (Fig. 44).



**Fig. 44.** Single Stage Glass Impinger.

A water/ethanol 8:2 (v/v) mixture was introduced in the upper (7 mL) and lower (30 mL) stages of the SSGI. Hard gelatine capsules (size 2) were filled manually with  $20.0 \pm 0.5$  mg of spray-dried powders. Then, the capsule was introduced into the Turbospin<sup>®</sup> (Fig. 45) and pierced twice.



**Fig. 45.** Turbospin<sup>®</sup>.

The vacuum pump was operated at a flow rate of 60 L/min for 5 s (Erweka vacuum pump VP 1000 equipped with an electronic digital flowmeter type DFM, Erweka Italia, Seveso (MI), Italy). Each deposition experiment was

performed on 10 capsules and repeated in triplicate. Upper and lower stages were washed with 500 ml of an 8:2 (v/v) water/ethanol mixture.

The N deposited into the upper and lower stages of the impinger was evaluated by UV detection (UV/vis spectrometer Lambda 25, Perkin Elmer instruments, MA, USA) at a wavelength of 283 nm, using 1 mm spectroscopy SUPRASIL<sup>®</sup> quartz cell (100-QS, Hellma Italia srl, Milan, I). Calibration curves were previously worked out and proportionality between N concentration and absorption was verified in the range of 70–400 mg/L. The emitted dose (ED) was gravimetrically determined and expressed as percentage of powder exiting the device *vs* amount of powder introduced into the capsule (Giry et al., 2006). The fine particle fraction (FPF), defined as ratio of N recovered from the lower stage of SSGI *vs* total N charged into the capsules, was expressed as a percentage (Sansone et al., 2009).

The powders showing promising aerosolisation properties were also tested with an Andersen cascade impactor (apparatus D, European Pharmacopoeia 6.0, ACI, Westech Instrument Services Ltd., Bedfordshire, UK) (Fig. 46), modified for use at a flow rate of 60 L/min as described elsewhere (Gilani et al., 2005 and Seville et al., 2007).

The effective cut-off diameters of the modified ACI, provided by the producer, were: Stage -1, 8.6  $\mu\text{m}$ ; Stage -0, 6.5  $\mu\text{m}$ ; Stage 1, 4.4  $\mu\text{m}$ ; Stage 2, 3.2  $\mu\text{m}$ ; Stage 3, 2.0  $\mu\text{m}$ ; Stage 4, 1.1  $\mu\text{m}$ ; Stage 5, 0.54  $\mu\text{m}$ ; Stage 6, 0.25  $\mu\text{m}$ . To minimize particle bounce, metal impaction plates were dipped into an *n*-hexane solution of SPAN 80 (0.1%, w/v) and the solvent was allowed to evaporate, leaving a thin film of SPAN 80 on the plate surface. The ACI was assembled placing a filter paper on the filter and the Turbospin<sup>®</sup> was fitted into a rubber mouth piece attached to the throat. The vacuum pump was actuated for 4 s.



**Fig. 46.** Andersen cascade impactor.

The powder deposited into the different stages was recovered by plunging each plate and the stage below into a water/ethanol mixture 8:2 (v/v) (5–200 mL depending on the stage number). N content was assessed by UV measurements and the emitted dose (ED) was determined as described above for SSGI experiments. The cumulative mass of powder with a diameter lower than the stated size of each stage was calculated and plotted as a percentage of recovered powder *vs* cut-off diameter. The mass median aerodynamic diameter (MMAD) of the particles was extrapolated from the graph, according to the European Pharmacopoeia 6.0. From the same plot, the fine particle dose (FPD), i.e. the mass of N with a particle size less than 5  $\mu\text{m}$ , and the fine particle fraction (FPF), i.e. the fraction of N emitted from the device with a particle size less than 5  $\mu\text{m}$ , were determined (European Pharmacopoeia 6.0). *In vitro* deposition experiments were performed on three batches with three replicates each.

### 3A.5 Dissolution study

Information about immediate solubility of the powders was obtained by a modified dissolution test (Hancock and Parks, 2000). Briefly, an excess of micronized powder (1.6 g) was introduced together with a magnetic bar into a

40 mL closed, flat-bottomed glass vial, and 25 mL of distilled water heated at 37 °C were added. The dissolution medium was kept at 37 °C in a water bath under magnetic stirring at 300 rpm: at regular time intervals the liquid phase was withdrawn, replaced with distilled water at the same temperature, filtered with 0.45 µm filters, diluted and analyzed by UV–visible spectroscopy for N content. Dissolution tests were carried out in triplicate and monitored for 120 min. Results obtained after 30 min are reported.

### **3A.6 Biological activity**

#### **3A.6a Cell lines and culture conditions**

CuFi1 and NuLi1 cell lines, derived from human bronchial epithelium of a CF (CuFi1, CFTR  $\Delta$ F508/ $\Delta$ F508 mutant genotype) and a non-CF subject respectively (NuLi1, WT CFTR), (Zabner et al., 2003) were purchased from American Type Culture Collection (ATCC, Manassas, VA, USA). CuFi1 and NuLi1 cells were grown in human placental collagen type VI coated flasks (Sigma–Aldrich, Milan, Italy) in BEGM medium (Lonza Walkersville, Inc). Cells were incubated at 37 °C in a humidified atmosphere containing 5% CO<sub>2</sub>.

#### **3A.6b Proliferation assay**

Cell growth was assessed by using a colorimetric bromodeoxyuridine (BrdU) cell proliferation ELISA kit (Roche Diagnostics, Milan, Italy). Briefly,  $5 \times 10^3$  cells were seeded into each coated well of a 96-well plate and left to adhere to the plate. The cells were then treated with increasing concentrations (from 15 to 150 µM) of rawN, N-1 and N-leu 1 for 24 h, and BrdU was added for the final 16 h ( $10^{-5}$  mol/L). At the end of the whole cell culture period, the medium was removed and the ELISA BrdU immunoassay was performed as described by the manufacturer. The colorimetric reaction was stopped by

adding H<sub>2</sub>SO<sub>4</sub>, and the absorbance at 450 nm was measured using a microplate reader (Bio-Rad Laboratories, Milan, Italy).

DMSO alone (0.1% final concentration in cell culture medium) did not give any significant result in all biological *in vitro* assays.

### 3A.6c Western blot analysis

For *in vitro* biological studies, the powders were dissolved in the cell culture medium and immediately administered to the cells at a concentration of 30 μM.

CuFi1 and NuLi1 cells, treated with rawN, N-1 and N-leu 1 were collected by centrifugation, washed twice with PBS and resuspended in RIPA buffer (NaCl 150 mM, 1% triton X-100 pH 8.0, 0.5% sodium deoxycholate, 0.1% SDS, 50 mM Tris, pH 8.0) at 4 °C and centrifugated at 13,000 rpm for 30 min. Supernatants were collected and protein concentrations determined by Bio-Rad protein assay. Equal amounts of protein extracts (30 μg) were boiled in Laemmli's buffer, fractioned on 12% SDS-PAGE and then transferred to nitrocellulose membranes (Amersham GE Healthcare, Milan, Italy). Membranes were blocked in TBS-T (50 mM Tris, 135 mM NaCl, and 5 mM KCl, 0,1% Tween-20) containing 5% fat free dry milk, washed in TBS-T, then incubated overnight at 4 °C with anti-IKKα, anti-IKKβ, phosphoERK1/2 (Thr202/Tyr204) and anti-phospho-IkBα (Ser32) (all from Cell Signaling Technology Inc). After three washes, blots were probed with mouse or rabbit horseradish peroxidase-conjugated secondary antibodies (Cell Signaling Technology) for 1 h at room temperature and then developed using the ECL chemiluminescence system (Amersham GE Healthcare). Finally, membranes were stripped and re-probed with total anti-ERK1/2, total anti-IkBα (Cell Signaling Technology) and anti-actin used as loading control (Abcam, Cambridge, UK). Results are the mean of at least three independent

experiments with three replicates each and immunoreactive bands were quantified using Quantity One I-D analysis software (Bio-Rad).

### **3A.6d Interleukin-8 (IL-8) and interleukin-6 (IL-6) release determinations in CuFi1 cells**

200,000 cells were plated on human placental collagen type VI coated plates as previously described. The cells were left to adhere to the plate and then were pretreated with N-leu 1 (at a concentration of 30 and 60  $\mu\text{M}$ ) for 2 hours and stimulated with LPS from *Pseudomonas aeruginosa* (100 ng/mL) for 14 hours. The cultured media were then collected, centrifuged for 5 min at 2000 rpm and the release of IL-8 and IL-6 was determined by Enzyme-linked immunosorbent assay ELISA (R&D Systems) following manufacture's instructions. The used ELISAs for IL-8 and IL-6 were sensitive at 3.5 pg/mL and 0.7 pg/mL respectively. Cytokine concentration in cell free media was calculated as pg/mL/ $10^6$  cells and expressed as the percentage of the control in absence of any stimulation or treatment.

### **3A.7 Statistical analysis**

Measurements were performed in triplicate, unless otherwise stated. Values were expressed as means of at least three experiments with three replicates each  $\pm$  SD. Statistical differences between the treatments and the control were evaluated by the Student's *t*-test A (*P* values less than 0.05 were considered statistically significant).

**SECTION B**

***DESIGN AND DEVELOPMENT OF STABLE GENTAMICIN  
MICRONIZED POWDERS BASED  
ON SUPERCRITICAL ASSISTED ATOMIZATION  
OR SPRAY-DRYING TECHNIQUES***



**PART 1: PRODUCTION OF MICRONIZED GENTAMICIN  
POWDER BY SAA (Supercritical Assisted Atomization)**

**Based on the article:** G. Della Porta, R. Adami, P. Del Gaudio, **L. Prota**, R.P. Aquino, E. Reverchon. “Albumin/Gentamicin Microspheres Produced by Supercritical Assisted Atomization: Optimization of Size, Drug Loading and Release”. *Journal Pharmaceutical Sciences*. **2010**, 99: 4720 – 9.



### **3B 1.1 Material**

BSA (purity 99.9%), GS and water (purity 99.5%) were supplied by Sigma–Aldrich (Milan, Italy). Other solvents used were of analytical grade. Carbon dioxide (CO<sub>2</sub>, purity 99.9%) and nitrogen (N<sub>2</sub>, purity 99.9%) were purchased from SON (Naples, Italy).

### **3B 1.2 Supercritical Apparatus**

The SAA laboratory apparatus consists of two high-pressure pumps (mod. 305, Gilson, FR) delivering the liquid solution and liquid CO<sub>2</sub> to a heated bath (Forlab mod. TR12, Carlo Erba, IT) and, then, to the saturator. The saturator is a high pressure vessel (25 cm<sup>3</sup> internal volume) loaded with stainless steel perforated saddles which assure a large contact surface between liquid solution and CO<sub>2</sub>. The solution obtained in the saturator is sprayed through a thin wall (80 μm internal diameter) injection nozzle into the precipitator (3 dm<sup>3</sup> internal volume) operating at atmospheric pressure. A controlled flow of N<sub>2</sub> is taken from a cylinder, heated in an electric heat exchanger (mod. CBEN 24G6, Watlow) and sent to the precipitator to facilitate liquid droplet evaporation. The saturator and the precipitator are electrically heated using thin band heaters. A stainless steel filter located at the bottom of the precipitator allows powder collection and the gaseous stream flow out.

### **3B 1.3 Morphology and Particle Size Distribution**

The morphologies of the coprecipitated powder were observed by a field emission-scanning electron microscope (FESEM, mod. LEO 1525, Carl Zeiss

SMT AG, Oberkochen, Germany). Powders were dispersed on a carbon tab previously stuck to an aluminum stub (Agar Scientific, Stansted, UK). Samples were coated with gold-palladium (layer thickness 250 Å) using a sputter coater (mod. 108 Å, Agar Scientific). At least 20 SEM images were taken for each run to verify the powder uniformity.

Particle size (PS) and the particle size distribution (PSD) were evaluated from SEM images using the Sigma Scan Pro Software (rel. 5.0, Jandel Scientific, Erkrath, Germany); about 3000 particle diameters were considered in each PSD calculation. Histograms representing PSDs in terms of particles number were calculated using Microcal Origin Software (rel. 7.0, Microcal Software, Inc., Northampton, MA); then, they were converted in volumetric distributions and plotted in a cumulative form.

PSDs were also measured by static light scattering (LS) (Coulter LS 13320, Beckman Coulter, Inc., Fullerton, CA). The Coulter LS 13320 software uses Mie theory to produce an optimal analysis of the light energy distribution and to obtain the size distribution of the particles. Analyses were performed on microspheres suspensions using 30 mg of each sample dispersed in dichloromethane by sample sonication. We verified the effectiveness of the microspheres dispersion performing the PSD measurement after different sonication times ranging between 10 and 60 min. Moreover, measurements on each sample loaded in the instrument were repeated at different time intervals, that is, every 5 min for 1 h. In all cases, good reproducibility of results was obtained and the obtained PSDs practically overlapped.

### **3B 1.4 Solid State Characterization**

Diffraction patterns of coprecipitated powders were obtained using an X-ray diffractometer (mod. D8 Discover, Bruker AXS, Inc., Madison, WI) with a Cu

sealed tube source. Samples were placed in the holder and flattened with a glass slide to assure a good surface texture. The measuring conditions were as follows: Ni-filtered Cu K radiation,  $\lambda = 1.54 \text{ \AA}$ ,  $2\theta$  angle ranging between  $5^\circ$  and  $60^\circ$  with a scan rate of 3 s/step and a step size of  $0.2^\circ$ .

Thermograms of powder samples were obtained using a differential scanning calorimeter (DSC mod. TC11, Mettler Toledo, Inc., Columbus, OH). Fusion temperature and enthalpy were calibrated with an indium standard (melting point  $156.6^\circ\text{C}$ ). The samples ( $\pm 5 \text{ mg}$ ) were accurately weighed, crimped in an aluminum pan and heated from 25 to  $300^\circ\text{C}$  at  $10^\circ\text{C}/\text{min}$ , under a nitrogen purge of 50 mL/min. X-ray and DSC analyses were performed in three replicates for each batch of material.

Fourier transform infrared (FT-IR) spectra were obtained via M2000 FTIR (MIDAC Co), at a resolution of  $0.5 \text{ cm}^{-1}$ . The scan wavenumber range was  $4000\text{--}400 \text{ cm}^{-1}$ , and 16 scan signals were averaged to reduce the noise. The powder samples were ground and mixed thoroughly with potassium bromide (KBr) as infrared transparent matrix. KBr discs were prepared by compressing the powders in a hydraulic press. The effect of temperature on BSA has been analyzed increasing the temperature of the sample of  $10^\circ\text{C}$  from 30 to  $150^\circ\text{C}$  at  $10^\circ\text{C}/\text{min}$ , keeping the sample at each temperature for 10 min.

### **3B 1.5 Drug Content and Encapsulation Efficiency**

Samples of each manufactured batch were dissolved under vigorous stirring in PBS buffer at  $37^\circ\text{C}$ . GS drug content was obtained using Pharmacopoeia HPLC method (USP 30). Briefly, 25 mg of GS/BSA powder was stirred in 25 mL of PBS buffer (0.1 M) until the powder was completely dissolved. Ten milliliter of the solution were transferred in a suitable test tube, then, 5 mL of isopropyl alcohol and 4 mL of a previously prepared phthalaldehyde solution

were added. The solution was stirred and isopropyl alcohol was added to obtain a 25 mL solution. The solution was heated for 15 min in a water bath at 60°C, then cooled at room temperature and analyzed by HPLC (Chromatopac L-10AD system equipped with a Model SPD-10AV UV-vis detector and a Rheodyne Model 7725 injector loop 20 µL, Shimadzu, Kyoto, Japan). Peak areas were calculated with a Shimadzu C-R6A integrator. Phthalaldehyde solution was obtained dissolving 1.0 mg of *o*-phthalaldehyde (Sigma-Aldrich) in 5 mL of methanol and adding 95 mL of 0.4 M boric acid, previously adjusted with 8 N KOH to a pH of 10.4, and 2 mL of thioglycolic acid. The pH of the resulting solution was adjusted a 10.4 by 8 N KOH solution.

Encapsulation efficiency was calculated as the ratio of the actual to the theoretical drug content. Each analysis was performed in triplicate and the results were expressed as mean ± standard deviation. Both, drug content and encapsulation efficiency were calculated correcting the weight for the residual water contained in the coprecipitates previously determined by Karl Fischer titration (Titromatic KF 1S, Crison, Barcelona, Spain).

### **3B 1.6 Drug Release Studies**

Drug release experiments were performed in vertical Franz-type diffusion cells (Disa, Milan, Italy), with an exposed surface area of 0.6 cm<sup>2</sup>. A cellulose acetate filter with pore size 0.45 µm (Sartorius, Goettingen, Germany) was used as the barrier. The donor compartment was filled with 25 mg of GS/BSA formulation and 100 µL of the receptor phase. The receptor phase was 0.1 M PBS buffer solution, thermostated at 37°C and magnetically stirred in order to prevent any boundary layer effects. The receptor solution was sampled, derivatized and analyzed by HPLC (USP 30, gentamicin content method) for the determination of permeated GS.

**PART 2: PRODUCTION OF MICRONIZED INHALABLE  
GENTAMICIN POWDER BY SPRAY-DRYING**

**Based on the article:** R.P. Aquino, **L. Prota**, G. Auriemma, A. Santoro, T. Mencherini, G. Colombo, P. Russo. “Dry powder inhalers of gentamicin and leucine: formulation parameters, aerosol performance and *in vitro* toxicity on CuFi1 cells”. *International Journal of Pharmaceutics*. **2012**, *In press*.



### **3B 2.1 Materials**

Gentamicin sulphate, L-leucine, o-phthalaldehyde and sodium hydroxide anhydrous pellets were supplied by Sigma Aldrich (Milan, Italy). Ethanol 96% (for analysis, USP grade), dichloromethane (for analysis, USP grade), n-hexane (for analysis, Ph Eur grade), were purchased from Carlo Erba Reagents (Milan, Italy). Other solvents and chemicals were of analytical grade. Size 2 gelatine capsules were kindly offered by Qualicaps Europe S.A. (Madrid, Spain). The Turbospin<sup>®</sup> was kindly donated by PH&T SpA (Milan, Italy). All the cell culture reagents were purchased from Lonza.

### **3B 2.2 Powders Preparation**

Micronized particles were prepared by spray drying GS alone or with leu from different solvents i.e., water, water/ethanol or water/isopropyl alcohol (IPA) mixtures. GS and leu were both solubilized in water, then the organic solvent was added under continuous magnetic stirring, reaching a total powder concentration of 5% w/v. The parameters changed in the formulation regarded: i) kind of solvent, ii) water to organic solvent ratio, iii) GS to leu ratio (from 100:0 to 8:2 w/w).

The liquid feeds were neutralized with few drops of a 1 M sodium hydroxide solution and dried using a Buchi mini spray dryer B-191 (Buchi Laboratoriums-Tecnik, Flawil, Switzerland) under the following operative conditions: inlet temperature 125 °C for aqueous solutions, 110 °C for hydroalcoholic solutions, outlet temperature 72-75 °C, drying air flow 500 L/min, aspiration rate 100%, air pressure 6 atmospheres, feed rate 5 ml/min, nozzle 0.5 mm, set in preliminary experiments.

Each preparation was carried out in triplicate. All the spray-dried powders were collected and stored under vacuum for 48 h at room temperature. Production yields were expressed as weight percentage of the final product compared to total amount of the material sprayed. Powders produced were solubilized in distilled water and analyzed in terms of drug content by means of HPLC method described below.

### **3B 2.3 Powders physico-chemical Properties**

#### **3B 2.3a GS and leu quantification**

GS quantitative determination by HPLC followed the Pharmacopoeia method (USP 30) as reported elsewhere (Della Porta et al., 2010). Briefly, 25 mg of GS raw material was stirred in 25 ml of distilled water until complete dissolution. Five ml of IPA and 4 ml of a previously prepared phthalaldehyde solution were then added to 10 ml of this solution. The solution was stirred and IPA was added to reach a 25 ml volume. Finally, it was heated for 15 min in a water bath at 60 °C, cooled at room temperature, filtered through 0.45 µm filters and analyzed by HPLC at a wavelength of 330 nm (Chromatopac L-10AD system equipped with a Model SPD-10AV UV-vis detector and a Rheodyne Model 7725 injector loop 20 µl, Shimadzu, Kyoto, Japan). Peak areas were calculated with a Shimadzu C-R6A integrator. Phthalaldehyde solution was obtained dissolving 1.0 mg of o-phthalaldehyde in 5 ml of methanol and adding 95 ml of 0.4 M boric acid, previously adjusted with 8 N KOH to a pH of 10.4, and 2 ml of thioglycolic acid. The pH of the resulting solution was adjusted to 10.4 by a 8 N KOH solution. Calibration curves were worked out and proportionality between G concentration and AUC was checked in the range of 5-500 µg/ml.

After adding the phthalaldehyde solution to a sample containing both GS and leu, the amino acid reacted with phthalaldehyde, giving rise to a chromophore absorbing at 330 nm, as observed for GS, with no interference with GS. Calibration curves were worked out for leu, too, and proportionality between leu concentration and AUC was tested in the range of 1-20 µg/ml.

### **3B 2.3b GS and leu solubility**

GS and leu solubility in water and hydro-alcoholic solutions used for spray drying process (pH 7.0 ± 0.1) was evaluated according to USP 31. An excessive amount of powder was introduced into glass vials containing 8 ml of solvents; the samples were stirred and stored at 25 °C for 3 days. After that, samples were centrifuged for 15 min at 3.000 rpm, in order to remove the extra powder required to saturate the solutions. Supernatants were filtered with 0.45 µm filters and the concentration of dissolved Gs or leu was determined by HPLC method as described before. The solubility measurements were performed in triplicate.

### **3B 2.3c Particle size**

Particle size of both raw materials and spray-dried powders was determined using a laser light-scattering granulometer equipped with a micro liquid module (LS 13 320 Beckman Coulter Inc., FL, USA). In preliminary studies, dichloromethane was chosen as suspending medium among the other chemicals. Samples were suspended in dichloromethane and sonicated for 2 min: few drops of each sample were poured into the small-volume cell to obtain an obscuration between 8 and 12%. Particle size distributions were calculated by instrument software, using the Fraunhofer model. Results were expressed as  $d_{50}$  and span defined as  $[d_{90}-d_{10}]/d_{50}$ , where  $d_{90}$ ,  $d_{50}$  and  $d_{10}$  indicate the volume diameters at the 90<sup>th</sup>, 50<sup>th</sup> and 10<sup>th</sup> percentiles respectively.

### **3B 2.3d Scanning Electron Microscopy (SEM)**

Morphology of raw materials and microparticles was investigated using a scanning electron microscope (SEM) Zeiss EVO MA10 (Carl Zeiss SMT AG, München-Hallbergmoos, Germany) operating at 14 kV.

### **3B 2.3e Bulk and tapped density**

Bulk and tapped densities of the spray-dried powders were measured as described elsewhere (Sansone et al., 2009). Briefly, powders were loaded into a bottom-sealed 1 ml plastic syringe (Terumo Europe, Leuven, Belgium) capped with laboratory film (Parafilm® “M”, Pechiney Plastic Packaging, Chicago, IL, USA) and tapped on a hard bench until no change in the volume of the powder was observed. The bulk and tapped densities were calculated from the net weight of the plastic syringe content divided by the powder volume in the syringe before and after tapping, respectively. Experiments were performed in triplicate.

### **3B 2.3f Moisture uptake**

The moisture uptake kinetics of raw materials and spray-dried powders was determined after their removal from the spray-drying chamber. About 20 mg of powder were inserted into an aluminum pan and transferred onto the plate of the balance (MTS Mettler Toledo microbalance, OH, USA) at 60% RH and 25 °C. The balance was left open during the experiment and the increase in powder weight was measured each 10 min up to 80 min. Results were expressed as the percentage of weight gained by the sample during the time.

### 3B 2.4 Aerodynamic Behaviour Evaluation

A first screening of the *in vitro* deposition of the micronized powders was carried out using a single-stage glass impinger (SSGI, apparatus A Eur. Ph. 6.0, Copley Scientific Ltd., Nottingham, UK) and the Turbospin® as inhalation device. The Turbospin® is a breath-activated, reusable DPI, working with a single unit capsule. The capsule is vertically inserted into the pulverization chamber and pierced by a needle at the bottom side: the inhaled air creates a turbulence that shakes and twists the capsule, facilitating its empty. The selected device has an optimal resistance rate, able to assure an effective particle deaggregation even with a moderate inspiration potency.

For the SSGI experiments, 30 and 7 ml of distilled water were introduced in the lower and upper stages of the SSGI, respectively. Hard gelatine capsules (size 2) were filled manually with different amounts of spray-dried powder (60-120 mg), according to its bulk density. Then, the capsule was introduced into the Turbospin® and pierced twice. The vacuum pump was operated at a flow rate of 60 l/min for 5 s (Erweka vacuum pump VP 1000 equipped with an electronic digital flowmeter type DFM, Erweka Italia, Seveso, MI, Italy). Each deposition experiment was performed on 3 capsules and repeated in triplicate. Upper and lower parts were washed with 500 ml of distilled water, in order to recover the powder deposited on each stage, the GS content of which was evaluated by HPLC as described above. The emitted dose (ED) was gravimetrically determined and expressed as percentage of powder exiting the device *vs* amount of powder introduced into the capsule. The fine particle fraction (FPF), defined as ratio of GS recovered from the lower stage of SSGI *vs* total GS charged into the capsules, was expressed as a percentage (Sansone et al., 2009).

The powders showing promising aerosolisation properties were also tested by Andersen cascade impactor (apparatus D, Eur. Ph. 6.0, ACI, Westech Instrument Services Ltd., Bedfordshire, UK), adjusted for use at a flow rate of 60 L/min as described elsewhere (Gilani et al., 2005; Seville et al., 2007). The effective cut-off diameters of the modified ACI, provided by the producer, were: Stage -1, 8.6  $\mu\text{m}$ ; Stage -0, 6.5  $\mu\text{m}$ ; Stage 1, 4.4  $\mu\text{m}$ ; Stage 2, 3.2  $\mu\text{m}$ ; Stage 3, 2.0  $\mu\text{m}$ ; Stage 4, 1.1  $\mu\text{m}$ ; Stage 5, 0.54  $\mu\text{m}$ ; Stage 6, 0.25  $\mu\text{m}$ . In order to minimize particle bounce, metal impaction plates were dipped into an *n*-hexane solution of SPAN 80 (0.1% w/v) and the solvent was allowed to evaporate, leaving a thin film of SPAN 80 on the plate surface. The ACI was assembled placing a filter paper on the filter stage and the Turbospin<sup>®</sup> was fitted into a rubber mouth piece attached to the throat. Four hard gelatine capsules (size 2) were filled manually with  $120 \pm 0.5$  mg of sample. Each capsule was introduced into the Turbospin<sup>®</sup> and pierced twice. The vacuum pump was actuated for 4 s. The powder deposited into the different stages was recovered by plunging each plate and the stage below into distilled water (5-500 ml depending on the stage number). GS content was assessed by HPLC measurements. The emitted dose (ED) was determined as described above for SSGI experiments. The cumulative mass of powder with a diameter lower than the stated size of each stage was calculated and plotted as a percentage of recovered powder *vs* cut-off diameter. The mass median aerodynamic diameter (MMAD) of the particles was extrapolated from the graph, according to the Eur. Ph. 6.0. From the same plot, the fine particle dose (FPD), i.e. the mass of GS with a particle size less than 5  $\mu\text{m}$ , and the fine particle fraction (FPF), i.e. the fraction of GS emitted from the device with a particle size less than 5  $\mu\text{m}$ , were determined. *In vitro* deposition experiments were performed on three batches with three replicates each.

### **3B 2.5 Powder stability**

Physicochemical stability of GS powders dried from hydroalcoholic solutions and containing 15% w/w of leu was assessed after 6 months of storage at 25 °C ± 2 °C/60% RH ± 5% RH in a climatic chamber (Climatic and Thermostatic Chamber Mod. CCP37, AMT srl, MI, Italy), with emphasis on drug content, surface morphology and aerodynamic properties. All measurements were performed in triplicate.

### **3B 2.6 *In vitro* toxicity**

#### **3B 2.6a Cell line and culture conditions**

CuFi1 cell line, derived from human bronchial epithelium of a CF patient (CuFi1, CFTR  $\Delta$ F508/  $\Delta$ F508 mutant genotype), was purchased from American Type Culture Collection (ATCC, Manassas, VA, USA). CuFi1 cells were grown in human placental collagen type VI coated flasks (Sigma Aldrich, Milan, Italy) in bronchial epithelial basal medium, BEBM (Clonetics, Lonza, Walkersville, Inc) supplemented with BPE, hydrocortisone, hEGF, epinephrine, insulin, triiodothyronine, transferrine and retinoic acid (all from Lonza) and penicillin/streptomycin (50 mg/ml). Cells were incubated at 37 °C in a humidified atmosphere containing 5% CO<sub>2</sub>.

For *in vitro* biological studies, the powders were dissolved in sterile water, and immediately administered to the cells.

#### **3B 2.6b Proliferation assay**

Cell growth was assessed by using a colorimetric bromodeoxyuridine (BrdU) cell proliferation ELISA kit (Roche Diagnostics, Milan, Italy). Briefly, 10 x 10<sup>3</sup> cells were seeded into each coated well of a 96-well plate and left to

adhere to the plate. The cells were then treated with increasing concentrations (from zero to 2  $\mu\text{M}$ ) of rawG, Get3 and Get3-Leu15 for 24 h. BrdU was added for the final 16 h (10  $\mu\text{M}$  final concentration). At the end of the cell culture period, the medium was removed and the ELISA BrdU immunoassay was performed as described by the manufacturer. The colorimetric reaction was stopped by adding  $\text{H}_2\text{SO}_4$ , and the absorbance at 450 nm was measured using a microplate reader (Bio-Rad Laboratories, Milan, Italy).

### **3B 2.6c Viability assay**

Cell viability was analyzed using the MTT assay. Briefly, cells were seeded at the density of  $10 \times 10^3$ /well, left to adhere to the plate and then treated with rawG, Get3 and Get3-Leu15 for 24 h. 3-(4,5-methylthiazol-2-yl)-2,5-diphenyl-tetrazolium bromide (MTT) was added (0.5 mg/ml final concentration) to each well of the 96-well plate and incubated in 37 °C for 4 h. Formazan products were solubilised with 10% Triton X-100, 0.1 N HCl in 2-propanol. Absorbance was determined at 595 nm using a microplate reader (Bio-Rad Laboratories srl, MI, Italy).

### **3B 2.7 Statistical analysis**

Measurements were performed in triplicate, unless differently stated. Values expressed as mean of at least three experiments with three replicates each  $\pm$  SD. Statistical differences between the treatments and the controls were evaluated by the Student's *t*-test A (*P* values less than 0.05 were considered statistically significant).

**List of Abbreviations**

4-PBA	Sodium-4-phenylbutyrate
AA	Amino acid
ACI	Andersen cascade impactor
BALF	Bronchoalveolar lavage fluid
BEBM	Bronchial epithelial basal medium
BSA	Bovine serum albumin
CF	Cystic fibrosis
CFTR	Cystic fibrosis transmembrane conductance regulator
$d_{ae}$	Aerodynamic diameter
DPI	Dry powder inhaler
DSC	Differential scanning calorimetry
ED	Emitted dose
ERK	Extracellular signal-regulated kinase
FPD	Fine particle dose;
FPF	Fine particle fraction
GS	Gentamicin sulfate
HAE	Cells human airway epithelial cells
IKKs	I $\kappa$ B kinases
IL-6	Interleukin-6
IL-8	Interleukin-8
IP	Isoelectric point
IPA	Isopropyl alcohol

*List of Abberiations*

---

Leu	L-leucine
MAPK	Mitogen-activated protein kinase
MMAD	Mass median aerodynamic diameter
N	Naringin
NBD	Nucleotide-binding domain
NF- $\kappa$ B	Nuclear factor- $\kappa$ B
<i>Pa</i>	<i>Pseudomonas aeruginosa</i>
pMDI	Pressurized metered dose inhalers
PSDs	Particle size distributions
ROS	Reactive oxygen species
SAA	Supercritical assisted atomization
SEM	Scanning electron microscopy
SSGI	Single stage glass impinge
TMD	Transmembrane domain

## References

- Adjei, A.L., Gupta, P.K., 1997. *Inhalation Delivery of Therapeutic Peptides and Proteins*. Marcel Dekker Inc., New York, Basel, Hong Kong.
- Akabas, M.H., 2000. Cystic fibrosis transmembrane conductance regulator. Structure and function of an epithelial chloride channel. *J. Biol. Chem.* 275, 3729–3732.
- Al-Nakkash, L., Hu, S., Li, M., Hwang, T.C., 2001. A common mechanism for cystic fibrosis transmembrane conductance regulator protein activation by genistein and benzimidazolone analogs. *J. Pharmacol. Exp. Ther.* 296, 464–472.
- Andersson, C., Roomans, G.M., 2000. Activation of deltaF508 CFTR in a cystic fibrosis respiratory epithelial cell line by 4-phenylbutyrate, genistein and CPX. *Eur Respir J.* 15, 937–941.
- Ashlock, M.A. and Olson, E.R. (2011) Therapeutics development for cystic fibrosis: a successful model for a multisystem genetic disease. *Annu. Rev. Med.* 62, 107–125.
- Atkins, P.J., 2005. Dry powder inhalers: an overview. *Resp. Care* 50, 1304–1312.
- Azbell, C., Zhang, S., Skinner, D., Fortenberry, J., Sorscher, E.J., Woodworth, B.A., 2010. Hesperidin stimulates cystic fibrosis transmembrane conductance regulator-mediated chloride secretion and ciliary beat frequency in sinonasal epithelium. *Otolaryngol. Head Neck Surg.* 143, 397–404.
- Balfour-Lynn, I.M., Lees, B., Hall, P., Phillips, G., Khan, M., Flather, M., Elborn, J.S.; CF WISE (Withdrawal of Inhaled Steroids Evaluation), 2006. Investigators et al. Multicenter randomized controlled trial of withdrawal of inhaled corticosteroids in cystic fibrosis. *Am. J. Respir. Crit. Care Med.* 173, 1356–62.
- Balough, K., McCubbin, M., Weinberger, M., Smits, W., Ahrens, R., Fick, R., 1995. The relationship between infection and inflammation in the early stages of lung disease from cystic fibrosis. *Pediatr. Pulmonol.* 20, 63–70.
- Barton-Davis, E., Cordier, L., Shorturma, D., Leland, S.E., Sweeney, H.L., 1999. Aminoglycoside antibiotics restore dystrophin function to skeletal muscles of mdx mice. *J Clin Invest.* 104, 375-81.
- Becq, F., Mall, M.A., Sheppard, D.N., Conese, M., Zegarra-Moran, O., 2011. Pharmacological therapy for cystic fibrosis: from bench to bedside. *J Cyst Fibros. Suppl* 2, S129-45.
- Bedwell, D.M., Kaenjak, A., Benos, D.J., Bebok, Z., Bubien, J.K., Hong, J., Tousson, A., Clancy, J.P., Sorscher, E.J., 1997. Suppression of a CFTR premature stop mutation in a bronchial epithelial cell line. *Nat Med.* 3, 1280-4.
- Benavente-Garcia, O., Castillo, J., 2008. Update on uses and properties of citrus flavonoids: new findings in anticancer, cardiovascular, and anti-inflammatory activity. *J. Agric. Food Chem.* 56, 6185–6205.

## References

---

- Boncoeur, E., Bonvin, E., Muselet-Charlier, C., Henrion-Caude, A., Gruenert, D., Clement, A., Jacquot, J., Tabary, O., 2008. Oxidative stress induces ERK1/2 signaling in cystic fibrosis lung epithelial cells: potential mechanism for excessive IL-8 expression. *Int. J. Biochem. Cell Biol.* 40, 432–446.
- Boncoeur, E., Roque, T., Bonvin, E., Saint Cricq, V., Bonora, M., Clement, A., Tabary, O., Henrion-Caude, A., Jacquot, J., 2008. Cystic fibrosis transmembrane conductance regulator controls lung proteasomal degradation and NF- $\kappa$ B activity in conditions of oxidative stress. *Am. J. Pathol.* 172, 1184–94.
- Brain, J.D., Knudson, D.E., Sorokin, S.P., Davis, M.A., 1976. Pulmonary distribution of particles given by intratracheal instillation or by aerosol inhalation. *Environ. Res.* 11(1):13–33.
- Buchanan, J.H., Stevens, A., Sidhu, J., 1987. Aminoglycoside antibiotic treatment of human fibroblasts: intracellular accumulation, molecular changes and the loss of ribosomal accuracy. *Eur J Cell Biol.* 43, 141–7.
- Burke, J.F., Mogg, A.E., 1985. Suppression of a nonsense mutation in mammalian cells *in vivo* by the aminoglycoside antibiotics G-418 and paromomycin. *Nucleic Acids Res.* 13, 6265–72.
- Cantin, A.M., Bilodeau, G., Ouellet, C., Liao, J., Hanrahan, J.W., 2006. Oxidant stress suppresses CFTR expression. *Am. J. Physiol. Cell. Physiol.* 290, C262–C270.
- Cheng, S.H., Gregory, R.J., Marshall, J., Paul, S., Souza, D.W., White, G.A., O'Riordan, C.R., Smith, A.E., 1990. Defective intracellular transport and processing of CFTR is the molecular basis of most cystic fibrosis. *Cell.* 63(4), 827–34.
- Chew, N.Y., Chan, H.K., 2001. Use of solid corrugated particles to enhance powder aerosol performance. *Pharm. Res.* 18, 1570–1577.
- Chew, N.Y., Shekunov, B.Y., Tong, H.H., Chow, A.H., Savage, C., Wu, J., Chan, H.K., 2005a. Effect of amino acids on the dispersion of disodium cromoglycate powders. *J. Pharm. Sci.* 94, 2289–2300.
- Chew, N.Y., Tang, P., Chan, H.K., Raper, J.A., 2005b. How much particle surface corrugation is sufficient to improve aerosol performance of powders? *Pharm. Res.* 22, 148–152.
- Chmiel, J.F., Davis, P B., 2003. State of the Art: why do the lungs of patients with cystic fibrosis become infected and why can't they clear the infection? *Respir. Res.* 4, 8.
- Chono, S., Fukuchi, R., Seki, T., Morimoto, K., 2009. Aerosolized liposomes with dipalmitoyl phosphatidylcholine enhance pulmonary insulin delivery. *J. Control. Release* 137, 104–109.
- Chrystyn, H., 1997. Is total particle dose more important than particle distribution? *Respir Med.* 91(suppl), 17–19.
- Chuchalin, A., Amelina, E., Bianco, F., 2009. Tobramycin for inhalation in cystic fibrosis: beyond respiratory improvements. *Pulm. Pharmacol. Ther.* 22, 526–532.

- Clancy, J.P., Bebok, Z., Ruiz, F., King, C., Jones, J., Walker, L., Greer, H., Hong, J., Wing, L., Macaluso, M., Lyrene, R., Sorscher, E.J., Bedwell, D.M., 2001. Evidence that systemic gentamicin suppresses premature stop mutations in patients with cystic fibrosis. *Am J Respir Crit Care Med.* 163, 1683–1692.
- Clunes, M.T., Boucher, R.C., 2008. Front-runners for pharmacotherapeutic correction of the airway ion transport defect in cystic fibrosis. *Curr. Opin. Pharmacol.* 8, 292–299.
- Collins, F.S., Riordan, J.R., Tsui, L.C., 1990. The cystic fibrosis gene: isolation and significance. *Hosp. Pract. (Off. Ed).* 25, 47–57.
- Conway, S., Pond, M., Watson, A., Etherington, C., Robey, H., Goldman, M., 1997. Intravenous colistin sulphomethate in acute respiratory exacerbations in adult patients with cystic fibrosis. *Thorax.* 52, 987–93.
- Crowther Labiris, N.R., Holbrook, A.M., Chrystyn, H., Macleod, S.M., Newhouse, M.T., 1999. Dry powder versus intravenous and nebulized gentamicin in cystic fibrosis and bronchiectasis. A pilot study. *Am J Respir Crit Care Med* 160, 1711–6.
- Cuthbert, A.W. (2011) New horizons in the treatment of cystic fibrosis. *Br. J. Pharmacol.* 163, 173–183
- Dailey, L.A., Jekel, N., Fink, L., Gessler, T., Schmehl, T., Wittmar, M., Kissel, T., Seeger, W., 2006. Investigation of the proinflammatory potential of biodegradable nanoparticle drug delivery systems in the lung. *Toxicol. Appl. Pharmacol.* 215, 100–108.
- Dalby, R.N., Tiano, S.L., Hickey, A.J., 1996. Medical devices for the delivery of therapeutic aerosols to the lungs. In: Hickey, A.J. (Ed.), *Inhalation Aerosols, Physical and Biological Basis for Therapy*, vol. 94. Marcel Dekker, New York, NY, pp. 441–473.
- Darquenne, C., 2004. Aerosol deposition in the human respiratory tract breathing air and 80:20 Heliox. *J Aerosol Med.* 17(3), 278–285.
- Das, S., Banerjee, R., Bellare, J., 2005. Aspirin Loaded Albumin Nanoparticles by Coacervation: Implications in Drug Delivery. *Trends Biomater. Artif. Organs.* Vol 18, no. 2, pp. 203–212.
- Davis, P.B., Drumm, M., Konstan, M.W., 1996. Cystic fibrosis. *Am. J. Respir. Crit. Care Med.* 154, 1229–1256.
- de Boer, A.H., Gjaltema, D., Hagedoorn, P., Frijlink, H.W., 2002. Characterization of inhalation aerosols: a critical evaluation of cascade impactor analysis and laser diffraction technique. *Int. J. Pharm.* 249, 219–231.
- Dehecchi, M.C., Nicolis, E., Norez, C., Bezzerri, V., Borgatti, M., Mancini, I., Rizzotti, P., Ribeiro, C.M., Gambari, R., Becq, F., Cabrini, G., 2008. Anti-inflammatory effect of miglustat in bronchial epithelial cells. *J. Cyst. Fibros.* 7, 555–565.
- Della Porta, G., Adami, R., Del Gaudio, P., Protta, L., Aquino, R., Reverchon, E., Albumin/gentamicin microspheres produced by supercritical assisted atomization: optimization of size, drug loading and release. *J Pharm Sci* 99, 4720–9.

## References

---

- Della Porta, G., Reverchon, E., 2007. Supercritical fluid-based technologies for particulate drug delivery. In: Ravi Kumar MNV editor. Handbook of particulate drug delivery, CA, U S A; American Scientific Publisher. pp. 35–59. ISBN 1-58883-079-9.
- Descargues, P., Sil, A.K., Karin, M., 2008. IKKalpha, a critical regulator of epidermal differentiation and a suppressor of skin cancer. *EMBO J.* 27, 2639–2647.
- DiMango, E., Ratner, A.J., Bryan, R., Tabibi, S., Prince, A., 1998. Activation of NF-kappaB by adherent *Pseudomonas aeruginosa* in normal and cystic fibrosis respiratory epithelial cells. *J. Clin. Invest.* 101, 2598–2605.
- DiMango, E., Zar, H.J., Bryan, R., Prince, A., 1995. Diverse *Pseudomonas aeruginosa* gene products stimulate respiratory epithelial cells to produce interleukin-8. *J. Clin. Invest.* 96, 2204–2210.
- Doring, G., Conway, S.P., Heijerman, H.G., Hodson, M.E., Høiby, N., Smyth, A., Touw, D.J., 2000. Antibiotic therapy against *Pseudomonas aeruginosa* in cystic fibrosis: a European consensus. *Eur. Respir. J.* 16, 749–67.
- Du, M., Jones, J.R., Lanier, J., Keeling, K.M., Lindsey, J.R., Tousson, A., Bebok, Z., Whitsett, J.A., Dey, C.R., Colledge, W.H., Evans, M.J., Sorscher, E.J., Bedwell, D.M., 2002. Aminoglycoside suppression of a premature stop mutation in a *Cftr*<sup>-/-</sup> mouse carrying a human CFTR-G542X transgene. *J Mol Med* 80, 595-604.
- Emmen, H.H., Hoogendijk, E.M.G., Klopping-Ketelaars, W.A.A., Muijser, H., Duistermaat, E., Ravensberg, J.C., Alexander, D.J., Borkhataria, D., Rusch, G.M., Schmit, B., 2000. Human safety and pharmacokinetics of the CFC alternative propellants HFC 134a (1,1,1,2-tetrafluoroethane) and HFD 227 (1,1,1,2,3,3,3-heptafluoropropane) following whole-body exposure. *Regul. Toxicol. Pharmacol.* 32, 22–35.
- Evans, M.J., Cabral-Anderson, L.J., Freeman, G., 1978. Role of the Clara cell in renewal of the bronchiolar epithelium. *Lab Invest.* 38, 648-655.
- Fehrenbach, H., 2001. Alveolar epithelial type II cell: defender of the alveolus revisited. *Respir Res.* 2, 33-46.
- Flume, P.A., O’Sullivan, B.P., Robinson, K.A., Goss, C.H., Mogayzel, P.J.Jr, Willey-Courand, D.B., Bujan, J., Finder, J., Lester, M., Quittell, L., Rosenblatt, R., Vender, R.L., Hazle, L., Sabadosa, K., Marshall, B.; Cystic Fibrosis Foundation, Pulmonary Therapies Committee, 2007. Cystic fibrosis pulmonary guidelines: chronic medications for maintenance of lung health. *Am. J. Respir. Crit. Care Med.* 176, 957–69.
- Gail, D.B., Lenfant, C.J.M., 1983. Cells of the lung: biology and clinical implications. *Am Rev Respir Dis.* 127, 366-387.
- Gehr, P., Bachofren, M., Weibel, E.R., 1978. The normal human lung: ultrastructure and morphometric estimation of diffusion capacity. *Respir Physiol.* 32, 121-140.
- Geller, D.E., 2009. Aerosol antibiotics in cystic fibrosis. *Respir Care* 54, 658-70.

- Gerrity, T.R., Garard, C.S., Yeates, D.B., 1983. A mathematical model of particle retention in the air-spaces of human lungs. *Brit.J.Indust.Med.* 40, 121-130.
- Gilani, K., Najafabadi, A.R., Barghi, M., Rafiee-Tehrani, M., 2005. The effect of water to ethanol feed ratio on physical properties and aerosolization behavior of spray dried cromolyn sodium particles. *J. Pharm. Sci.* 94, 1048–1059.
- Giry, K., Pean, J.M., Giraud, L., Marsas, S., Rolland, H., Wuthrich, P., 2006. Drug/lactose co-micronization by jet milling to improve aerosolization properties of a powder for inhalation. *Int. J. Pharm.* 321, 162–166.
- Gomez, M.I., Prince, A., 2008. Airway epithelial cell signaling in response to bacterial pathogens. *Pediatr. Pulmonol.* 43, 11–19.
- Grenha, A., Remunan-Lopez, C., Carvalho, E.L., Seijo, B., 2008. Microspheres containing lipid/chitosan nanoparticles complexes for pulmonary delivery of therapeutic proteins. *Eur. J. Pharm. Biopharm.* 69, 83–93.
- Grossman, J., 1994. The evolution of inhaler technology. *J. Asthma.* 31(1), 55-64.
- Gruenert, D.C., Willems, M., Cassiman, J.J., Frizzell, R.A., 2004. Established cell lines used in cystic fibrosis research. *J. Cyst. Fibros.* 3(Suppl 2), 191–196.
- Haardt, M., Benharouga, M., Lechardeur, D., Kartner, N., Lukacs, G.L., 1999. C-terminal truncations destabilize the cystic fibrosis transmembrane conductance regulator without impairing its biogenesis. A novel class of mutation. *J Biol Chem.* 274(31), 21873-7.
- Hallows, K.R., Fitch, A.C., Richardson, C.A., Reynolds, P.R., Clancy, J.P., Dagher, P.C., Witters, L.A., Kolls, J.K., Pilewski, J.M., 2006. Up-regulation of AMP-activated kinase by dysfunctional cystic fibrosis transmembrane conductance regulator in cystic fibrosis airway epithelial cells mitigates excessive inflammation. *J. Biol. Chem.* 281, 4231–4241.
- Hancock, B.C., Parks, M., 2000. What is the true solubility advantage for amorphous pharmaceuticals? *Pharm. Res.* 17, 397–404.
- Haswani, D.K., Nettey, H., Oettinger, C.D., Souza, M.J., 2006. Formulation, characterization and pharmacokinetic evaluation of gentamicin sulphate loaded microspheres. *Microencaps J.* 23, 875–886.
- Hayden, M.S., Ghosh, S., 2004. Signaling to NF-kappaB. *Genes Dev.* 18, 2195–2224.
- Heijerman, H., Westerman, E., Conway, S., Touw, D., Doring, G., 2009. Inhaled medication and inhalation devices for lung disease in patients with cystic fibrosis: a European consensus. *J Cyst. Fibros.* 8, 295–315.
- Helip-Wooley, A., Park, M.A., Lemons, R.M., Thoene, J.G., 2002. Expression of CTNS alleles: subcellular localization and aminoglycoside correction *in vitro*. *Mol Genet Metab.* 75, 128-33.
- Heyder, J., Gebhart, J., Rudolf, G., Schiller, C.F., Stalhofen, W., 1986. Deposition of particles in the human respiratory tract in the size range 0.005-15  $\mu\text{m}$ . *J. Aerosol Sci.* 17.
- Hinds, W.C., 1999. *Aerosol Technology: Properties, Behaviour, and Measurement of Airborne Particles*, 2nd edition. John Wiley & Sons, New York.

## References

---

- Hodson, M.E., Gallagher, C.G., Govan, J.R., 2002. A randomised clinical trial of nebulised tobramycin or colistin in cystic fibrosis. *Eur. Respir. J.* 20, 658–64.
- Holt, T.L., Ward, L.C., Francis, P.J., Isles, A., Cooksley, W.G., Shepherd, R.W., 1985. Whole body protein turnover in malnourished cystic fibrosis patients and its relationship to pulmonary disease. *Am. J. Clin. Nutr.* 41, 1061–1066.
- Howard, M., Frizzell, R.A., Bedwell, D.M., 1996. Aminoglycoside antibiotics restore CFTR function by overcoming premature stop mutations. *Nat Med.* 2, 467-9.
- Huang, X., Brazel, C.S., 2001. On the importance and mechanism of burst release in matrix-controlled drug delivery system. *J Contr Rel.* 73, 121–136.
- Huang, Y.C., Vieira, A., Huang, K.L., Yeh, M.K., Chiang, C.H., 2005. Pulmonary inflammation caused by chitosan microparticles. *J. Biomed. Mater. Res.* 75A, 238–287.
- Hussain, A., Arnold, J., Khan, M., Ahsan, F., 2004. Absorption enhancers in pulmonary protein delivery. *J. Control. Release.* 94, 15–24.
- Ibrahim, B.M., Jun, S.W., Lee, M.Y., Kang, S.H., Yeo, Y., 2010. Development of inhalable dry powder formulation of basic fibroblast growth factor. *Int. J. Pharm.* 385, 66-72.
- Iskandara, F., Gradonb, L., Okuyama, K. 2003. Control of the morphology of nano-structured particles prepared by the spray drying of a nanoparticle sol. *J Colloid Interface Sci.* 265, 296–303.
- Jacquot, J., Tabary, O., Le Rouzic, P., Clement, A., 2008. Airway epithelial cell inflammatory signalling in cystic fibrosis. *Int. J. Biochem. Cell Biol.* 40, 1703–1715.
- Jeffrey, P.K., 1983. Morphological features of airway surface epithelial cells and glands. *Am Rev Respir Dis.* 128, S14-S18.
- Jensen, T., Pedersen, S.S., Garne, S., Heilmann, C., Hoiby, N., Koch, C., 1987. Colistin inhalation therapy in cystic fibrosis patients with chronic *Pseudomonas aeruginosa* lung infection. *J. Antimicrob. Chemother.* 19, 831–38.
- Johannson, F., Hjertberg, E., Eirefelt, S., Tronde, A., Bengtsson, U.H., 2002. Mechanisms for absorption enhancement of inhaled insulin by sodium taurocholate. *Eur. J. Pharm. Sci.* 17, 63–71.
- John, G., Yildirim, A.O., Rubin, B.K., Gruenert, D.C., Henke, M.O. 2010. TLR-4-mediated innate immunity is reduced in cystic fibrosis airway cells. *Am J Respir Cell Mol Biol.* 42(4), 424-31.
- Johnson, C., Butler, S.M., Konstan, M.W., Morgan, W., Wohl, M.E., 2003. Factors influencing outcomes in cystic fibrosis: a center-based analysis. *Chest.* 123, 20–27.
- Karin, M., 1995. The regulation of AP-1 activity by mitogen-activated protein kinases. *J. Biol. Chem.* 270, 16483–16486.

- Keeling, K.M., Bedwell, D.M., 2002. Clinically relevant aminoglycosides can suppress disease-associated premature stop mutations in the IDUA and P53 cDNAs in a mammalian translation system. *J Mol Med.* 80, 367-76.
- Keeling, K.M., Brooks, D.A., Hopwood, J.J., Li, P., Thompson, J.N., Bedwell, D.M., 2001. Gentamicin mediated suppression of Hurler syndrome stop mutations restores a low level of alpha- L-iduronidase activity and reduces lysosomal glycosaminoglycan accumulation. *Hum Mol Genet.* 10, 291-9.
- Kerem, E., 2005. Pharmacological induction of CFTR function in patients with cystic fibrosis: mutation-specific therapy. *Pediatr Pulmonol.* 40(3), 183-96.
- Kerem, E., 2006. Mutation specific therapy in CF. *Paediatr Respir Rev.* 7 Suppl 1, S166-9.
- Kettle, A.J., Chan, T., Osberg, I., Senthilmohan, R., Chapman, A.L., Mocatta, T.J., Wagener, J.S., 2004. Myeloperoxidase and protein oxidation in the airways of young children with cystic fibrosis. *Am. J. Respir. Crit. Care Med.* 170, 1317–1323.
- Khan, T.Z., Wagener, J.S., Bost, T., Martinez, J., Accurso, F.J., Riches, D.W., 1995. Early pulmonary inflammation in infants with cystic fibrosis. *Am. J. Respir. Crit. Care Med.* 151, 1075–1082.
- Khassawneh, B.Y., Al-Ali, M.K., Alzoubi, K.H., Batarseh, M.Z., Al-Safi, S.A., Sharara, A.M., Alnasr, H.M., 2008. Handling of inhaler devices in actual pulmonary practice: metered-dose inhaler versus dry powder inhalers. *Respir. Care* 53, 324-8.
- Kieninger, E., Regamey, N., 2010. Targeting inflammation in cystic fibrosis. *Respiration.* 79, 189–190.
- Kim, J-H., Bae, Y.H., 2004. Albumin loaded microsphere of amphiphilic poly(ethylene glycol)/poly(alpha-ester) multiblock copolymer. *Eur. J. Pharm. Sci.* 23, 245–251.
- Kube, D., Sontich, U., Fletcher, D., Davis, P.B., 2001. Proinflammatory cytokine responses to *P. aeruginosa* infection in human airway epithelial cell lines. *Am. J. Physiol. Lung Cell Mol. Physiol.* 280, L493–L502.
- Lechuga-Ballesteros, D., Charan, C., Stults, C.L., Stevenson, C.L., Miller, D.P., Vehring, R., Tep, V., Kuo, M.C., 2008. Trileucine improves aerosol performance and stability of spray-dried powders for inhalation. *J. Pharm. Sci.* 97, 287-302.
- Levy, L.D., Durie, P.R., Pencharz, P.B., Corey, M.L., 1985. Effects of long-term nutritional rehabilitation on body composition and clinical status in malnourished children and adolescents with cystic fibrosis. *J. Pediatr.* 107, 225–230.
- Li, H.Y., Seville, P.C., Williamson, I.J., Birchall, J.C., 2005. The use of amino acids to enhance the aerosolisation of spray-dried powders for pulmonary gene therapy. *J Gene Med* 7, 343-53.
- Li, J., Johnson, X.D., Iazvovskaia, S., Tan, A., Lin, A., Hershenson, M.B., 2003. Signaling intermediates required for NF-kappa B activation and IL-8 expression in CF bronchial epithelial cells. *Am. J. Physiol. Lung Cell Mol. Physiol.* 284, L307–L315.

## References

---

- Lim, M., McKenzie, K., Floyd, A.D., Kwon, E., Zeitlin, P.L., 2004. Modulation of deltaF508 cystic fibrosis transmembrane regulator trafficking and function with 4-phenylbutyrate and flavonoids. *Am J Respir Cell Mol Biol.* 31(3), 351-7.
- Limasset, B., le Doucen, C., Dore, J.C., Ojasoo, T., Damon, M., Crastes de Paulet, A., 1993. Effects of flavonoids on the release of reactive oxygen species by stimulated human neutrophils. Multivariate analysis of structure-activity relationships (SAR). *Biochem. Pharmacol.* 46, 1257-1271.
- Lucas, P., Anderson, K., Potter, U.J., Staniforth, J.N., 1999. Enhancement of small particle size dry powder aerosol formulations using an ultra low density additive. *Pharm. Res.* 16, 1643-1647.
- Lukacs, G.L., Mohamed, A., Kartner, N., Chang, X.B., Riordan, J.R., Grinstein, S., 1994. Conformational maturation of CFTR but not its mutant counterpart (delta F508) occurs in the endoplasmic reticulum and requires ATP. *EMBO J.* 13, 6076-6086.
- Lyczak, J.B., Cannon, C.L., Pier, G.B., 2002. Lung infections associated with cystic fibrosis. *Clin. Microbiol. Rev.* 15, 194-222.
- Manthey, J.A., Grohmann, K., Guthrie, N., 2001. Biological properties of citrus flavonoids pertaining to cancer and inflammation. *Curr. Med. Chem.* 8, 135-153.
- Mao, L., Blair, J., 2004. Effect of additives on the aerosolization properties of spray dried trehalose powders. *Resp. Deliv. Drugs* 9, 653-656.
- Martonen, T.B., Yang, Y., 1996. Deposition mechanics of pharmaceutical particles in human airways. In: Hickey, A.J. (Ed.), *Inhalation Aerosols, Physical and Biological Basis for Therapy*, vol. 94. Marcel Dekker, New York, NY, pp. 3-27.
- McCarty, N.A., Standaert, T.A., Teresi, M., Tuthill, C., Launspach, J., Kelley, T.J., Milgram, L.J., Hilliard, K.A., Regelman, W.E., Weatherly, M.R., Aitken, M.L., Konstan, M.W., Ahrens, R.C., 2002. A phase I randomized, multicenter trial of CPX in adult subjects with mild cystic fibrosis. *Pediatr. Pulmonol.* 33, 90-98.
- Mehta, A., 2005. CFTR: more than just a chloride channel. *Pediatr Pulmonol.* 39, 292-98.
- Mendelman, P.M., Smith, A.L., Levy, J., Weber, A., Ramsey, B., Davis, R.L., 1985. Aminoglycoside penetration, inactivation, and efficacy in cystic fibrosis sputum. *Am. Rev. Respir. Dis.* 132, 761-5.
- Muhlebach, M.S., Reed, W., & Noah, T.L., 2004. Quantitative cytokine gene expression in CF airway. *Pediatr. Pulmonol.* 37, 393-399.
- Mukhopadhyay, S., Singh, M., Cater, J.I., Ogston, S., Franklin, M., Olver, R.E., 1996. Nebulised antipseudomonal antibiotic therapy in cystic fibrosis: a meta-analysis of benefits and risks. *Thorax* 51, 364-8.

- Myers, M.A., Thomas, D.A., Straub, L., Soucy, W., Niven, R.W., Kaltenbach, M., Hood, C.I., Schreier, H., Gonzalez-Rothi, R.J., 1993. Pulmonary effects of chronic exposure to liposome aerosols in mice. *Exp. Lung Res.* 19, 1–19.
- Najafabadi, A.R., Gilani, K., Barghi, M., Rafiee-Tehrani, M., 2004. The effect of vehicle on physical properties and aerosolisation behaviour of disodium cromoglycate microparticles spray dried alone or with l-leucine. *Int. J. Pharm.* 285, 97–108.
- Nazer, D., Abdulhamid, I., Thomas, R., Pendleton, S., 2006. Home versus hospital intravenous antibiotic therapy for acute pulmonary exacerbations in children with cystic fibrosis. *Pediatr. Pulmonol.* 41, 744–49.
- Newman, S.P., 2005. Principles of metered-dose inhaler design. *Res. Care.* 50 (9), 1177–1190.
- Nicolis, E., Lampronti, I., Dehecchi, M.C., Borgatti, M., Tamanini, A., Bianchi, N., Bezzerri, V., Mancini, I., Giri, M.G., Rizzotti, P., Gambari, R., Cabrini, G., 2008. Pyrogallol, an active compound from the medicinal plant *Embllica officinalis*, regulates expression of pro-inflammatory genes in bronchial epithelial cells. *Int. Immunopharmacol.* 8, 1672–1680.
- Nozaki, Y., Tanford, C., 1971. The solubility of amino acids and two glycine peptides in aqueous ethanol and dioxane solutions. Establishment of a hydrophobicity scale. *J. Biol. Chem.* 246, 2211–2217.
- O’Sullivan, B.P., Freedman, S.D., 2009. Cystic fibrosis. *Lancet.* 373, 1891–904.
- Parlati, C., Colombo, P., Buttini, F., Young, P.M., Adi, H., Ammit, A.J., Traini, D., 2009. Pulmonary spray dried powders of tobramycin containing sodium stearate to improve aerosolization efficiency. *Pharm. Res.* 26, 1084–1092.
- Pedemonte, N., Lukacs, G.L., Du, K., Caci, E., Zegarra-Moran, O., Galiotta, L.J., Verkman, A.S., 2005. Small-molecule correctors of defective DeltaF508-CFTR cellular processing identified by high-throughput screening. *J. Clin. Invest.* 115, 2564–2571.
- Peijun, J., Jinxin Zou, Feng, W., 2009. Effect of alcohol on the solubility of amino acid in water. *J. Mol. Catal. B: Enzym.* 56, 185–188.
- Pilcer, G., Amighi, K., 2010. Formulation strategy and use of excipients in pulmonary drug delivery. *Int. J. Pharm.* 392, 1–19.
- Pilcer, G., Vanderbist, F., Amighi, K., 2009. Preparation and characterization of spray-dried tobramycin powders containing nanoparticles for pulmonary delivery. *Int. J. Pharm.* 365, 122–129.
- Prayle, A., Smyth, A.R., 2010. Aminoglycoside use in cystic fibrosis: therapeutic strategies and toxicity. *Curr Opin Pulm Med* 16, 604–10.
- Prior, S., Gamazo, C., Irache, J.M., Merkle, H.P., Gander, B., 2000. Gentamicin encapsulation in PLA/PLGA microspheres in view of treating *Brucella* infections. *Int J Pharm.* 196(1), 115–25.

## References

---

- Prota, L., Santoro, A., Bifulco, M., Aquino, R.P., Mencherini, T., Russo, P., 2011. Leucine enhances aerosol performance of Naringin dry powder and its activity on cystic fibrosis airway epithelial cells. *Int. J. Pharm.* 412, 8-19.
- Pyle, L.C., Fulton, J.C., Sloane, P.A., Backer, K., Mazur, M., Prasain, J., Barnes, S., Clancy, J.P., Rowe, S.M., 2009. Activation of CFTR by the flavonoid quercetin: potential use as a biomarker of  $\Delta$ F508 CFTR rescue. *Am. J. Respir. Cell. Mol. Biol.*
- Quinton, P.M., 2008. Cystic fibrosis: impaired bicarbonate secretion and mucoviscidosis. *Lancet.* 372, 415–17.
- Rabbani, N.R., Seville, P.C., 2004. The use of amino acids as formulation excipients in lactose based spray-dried powders. *J. Pharm. Pharmacol.* 56, 32–33.
- Ramsey, B.W., Pepe, M.S., Quan, J.M., Otto, K.L., Montgomery, A.B., Williams-Warren, J., Vasiljev, K.M., Borowitz, D., Bowman, C.M., Marshall, B.C., Marshall, S., Smith, A.L., 1999. Intermittent administration of inhaled tobramycin in patients with cystic fibrosis. Cystic Fibrosis Inhaled Tobramycin Study Group. *N Engl. J. Med.* 340, 23-30.
- Regelmann, W.E., Elliott, G.R., Warwick, W.J., Clawson, C.C., 1990. Reduction of sputum *Pseudomonas aeruginosa* density by antibiotics improves lung function in cystic fibrosis more than do bronchodilators and chest physiotherapy alone. *Am. Rev. Respir. Dis.* 141, 914–21.
- Reisin, I.L., Prat, A.G., Abraham, E.H., Amara, J.F., Gregory, R.J., Ausiello, D.A., Cantiello, H.F., 1994. The cystic fibrosis transmembrane conductance regulator is a dual ATP and chloride channel. *J. Biol. Chem.* 269, 20584–91.
- Reverchon, E., DeMarco, I., 2006. Supercritical fluid extraction and fractionation of natural matter. *Supercritical Fluid J.* 38, 146–166.
- Riordan, J.R., 2005. Assembly of functional CFTR chloride channels. *Annu. Rev. Physiol.* 67, 701–718.
- Ross, K.R., Chmiel, J.F., Konstan, M.W., 2009. The role of inhaled corticosteroids in the management of cystic fibrosis. *Paediatr. Drugs* 11, 101–113.
- Rottner, M., Kunzelmann, C., Mergey, M., Freyssinet, J.M., Martinez, M.C., 2007. Exaggerated apoptosis and NF-kappaB activation in pancreatic and tracheal cystic fibrosis cells. *FASEB J.* 21, 2939–2948.
- Rowe, S.M., Miller, S., Sorscher, E.J., 2005. Cystic fibrosis. *N Engl J Med.* 352, 1992–2001.
- Rubin, B.K., 2007. CFTR is a modulator of airway inflammation. *Am. J. Physiol. Lung Cell Mol. Physiol.* 292, L381–L382.
- Saadane, A., Masters, S., DiDonato, J., Li, J., Berger, M., 2007. Parthenolide inhibits IkappaB kinase, NF-kappaB activation, and inflammatory response in cystic fibrosis cells and mice. *Am. J. Respir. Cell Mol. Biol.* 36, 728–736.

- Sacchetti, M., Van Oort, M.M., 1996. Spray-drying and supercritical fluid particle generation techniques. In: Hickey, A.J. (Ed.), *Inhalation Aerosols, Physical and Biological Basis for Therapy*, vol. 94. Marcel Dekker, New York, NY, pp. 337–384.
- Sagel, S.D., Chmiel, J.F., Konstan, M.W., 2007. Sputum biomarkers of inflammation in cystic fibrosis lung disease. *Proc. Am. Thorac. Soc.* 4, 406–417.
- Salem, L., Bosquillon, C., Dailey, L.A., Delattre, L., Martin, G.P., Evrard, B., Forbes, B., 2009. Sparing methylation of  $\beta$ -cyclodextrin mitigates cytotoxicity and permeability induction in respiratory epithelial cell layers in vitro. *J. Control. Release.* 136, 110–116.
- Sansone, F., Aquino, R.P., Del Gaudio, P., Colombo, P., Russo, P., 2009. Physical characteristics and aerosol performance of Naringin dry powders for pulmonary delivery prepared by spray-drying. *Eur. J. Pharm. Biopharm.* 72, 206–213.
- Sato, S., Ward, C.L., Krouse, M.E., Wine, J.J., Kopito, R.R., 1996. Glycerol reverses the misfolding phenotype of the most common cystic fibrosis mutation. *J Biol Chem.* 271, 635–638.
- Schmidt, A., Hughes, L.K., Cai, Z., Mendes, F., Li, H., Sheppard, D.N. and Amaral, M.D., 2008. Prolonged treatment of cells with genistein modulates the expression and function of the cystic fibrosis transmembrane conductance regulator. *Br. J. Pharmacol.* 153, 1311–1323.
- Schwiebert, E.M., Benos, D.J., Egan, M.E., Stutts, M.J., Guggino, W.B., 1999. CFTR is a conductance regulator as well as a chloride channel. *Physiol Rev.* 79(1 Suppl), S145–66.
- Schwiebert, E.M., Egan, M.E., Hwang, T.H., Fulmer, S.B., Allen, S.S., Cutting, G.R., Guggino, W.B., 1995. CFTR regulates outwardly rectifying chloride channels through an autocrine mechanism involving ATP. *Cell.* 81: 1063–73.
- Sebti, Th., Amighi, K., 2006. Preparation and in vitro evaluation of lipidic carriers and fillers for inhalation. *Eur. J. Pharm. Biopharm.* 63, 51–58.
- Seville, P.C., Li, H.Y., Learoyd, T.P., 2007. Spray-dried powders for pulmonary drug delivery. *Crit. Rev. Ther. Drug Carrier Syst.* 24, 307–360.
- Sheppard, D.N., Welsh, M.J., 1999. Structure and function of the CFTR chloride channel. *Physiol Rev.* 79(1 Suppl), S23–45.
- Shur, J., Nevell, T.G., Ewen, R.J., Price, R., Smith, A., Barbu, E., Conway, J.H., Carroll, M.P., Shute, J.K., Smith, J.R., 2008. Cospray-dried unfractionated heparin with L-leucine as a dry powder inhaler mucolytic for cystic fibrosis therapy. *J. Pharm. Sci.* 97, 4857-68.
- Sleat, D.E., Sohar, I., Gin, R.M., Lobel, P., 2001. Aminoglycoside-mediated suppression of nonsense mutations in late infantile neuronal ceroid lipofuscinosis. *Eur. J. Paediatr. Neurol.* 5, Suppl. A:57-62.
- Springsteel, M.F., Galiotta, L.J., Ma, T., By, K., Berger, G.O., Yang, H., Dicus, C.W., Choung, W., Quan, C., Shelat, A.A., Guy, R.K., Verkman, A.S., Kurth, M.J., Nantz, M.H., 2003. Benzoflavone activators of the cystic fibrosis transmembrane conductance regulator: towards a pharmacophore model for the nucleotide-binding domain. *Bioorg Med Chem.* 11(18), 4113-20.

## References

---

- Starosta, V., Griese, M., 2006. Protein oxidation by chronic pulmonary diseases in children. *Pediatr. Pulmonol.* 41, 67–73.
- Steckel, H., Brandes, H.G., 2004. A novel spray-drying technique to produce low density particles for pulmonary delivery. *Int. J. Pharm.* 278, 187–195.
- Stevens, J. Lowe, *Istologia umana*, CEA.
- Stutts, M.J., Canessa, C.M., Olsen, J.C., Hamrick, M., Cohn, J.A., Rossier, B.C., Boucher, R.C., 1995. CFTR as a cAMP-dependent regulator of sodium channels. *Science.* 269, 847–50.
- Switzer, M., Rice, J., Rice, M., Hardin, D.S., 2009. Insulin-like growth factor-I levels predict weight, height and protein catabolism in children and adolescents with cystic fibrosis. *J. Pediatr. Endocrinol. Metab.* 22, 417–424.
- Szaff, M., Hoiby, N., Flensburg, E.W., 1983. Frequent antibiotic therapy improves survival of cystic fibrosis patients with chronic *Pseudomonas aeruginosa* infection. *Acta Paediatr. Scand.* 72, 651–57.
- Tabary, O., Escotte, S., Couetil, J.P., Hubert, D., Dusser, D., Puchelle, E., Jacquot, J., 2001. Relationship between IkappaBalpha deficiency, NFkappaB activity and interleukin-8 production in CF human airway epithelial cells. *Pflugers Arch.* 443(Suppl 1), S40–S44.
- Tabary, O., Zahm, J.M., Hinnrasky, J., Couetil, J.P., Cornillet, P., Guenounou, M., Gaillard, D., Puchelle, E., Jacquot, J., 1998. Selective up-regulation of chemokine IL-8 expression in cystic fibrosis bronchial gland cells in vivo and in vitro. *Am. J. Pathol.* 153, 921–930.
- Telko, M.J., Hickey, A.J., 2005. Dry powder inhaler formulation. *Resp. Care* 50, 1209–1227.
- Thai, A., Xiao, J., Ammit, A.J., Rohanizadeh, R., 2010. Development of inhalable formulations of anti-inflammatory drugs to potentially treat smoke inhalation injury in burn victims. *Int. J. Pharm.* 389, 41-52.
- Thornton, J., Elliott, R., Tully, M.P., Dodd, M., Webb, A.K., 2004. Long term clinical outcome of home and hospital intravenous antibiotic treatment in adults with cystic fibrosis. *Thorax.* 59, 242–46.
- Tsui, L.C., 1992. The spectrum of cystic fibrosis mutations. *Trends Genet.* 8(11), 392-8.
- UNEP, 1987. The Montreal Protocol on Substances that Deplete the Ozone Layer. United Nations Environment Programme, Nairobi, p. 54.
- Vankeerberghen, A., Cuppens, H., Cassiman, J.J., 2002. The cystic fibrosis transmembrane conductance regulator: an intriguing protein with pleiotropic functions. *J. Cyst. Fibros.* 1, 13–29.
- Vaughn, J., Wiederhold, N., McConville, J., Coalson, J., Talbert, R., Burgess, D., Johnston, K., Williams, R., Peters, J., 2007. Murine airway histology and intracellular uptake of inhaled amorphous itraconazole. *Int. J. Pharm.* 338, 219–224.
- Vehring, R., 2008. Pharmaceutical particle engineering via spray drying. *Pharm Res* 25, 999–1022.

- Venkatakrishnan, A., Stecenko, A.A., King, G., Blackwell, T.R., Brigham, K.L., Christman, J.W., Blackwell, T.S., 2000. Exaggerated activation of nuclear factor-kappaB and altered IkappaB- beta processing in cystic fibrosis bronchial epithelial cells. *Am. J. Respir. Cell Mol. Biol.* 23, 396–403.
- Verdugo, P., 1990. Goblet cells secretion and mucogenesis. *Annu. Rev. Physiol.* 52, 157-176.
- Verhaeghe, C., Remouchamps, C., Hennuy, B., Vanderplasschen, A., Chariot, A., Tabruyn, S.P., Oury, C., Bours, V., 2007. Role of IKK and ERK pathways in intrinsic inflammation of cystic fibrosis airways. *Biochem. Pharmacol.* 73, 1982–1994.
- Virgin, F., Zhang, S., Schuster, D., Azbell, C., Fortenberry, J., Sorscher, E.J., Woodworth, B.A., 2010. The bioflavonoid compound, sinupret, stimulates transepithelial chloride transport in vitro and in vivo. *Laryngoscope* 120, 1051–1056.
- Wang, L., Zhang, Y., Tang, X., 2009. Characterization of a new inhalable thymopentin formulation. *Int. J. Pharm.* 375, 1-7.
- Weber, A.J., Soong, G., Bryan, R., Saba, S., Prince, A., 2001. Activation of NF-kappaB in airway epithelial cells is dependent on CFTR trafficking and Cl<sup>-</sup> channel function. *Am. J. Physiol. Lung Cell Mol. Physiol.* 281, L71–L78.
- Wegrzyn, G., Jakobkiewicz-Banecka, J., Gabig-Ciminska, M., Piotrowska, E., Narajczyk, M., Kloska, A., Malinowska, M., Dziedzic, D., Golebiewska, I., Moskot, M., Wegrzyn, A., 2010. Genistein: a natural isoflavone with a potential for treatment of genetic diseases. *Biochem. Soc. Trans.* 38, 695–701.
- Weibel, E.R. Lung morphometry and models in respiratory physiology. In: Chang HK, Paiva M, eds. *Respiratory Physiology: An Analytical Approach*. New York: Marcel Dekker, 1989:1-56.
- Weibel, E.R. *Morphometry of the Human Lung*. Berlin: Springer Verlag, 1963:1.
- Weiler, C., Egen, M., Trunk, M., Langguth, P., 2010. Force control and powder dispersibility of spray dried particles for inhalation. *J. Pharm. Sci.* 99, 303-16.
- Welsh, M.J., Ramsey, B.W., Accurso, F., Cutting, G.R., 2001. Cystic Fibrosis. In: Scriver CR, Beaudet AL, Sly WS, Valle D., Eds. *The Metabolic and Molecular Basis of Inherited Disease*. New York: McGraw-Hill Inc. 5121–88.
- Welsh, M.J., Smith, A.E., 1993. Molecular mechanism of CFTR chloride channel dysfunction in cystic fibrosis. *Cell.* 73(7), 1251-4.
- Willmott, N., Cummings, J., Stuart, J.F., Florence, A.T., 1985. Adriamycin-loaded albumin microspheres: preparation, in vivo distribution and release in the rat. *Biopharm Drug Disp.* 6, 91–104.
- Wilschanski, M., Famini, C., Blau, H., Rivlin, J., Augarten, A., Avital, A., Kerem, B., Kerem, E., 2000. A pilot study of the effect of gentamicin on nasal potential difference measurements in cystic fibrosis patients carrying stop mutations. *Am. J. Respir. Crit. Care Med.* 161, 860–865.

## References

---

- Wilschanski, M., Yahav, Y., Yaacov, Y., Blau, H., Bentur, L., Rivlin, J., Aviram, M., Bdelah-Abram, T., Bebok, Z., Shushi, L., Kerem, B., Kerem, E., 2003. Gentamicin induced correction of CFTR function in patients with cystic fibrosis and CFTR stop mutations. *N Engl. J. Med.* 349, 1433–1441.
- Wiszniewski, L., Jornot, L., Dudez, T., Pagano, A., Rochat, T., Lacroix, J. S., Suter, S., Chanson, M., 2006. Long-term cultures of polarized airway epithelial cells from patients with cystic fibrosis. *Am. J. Respir. Cell Mol. Biol.* 34, 39–48.
- Wolter, J., Bowler, S., Nolan, P., McCormack, J., 1997. Home intravenous therapy in cystic fibrosis: a prospective randomized trial examining clinical, quality of life and cost aspects. *Eur. Respir. J.* 10, 896–900.
- Yamamoto, A., Okumura, S., Fukuda, Y., Fukui, M., Takahashi, K., Muranishi, S., 1997. Improvement of the pulmonary absorption of (Asu1,7)-eel calcitonin by various absorption enhancers and their pulmonary toxicity in rats. *J. Pharm. Sci.* 86, 1144–1147.
- Yamamoto, Y., Gaynor, R.B., 2001. Role of the NF-kappaB pathway in the pathogenesis of human disease states. *Curr. Mol. Med.* 1, 287–296.
- Yang, H., Shelat, A.A., Guy, R.K., Gopinath, V.S., Ma, T., Du, K., Lukacs, G.L., Taddei, A., Folli, C., Pedemonte, N., Galletta, L.J., Verkman, A.S., 2003. Nanomolar affinity small molecule correctors of defective Delta F508-CFTR chloride channel gating. *J. Biol. Chem.* 278, 35079–35085.
- Yeh, H.C., Phalen, R.F., Raabe, O.G., 1976. Factors influencing the deposition of inhaled particles, *Env. Health Persp.* 15, 147-156.
- You, C.P., Dju, C.K., 1983. Total and regional deposition of inhaled aerosol in humans. *J. Aerosol Sci.* 14, 599-609.
- Zabner, J., Karp, P., Seiler, M., Phillips, S.L., Mitchell, C.J., Saavedra, M., Welsh, M., Klingelutz, A.J., 2003. Development of cystic fibrosis and noncystic fibrosis airway cell lines. *Am. J. Physiol. Lung Cell Mol. Physiol.* 284, L844–L854.
- Zaman, M.M., Gelrud, A., Junaidi, O., Regan, M.M., Warny, M., Shea, J.C., Kelly, C., O’Sullivan, B.P., Freedman, S.D., 2004. Interleukin 8 secretion from monocytes of subjects heterozygous for the deltaF508 cystic fibrosis transmembrane conductance regulator gene mutation is altered. *Clin. Diagn. Lab. Immunol.* 11, 819–824.
- Zanen, P., Go, L.T., Lammers, J.W., 1996. Optimal particle size for beta 2 agonist and anticholinergic aerosols in patients with severe airflow obstruction. *Thorax.* 51, 977–980.
- Zeng, X.-M., Martin, G.P., Marriott, C., 1995. The controlled delivery of drugs to the lung. *Int. J. Pharm.* 124, 149–164.
- Zhang, X.M., Wang, X.T., Yue, H., Leung, S.W., Thibodeau, P.H., Thomas, P.J., Guggino, S.E., 2003. Organic solutes rescue the functional defect in DF508 cystic fibrosis transmembrane conductance regulator. *JBC.* 278, 51232–51242.

## *References*

---

Zsembery, A., Jessner, W., Sitter, G., Spirli, C., Strazzabosco, M., Graf, J., 2002. Correction of CFTR malfunction and stimulation of  $\text{Ca}^{2+}$ -activated  $\text{Cl}^-$  channels restore  $\text{HCO}_3^-$  secretion in cystic fibrosis bile ductular cells. *Hepatology*. 35, 95-104.

## *References*

---

## **Acknowledgements**

I never could have done this work without the enthusiasm and encouragements of the people who worked with me this three years way. First of all, I would thank sincerely my supervisor Prof. Rita Patrizia Aquino for her guidance, support and the opportunity that she gave me to attend the Research Doctorate Program.

My special thanks go to Dr. Paola Russo. Paola, thank you for your enthusiasm, inspiration and endless support.

I would also thank Dr. Francesca Sansone, Dr. Teresa Mencherini, Dr. Patrizia Picerno, Dr. Giulia Auriemma, Dr. Pasquale Del Gaudio for the continuous help, collaboration and for the special moments that we shared.

Francy, thank you for sharing your “desk” with me during these three years, for coming with me to my first congress-poster session in Cagliari (do you remember?!); your support was unique.

Terry, thank you for our friendly coffee break and for your encouragements and advices that I really appreciated.

Patty, thank you for your wise and valuable advices.

Giulia, thank you for all the moments we shared inside and outside the lab; how can we forget all the conferences together?!

Thank you Prof. Pasquale for your suggestion and advices.

My thanks and appreciation go to my students Valentina, Lucio Mario, Mariateresa and Gaetana who helped me in various way.

My thanks go also to Prof. Maurizio Bifulco for giving me the precious opportunity to collaborate to biological section of my research.

I would thank Dr. Antonietta Santoro for her help in developing of biological experiments. Anto, thank you for your advices and enthusiasm that made stronger my research passion.

I wish to thank Dr. Simona Pisanti for her scientific and personal support.

## *Acknowledgements*

---

A special thank goes to Dr. Paola Picardi who shared with me also this experience. Paola, thank you for our coffee break, chatters, going out, for being my hair stylist and personal shopper, for your support even from a distance with Skype, for putting up with me in my bad days that were not few.

Then, my thanks go to Dr. Luigi Margarucci for making enjoyable and less boring my daily trip (Agropoli-Fisciano) with friendly chats, for his support and valuable advices.

And my last few lines are dedicated to who have always believed in me more than I did, Valerio. I am grateful to you for everything, since I never could have done this work without your support, patience and love.

Finally, I would thank my family, especially my mother who makes wonderful my life. They encouraged and loved me every day.

*Lucia Prota*